# Characterizing Ferrofluid Spin-Up Flow in Rotating Uniform Magnetic Fields

by
Kahlil A. Dozier
S.B., EE, M.I.T., 2012

Submitted to the Department of Electrical Engineering and Computer Science in
Partial Fulfillment of the Requirements for the Degree of
Master of Engineering in Electrical Engineering and Computer Science
at the Massachusetts Institute of Technology
January 2014

Author: _____ **Signature redacted** _____
Department of Electrical Engineering and Computer Science
January 31, 2014

Certified by: _____ **Signature redacted** _____
Markus Zahn, Professor of Electrical Engineering, Thesis Supervisor
January 31, 2014

Accepted by: _____ **Signature redacted** _____
Prof. Albert R. Meyer, Chairman, Masters of Engineering Thesis
Committee
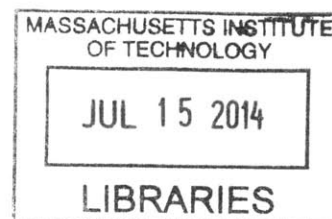
Characterizing Ferrofluid Spin-Up Flow in Rotating Uniform Magnetic Fields

By

Kahlil A. Dozier

January 30, 2014, In Partial Fulfillment of the Requirements for the Degree of
Master of Engineering in Electrical Engineering and Computer Science

## ABSTRACT

A ferrofluid is a collection of nanoscale ferromagnetic particles with a stabilizing
surfactant in a liquid to form a colloid. The dynamic behavior of ferrofluids in the
presence of magnetic fields has long been an area of research interest. A particular
area of interest deals with the "spin-up" mechanisms of ferrofluids, which describe
how a container of ferrofluid comes to a steady state of bulk flow when subjected to
a uniform rotating external magnetic field. There are two prevailing theories that
attempt to explain the spin-up mechanisms of ferrofluids: spin diffusion theory, and
the presence of non-uniformities in the magnetic field, due to "demagnetizing
factors" introduced by the shape of the container. This research attempts to confirm
previous measurements indicating that non-uniformities in the magnetic field are
the primary cause of ferrofluid bulk flow. Partial spheres and cylindrical containers
of different volumes—and thus different demagnetizing factors—were filled with
Ferrotec EFH1 oil-based ferrofluid and subjected to an external uniform rotating
magnetic field for various parameters of rotation direction and magnetic field.
Ferrofluid bulk flow was measured using ultrasound velocimetry, and the
magnitudes and shapes of the velocity profiles were compared. Despite the
complicated flows observed within the containers, enough of a trend was
established to safely conclude that demagnetizing factors are often the primary
cause of ferrofluid bulk flow.

## ACKNOWLEDGEMENTS

First of all, I would like to thank Professor Markus Zahn, firstly for giving me the opportunity to work on this project, and then for his support throughout the entire process.

This thesis would also not be possible without the tireless efforts of Dr. Shahriar Khushrushahi. His significant contribution of his time and knowledge was integral from the very beginning, and lasted throughout the duration of the project.

Finally, I would like to thank my family. Without their enduring love and support, this achievement would have never been possible.

**CONTENTS**

# CHAPTER 1

# INTRODUCTION

## 1.1 Ferrofluids

A ferrofluid is a collection of nanoscale ferromagnetic particles mixed in a stable suspension of liquid to form a colloid. Each ferromagnetic particle is coated with a surfactant, which inhibits individual particles' tendency to "clump together" within the homogenous fluid. The liquid in which the ferromagnetic particles are mixed (often called the "base liquid") is most commonly oil or water. A simple diagrammatic model of a ferrofluid is depicted in Figure 1 [1].

Ferrofluids have a host of unique properties, and as these properties have come to be understood better, many practical applications have surfaced. Some of the most useful properties of ferrofluids only become apparent when they are subjected to external magnetic fields. Under these conditions, the magnetic properties of the individual ferromagnetic particles, combined with the action of their surfactant coating, can result in very complex and interesting dynamic behavior. This behavior has lead to thousands of application patents for
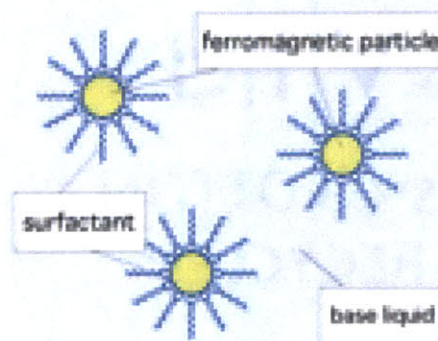
Figure 1: Ferromagnetic particles coated with a surfactant, suspended in a base liquid, forming a ferrofluid.

ferrofluids, such as for improved liquid rotary shafts on disk drives, inertia dampers in motors, improved heat transfer in speakers, or even magnetically controlled gates in microfluidic pumps [2].

## 1.2 Spin-up Flow

Spin-up flow is the term given to the process by which fluid in a container reaches a steady state of rotation in the presence of a rotating magnetic field, which can be uniform or non-uniform. The spin-up mechanisms of ferrofluid flow are closely related to the two distinct types of flows that can happen inside a container: "free surface" flow and "bulk" flow. Free surface flow can only happen when the container has an uncovered surface, because it refers to the rotation of the top of the fluid at that uncovered surface. Bulk flow refers to the rotation of the "body" of the fluid inside the container. These two flows need not coincide with one another; prior experiments have found that they often behave very differently depending on the external magnetic field [2].

The details of the physical phenomena that actually determine ferrofluid spin-up mechanisms have long been a point of dispute between researchers. Part of this dispute initially stemmed from the puzzling results researchers obtained when first investigating ferrofluid spin-up flow. Historically, before the ultrasound velocimetry technique of measurement was developed, free-surface flow was the only type of ferrofluid flow that could be easily measured and observed [2]. Various

researchers, all cited by Khushrushahi, performed experiments measuring ferrofluid free surface flow, all under the assumption of a uniform rotating magnetic field. Eventually, a distinct relationship between the direction of free surface flow and the shape of the ferrofluid meniscus at the surface of the container was found. With a concave-shaped meniscus, the free surface rotated opposite the magnetic field. With a flat meniscus, there was no significant free surface flow. And with a convex meniscus, the free surface co-rotated with the magnetic field. These results are summarized in Figure 2 [3].
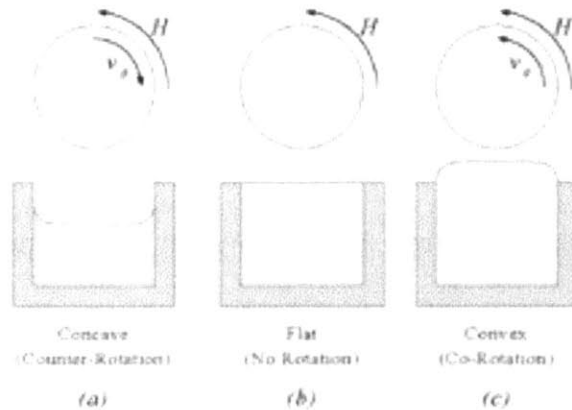


**Figure 2:** Relationship between free surface flow in a ferrofluid-filled container and the direction of the external rotating magnetic field.

However, when experiments were performed using ultrasound velocimetry techniques to measure ferrofluid bulk flow in identical experimental conditions, it was determined that the bulk flow of the ferrofluid is not necessarily in the same direction as the free surface flow. Instead, ferrofluid bulk flow always co-rotated with the direction of the external rotating field, independent of the direction of free surface flow. This initially was puzzling for researchers, and they tried to come up

with potential explanations for the observed dynamics. To date, there have been two prevailing theories offered to explain the phenomena of bulk flow in a ferrofluid-filled container: Spin Diffusion Theory, and the presence of non-uniformities in the magnetic field due to demagnetizing effects [2].

## 1.3 Spin Diffusion Theory

According to Spin Diffusion Theory, when a ferrofluid-filled container is subjected to a rotating external magnetic field, at any given instant, the individual magnetic particles of the ferrofluid try to align their magnetic moments with the external field. However, this alignment is not instantaneous, and as a result there is a time lag between the magnetization of the individual particles and the continually rotating field. This induces a spin velocity in each particle. Within the bulk of the ferrofluid, the spin velocity of each particle is cancelled out by the spin velocity of adjacent particles. But near the walls of the container, this is not the case, due to fluid drag on the wall. This causes a net body-torque density on the magnetic particles near the walls, which results in a transfer of angular momentum from these wall particles to the adjacent ones, which is quickly dispersed into the bulk of the fluid, inducing the bulk flow. Effectively, the spin of the particles on the wall is "diffused" into the surrounding liquid, hence the name "Spin Diffusion Theory." [3]

## 1.4 Non-uniformities in the Magnetic Field

The competing theory asserts that the presence of non-uniformities in the magnetic field within the body of the ferrofluid is the primary cause of bulk flow. When a ferrofluid filled container is subjected to an external magnetic field, the existing magnetic field within the body of the ferrofluid itself is distorted. This distorted

9

magnetic field is posited to be the main cause of bulk flow. A container of an asymmetric shape will have a much more distorted field. In general, a container of any given shape has an associated demagnetizing factor, which can be calculated, and which characterizes the extent to which the field within the container of fluid will be distorted [2].

Specifically, the theory predicts that ferrofluid within a perfectly spherical container, or a cylindrical container of infinite length, subjected to a uniform rotating magnetic field, will not have its inner field distorted at all. As a result, there should be negligible ferrofluid bulk flow in a perfectly spherical container, as well as a cylindrical container with a large height to radius ratio, despite the presence of the rotating field.

Khushrushahi, in his thesis, asserted that it was the latter theory that was correct. Non-uniformities in the magnetic field, caused primarily by asymmetric container shapes, were concluded to be the main cause of ferrofluid bulk flow; spin diffusion theory was found to be negligible. Khushrushahi performed experiments with MSGW11, a water-based ferrofluid, housed in a wide variety of containers of different shapes. A uniform rotating external field was generated using a spherical configuration of copper wire called a "fluxball, [3]" shown in Figure 3. Khushrushahi took velocity profiles of the ferrofluid using ultrasound velocimetry measurement to determine the resulting bulk flow. As predicted, negligible bulk flow was measured when using a perfectly spherical container of ferrofluid, while introducing non-uniformities in the field by using containers of different shapes lead to measurable bulk flow.
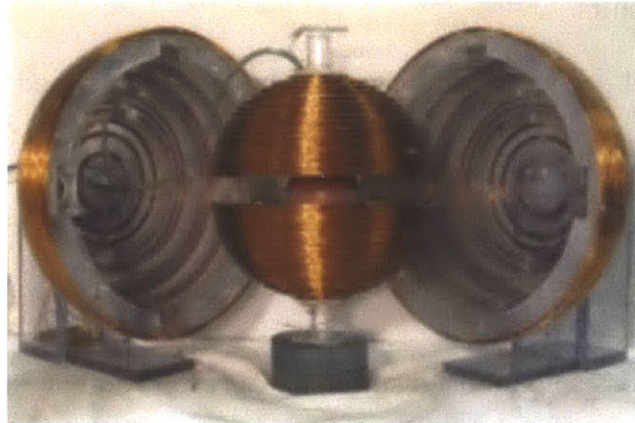
Figure 3: The fluxball, which is used to create a rotating magnetic field.

## 1.5 Overview of Thesis

The primary focus of this thesis will be to expand upon Khushrushahi's initial experiments, and to see if the collected data coincides with his own conclusions and the predictions of the theory of non-uniformities due to demagnetizing factors. Experiments are conducted with EFH1, an oil-based ferrofluid that Khushrushahi had minimal previous data on. Ultrasound measurements will be taken of ferrofluid in containers of both spherical and cylindrical geometries.

**Chapter 2** details the experimental setup and apparatus. It gives an overview of the basic properties of EFH1 ferrofluid, and then describes all the critical experimental apparatus, including the fluxball, the containers of different geometries, and the DOP-2000 Velocimeter, which is the instrument used to make ultrasound velocimetry measurements.

**Chapter 3** walks through the entire experimental procedure beginning to end, detailing the exact steps that must be taken in order to reproduce these

experiments. It also details the procedure used to verify the validity of the experimental results.

**Chapter 4** presents and discusses the results obtained from measurements taken in spherical geometry.

**Chapter 5** presents and discusses the results obtained from measurements taken in cylindrical geometry.

**Chapter 6** is a condensed summary of results and presents the conclusions of the thesis. It also makes note of how future experiments may be improved and contains suggestions for future work.

# CHAPTER 2

# EXPERIMENTAL APPARATUS

## 2.1 EFHI Ferrofluid

EFH1 is a type of oil-based ferrofluid produced by FerroTec Corporation. All experiments with ferrofluid in this thesis were carried out using EFH1. The volume composition of EFH1 is summarized in Table 2.1, and some of its chemical properties are summarized in Table 2.2 [2].

Table 2.1: Composition of EFH1 ferrofluid

| COMPONENT | PERCENTAGE BY VOLUME |
|---|---|
| Magnetite | 3-15% |
| Oil Soluble Dispersant | 6-30% |
| Carrier Liquid | 55-91% |

Table 2.2: Properties of EFH1 ferrofluid

| PROPERTY | VALUES |
|---|---|
| Boiling Point (F) | 401-491 |
| Specific Gravity | 0.92 to 1.47 |
| Vapor Pressure (mm Hg) | 1 at 100 °F |
| Percent Volatile by Volume | 55-91% |
| Vapor Density (AIR = 1) | 6.4 |
| Solubility in Water | Negligible |
| Speed of Sound | 1116 m/s |

## 2.2 Ferrofluid Containers

To determine the extent to which demagnetizing factors affected the dynamic behavior of ferrofluid in a uniform rotating magnetic field, containers of different shapes (and thus different demagnetizing factors) were used. Experiments were carried out using two main types of container geometries: spherical and cylindrical. In addition to holding the ferrofluid, the containers also had to allow for interface with ultrasonic transducers, so bulk flow velocity could be measured using ultrasound velocimetry.

## 2.2.1 Truncated Spherical Containers

For the spherical geometry, hollow propylene spheres of 3.937 inches in diameter were used as the containers. MIT student Michael Snively previously manufactured these containers in the process of completing his own Bachelor's thesis [3]. In

14

addition to a fully spherical container, other spherical containers were "truncated" at various volumes to provide for different demagnetizing factors. A cross-section of the whole sphere and the dimensions for the truncated spheres are diagrammed in figure 2.1 below.
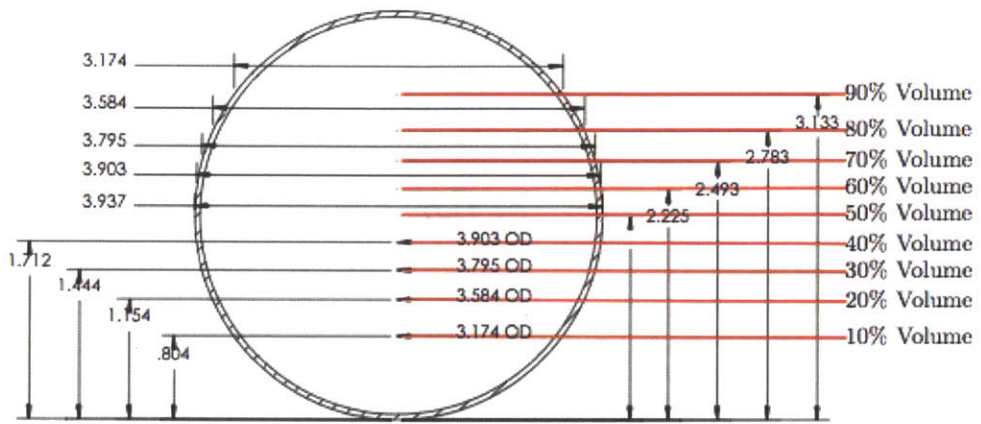


Figure 2.1: Cross-section of a full hollow sphere, with the height of cuts (in inches) made to truncate the spheres.

Initially, there were ten containers manufactured in total, one for the 100% sphere and one for truncated spheres at 90% volume down in 10-percent increments to 10% volume. However, in the course of experimentation, mechanical issues with the 60%, 50%, 40%, and 20% volume containers rendered them unusable. The adhesive material on the 60% and 50% containers interfered with the probe holder, and the 40% and 20% containers were deformed to the point of being unusable. As a result, data was only taken using the 100%, 90%, 80%, 70%, 30%, and 10% volumes.

Each container contained a cap which was re-sealable as well as a well at the top through which ferrofluid could be poured. The containers were secured with plastic screws after being filled with ferrofluid. Pictures of the individual containers are in figures 2.2-2.7 below.
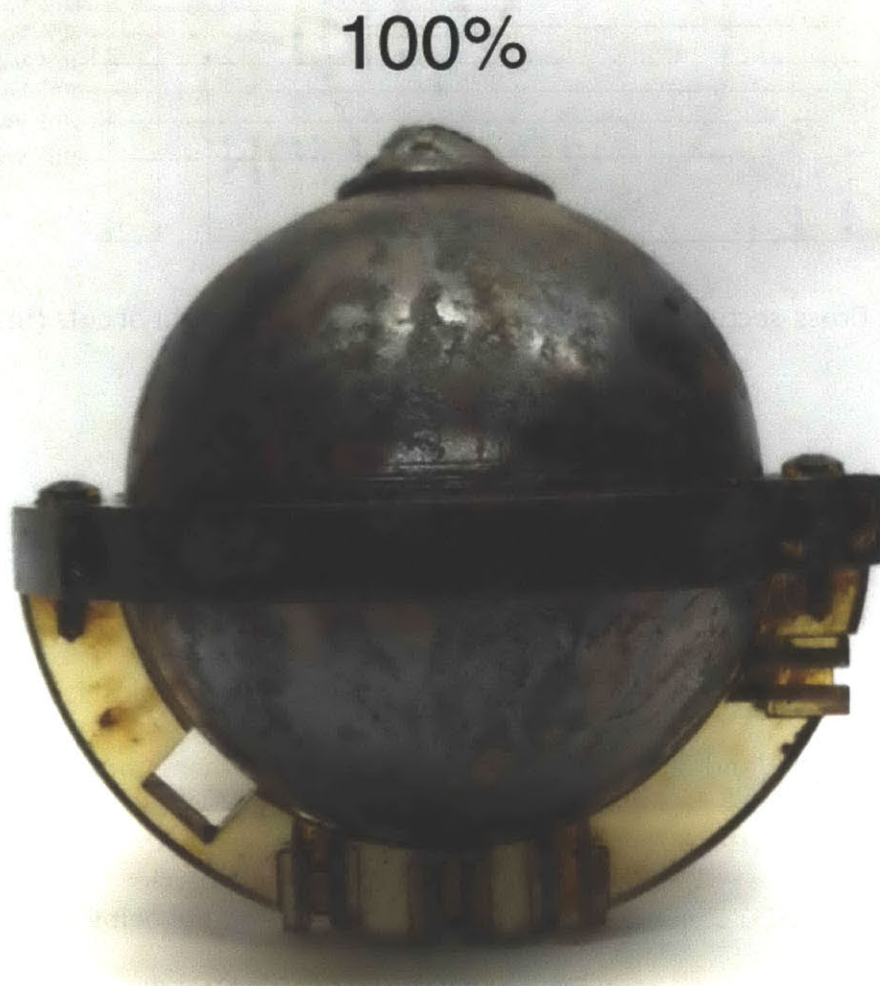


Figure 2.2: Spherical container of 100% volume.

90%
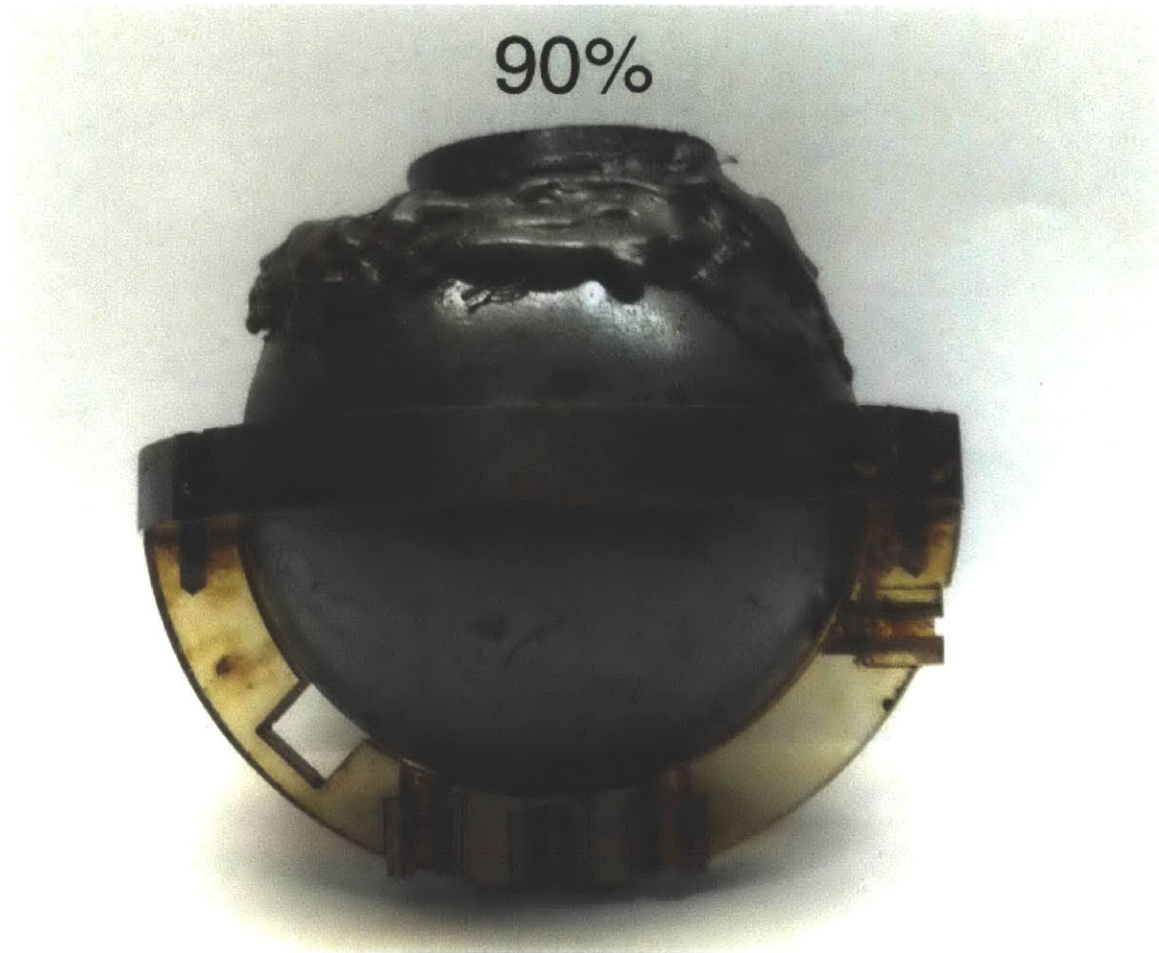


Figure 2.3: Spherical container of 90% volume.

80%



Figure 2.4: Spherical container of 80% volume.

70%



Figure 2.5: Spherical container of 70% volume.

30%
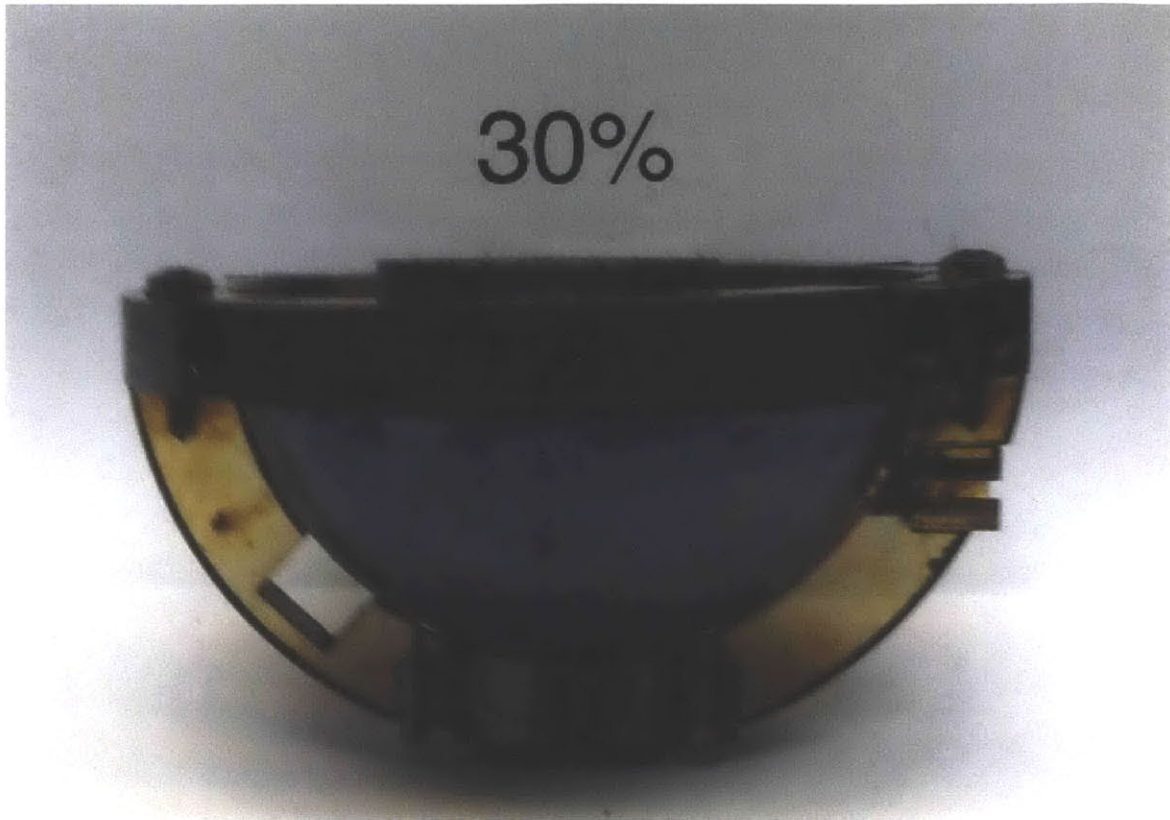


Figure 2.6: Spherical container of 30% volume.
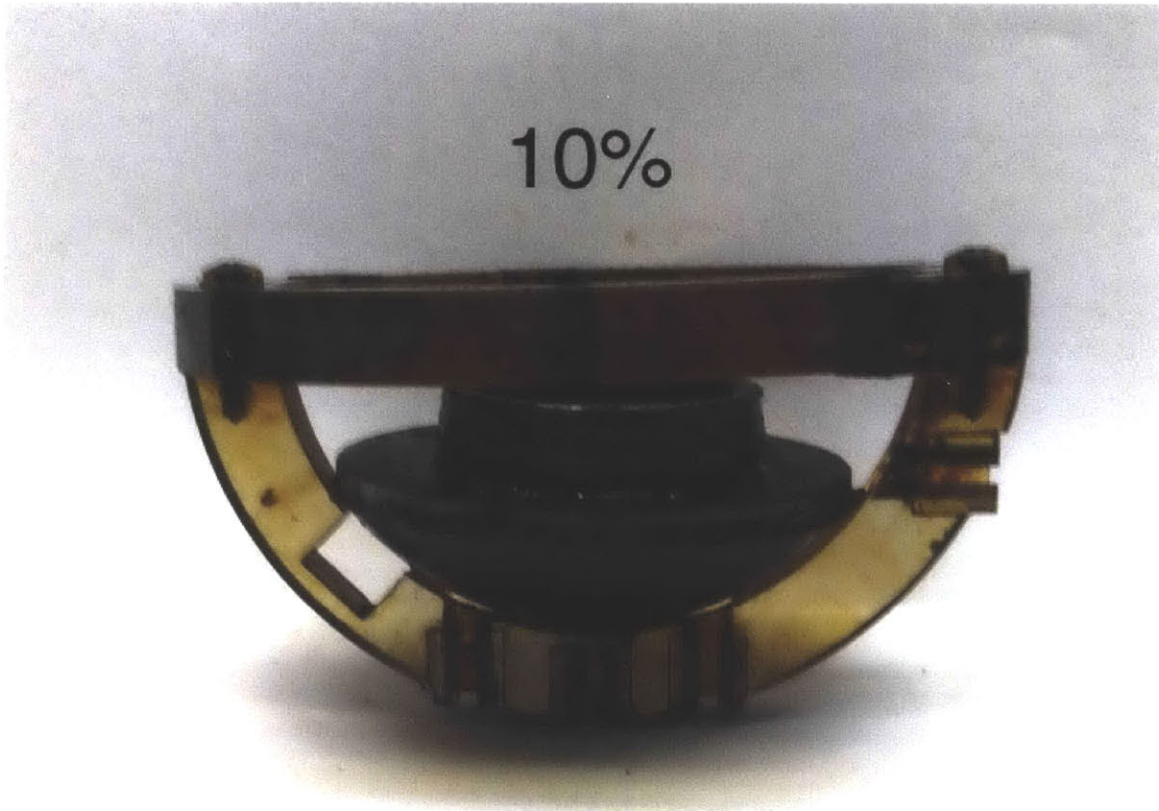
Figure 2.7: Spherical container of 10% volume.

## 2.2.2 Probe Holder

To allow the spheres to interface with ultrasound transducers for velocimetry measurements, a "probe holder" was used. Khushrushahi built this probe holder in his own doctoral thesis. The probe holder contains slots for ultrasound transducers, or "probes" to fit into, as well as a peg slot that allows it to be placed securely into the fluxball while the magnetic field is being generated.
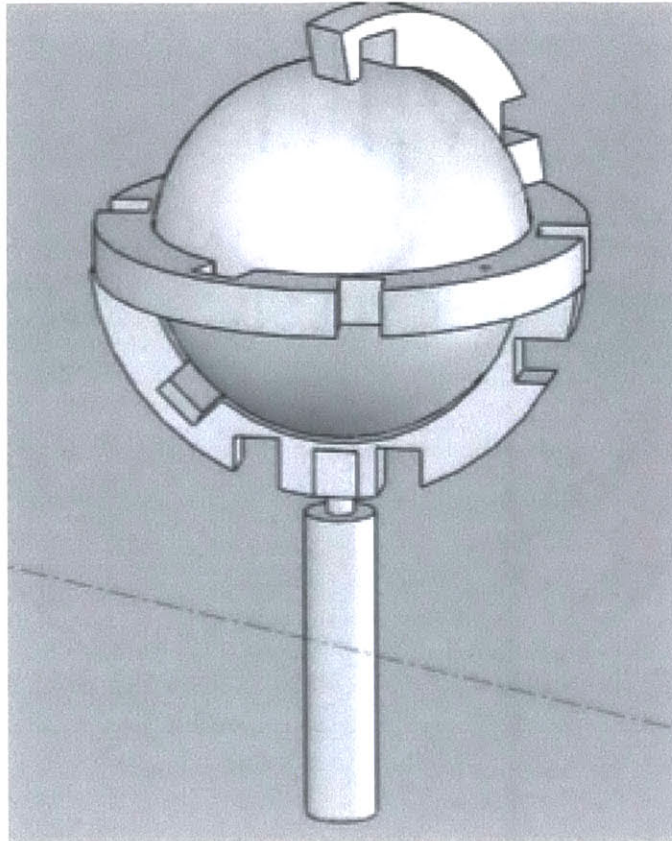
Figure 2.8: SolidWorks Graphic of Probe Holder, with support rod inserted into peg

slot.

Each probe slot corresponds to a specific channel for data taking on the DOP-2000

velocimeter, pictured in Figure 2.9. Pictures of the actual probe holder used, along

with the associated channel designations, are shown in Figures 2.10 and 2.11.

Figure 2.9: DOP-2000 Velocimeter.
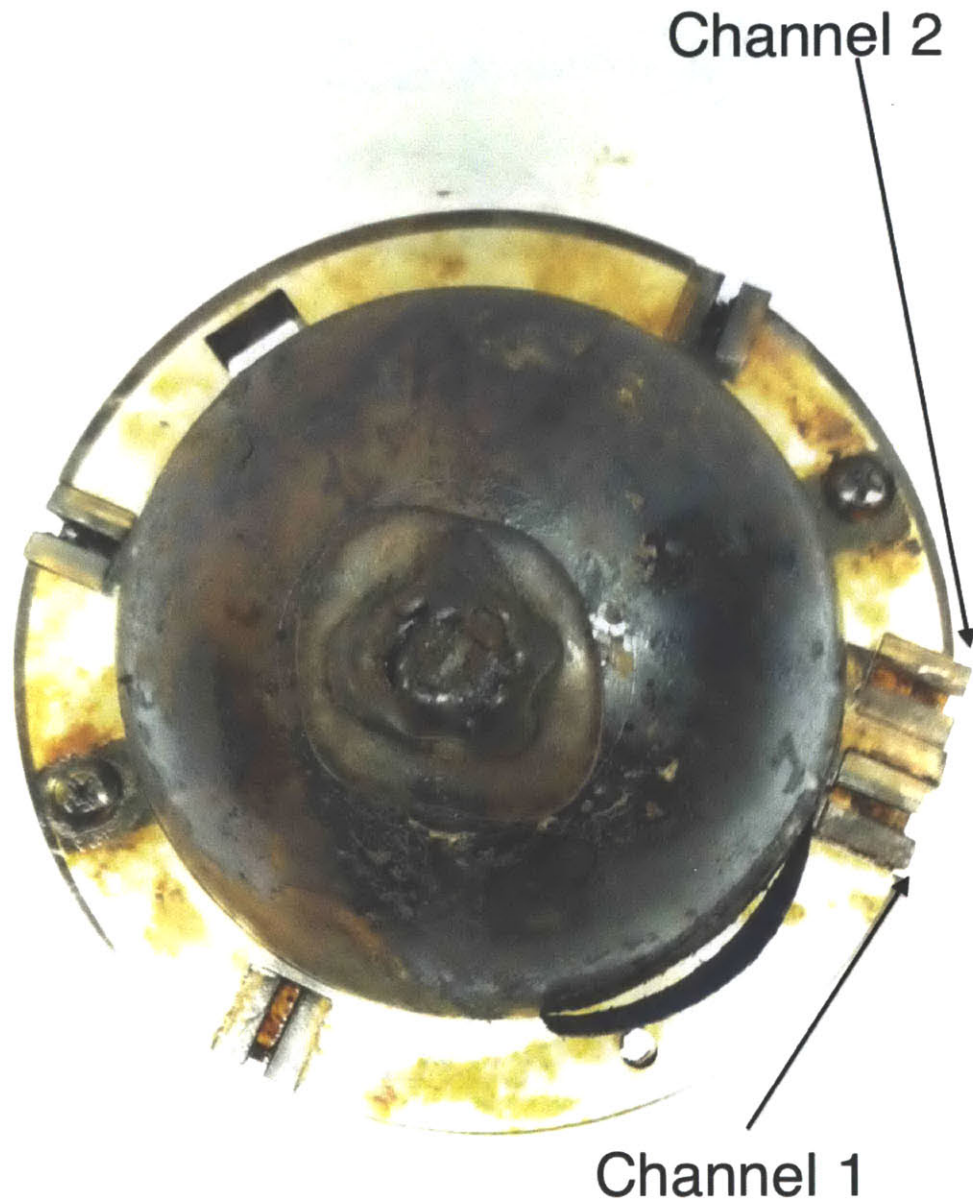
**Channel 2**

**Channel 1**

Figure 2.10: Top view of probe holder, with a ferrofluid-filled sphere inside. Two slots for ultrasound probes are marked, designated "channel 1" and "channel 2".
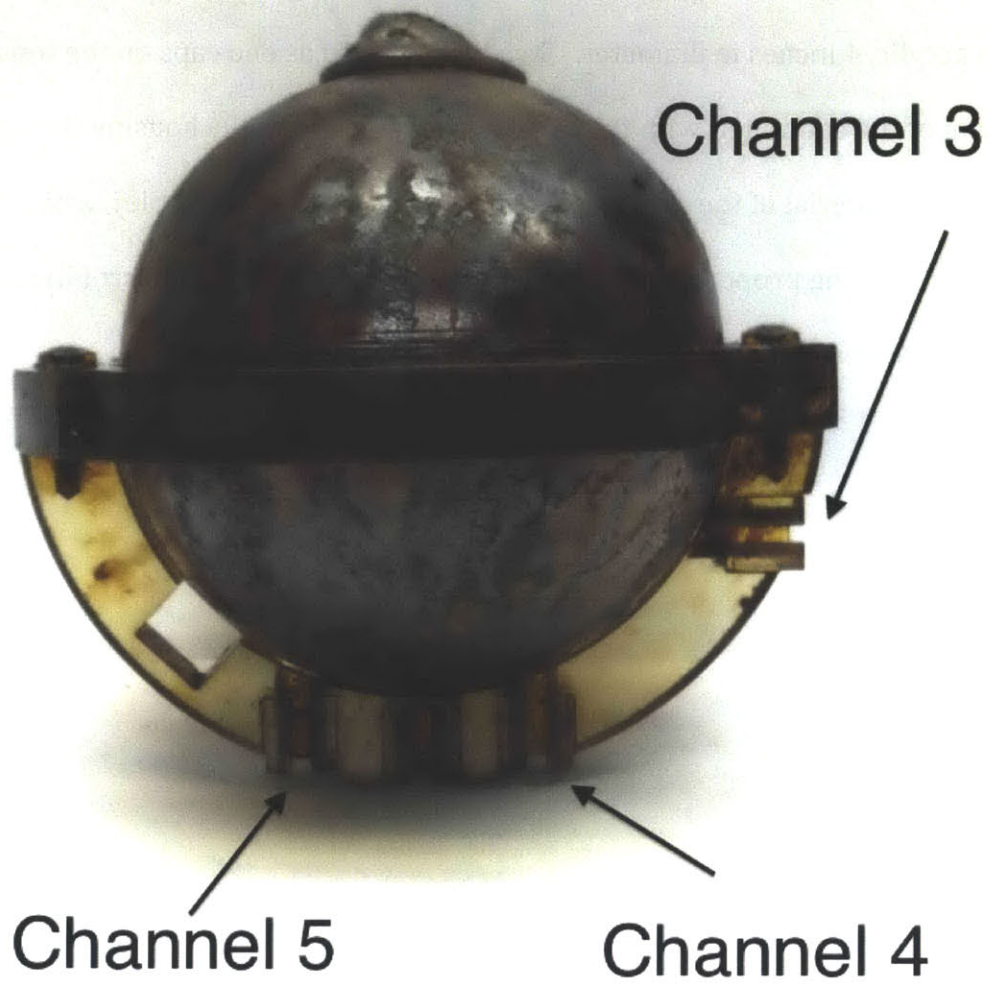
Figure 2.11: Side view of probe holder, with a ferrofluid-filled sphere inside. Three slots for ultrasound probes are marked, designated "channel 3", "channel 4", and "channel 5".

## 2.2.3 Cylindrical Containers

For experiments performed in the cylindrical geometry, containers were used that were manufactured by MIT student Katrina Schoen in the process of completing her own thesis [4]. The containers were comprised of stacked circular "disks," laser-cut from acrylic, 4 inches in diameter. Two disks served as end caps on the top and the bottom of the container, with the disks in the middle actually housing the ferrofluid. The inner material of the middle disks was made of Buna-N (nitrile), which has desirable sealing properties for both oil-based and water-based ferrofluids. All disks contained slots for ultrasound probes to be inserted into.
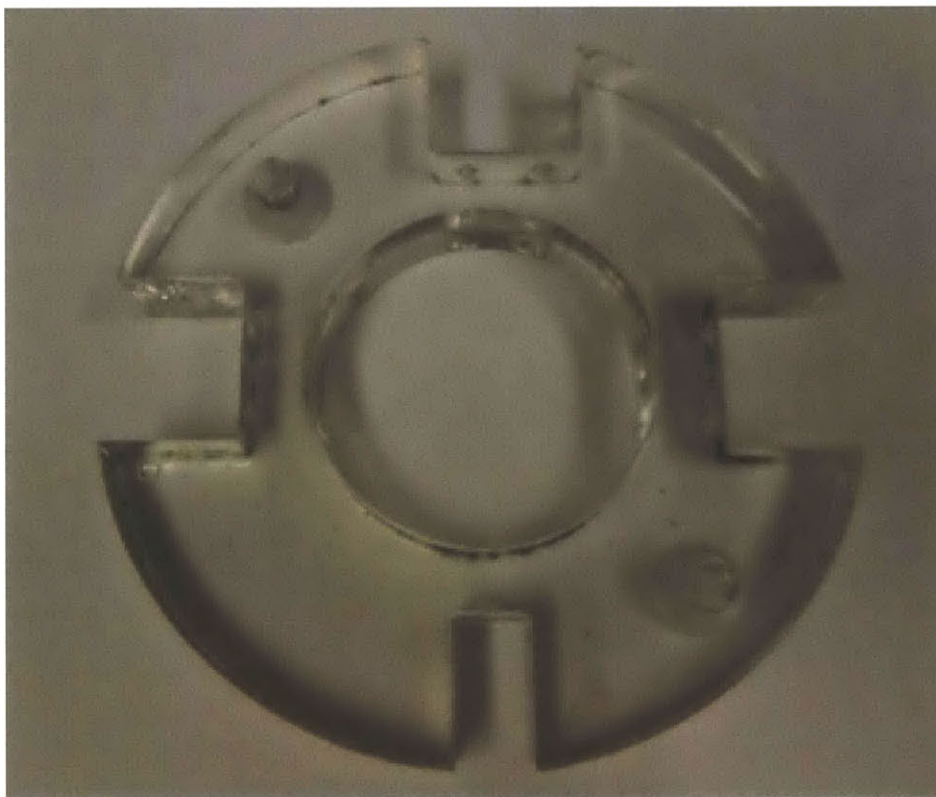


Figure 2.12: One of the acrylic disks that surround the cylindrical containers. A slot for an ultrasound probe is visible at the bottom.

There were two cylindrical containers used in experimentation, a "short" one with a height of a single disk (not including end caps), and a "long" one with a height of seven disks. A summary of the container aspect ratios is presented in Table 2.3, and actual pictures of the containers are presented in Figures 2.13-2.16.

Table 2.3: Aspect ratios of the short and long cylindrical containers

| Cylindrical Container | Aspect Ratio (height/diameter) |
|:---:|:---:|
| Short (1 disk) | 0.3175 |
| Long (7 disks) | 2.2225 |
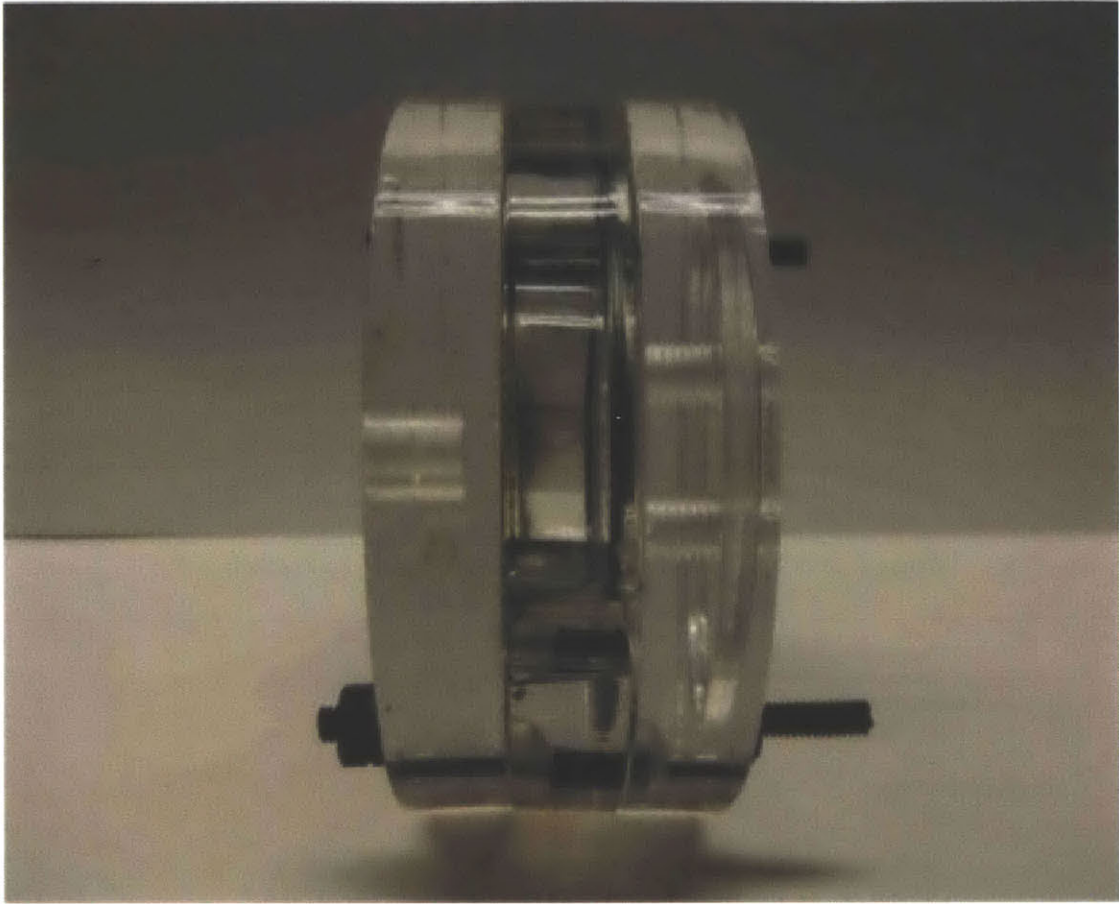
Figure 2.13 Side view of a fully assembled short cylinder. The container is made up of three disks. The single disk in the middle holds the ferrofluid, and is sealed by the two disks on the ends.
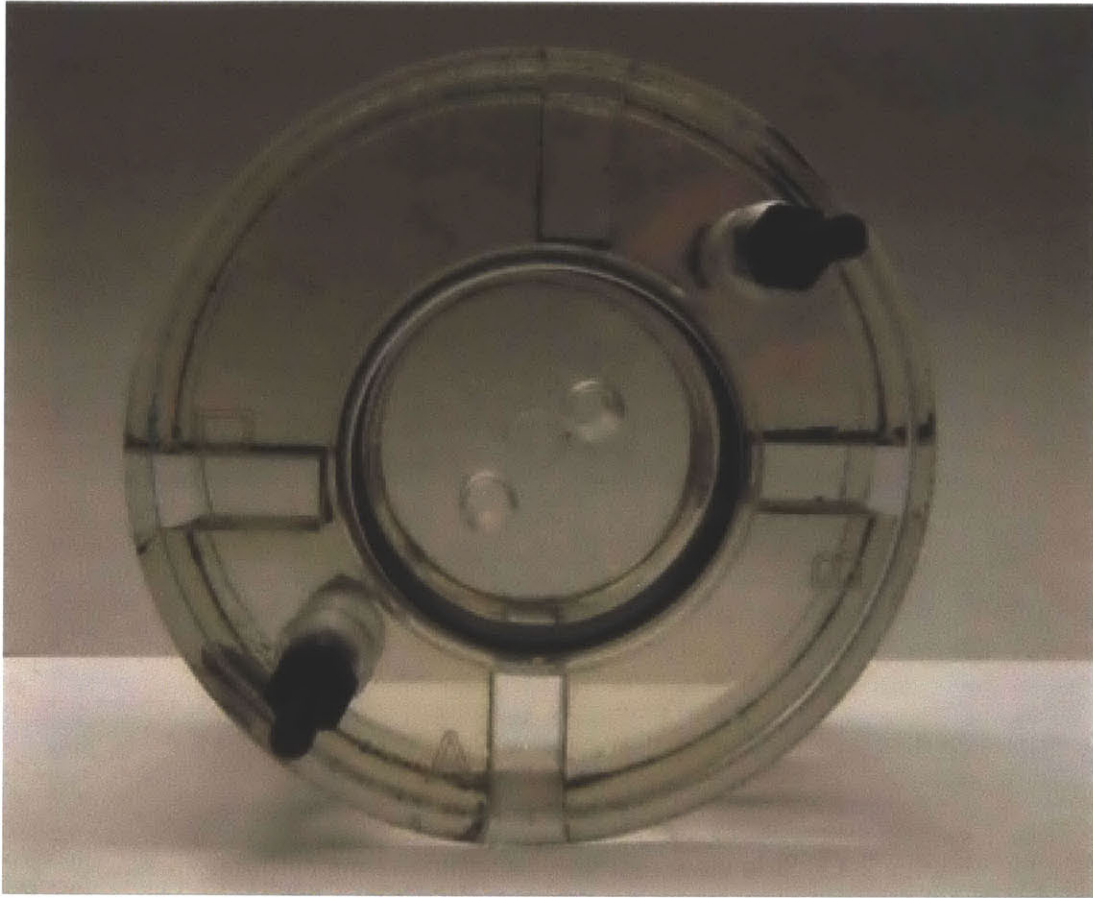
Figure 2.14: Top view of a short cylinder.

Figure 2.15: Side view of a fully assembled long cylinder.
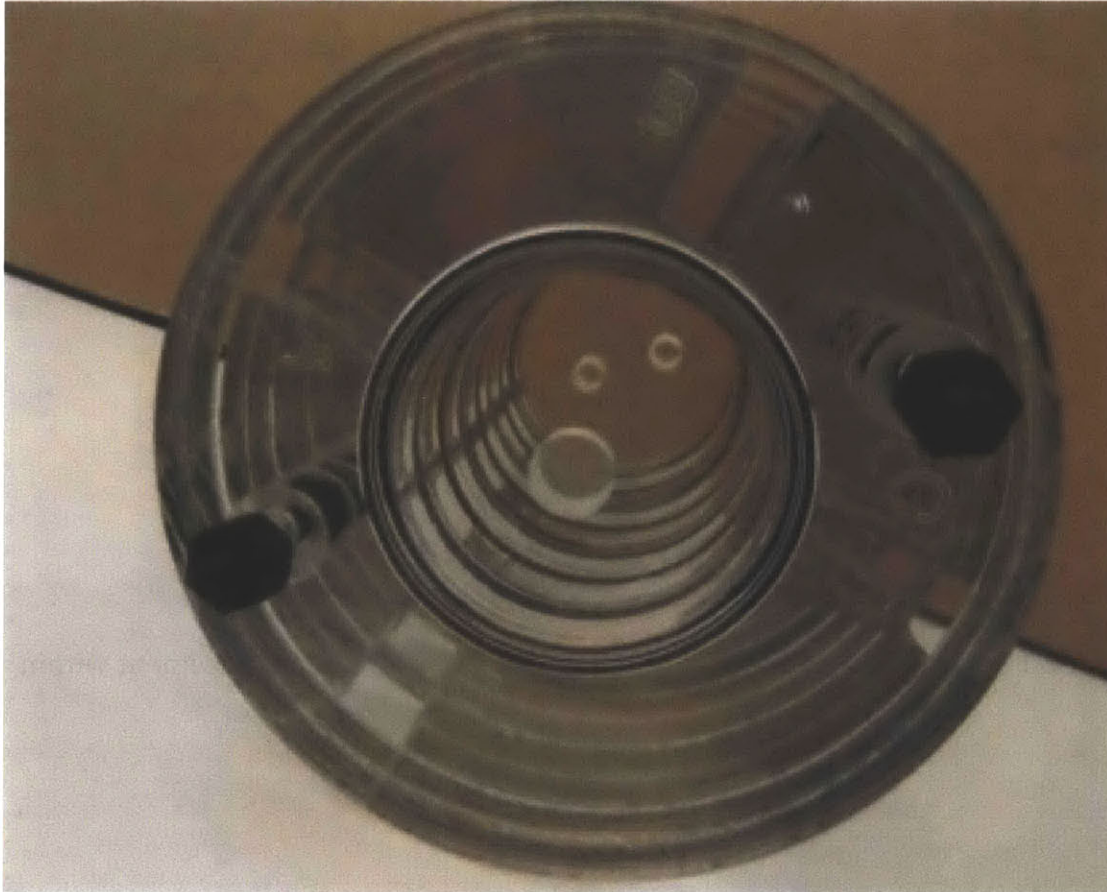
Figure 2.16: Top view of a fully assembled long cylinder.

To allow for secure placement within the fluxball, plastic fixtures were manufactured, shown in Figure 2.17. The cylinders were placed within these fixtures, and then the whole arrangement was placed into the fluxball, as shown in Figure 2.18.
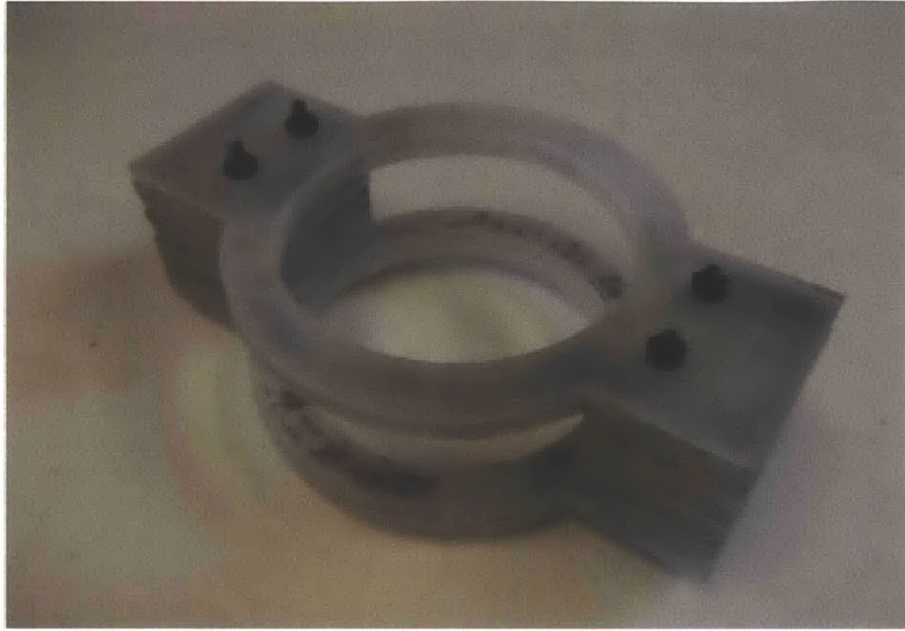
Figure 2.17: Fixture for cylindrical containers to allow for secure placement within

fluxball.
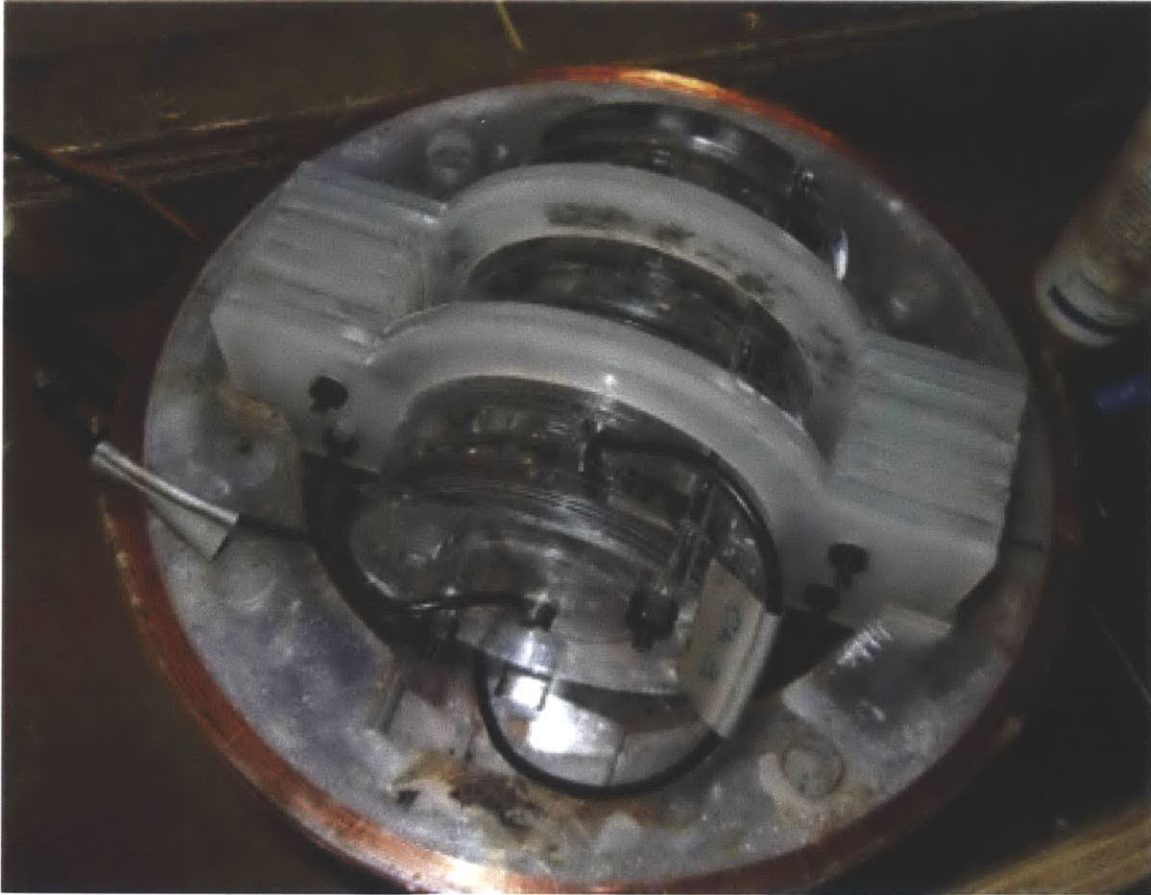
Figure 2.18: Long cylindrical container, with fixture, placed securely inside bottom

half of fluxball.

## 2.3 DOP-2000 Velocimeter

To actually measure bulk ferrofluid flow inside the containers, the DOP-2000

Velocimeter, made by Signal Processing SA, was utilized (Figure 2.19). The DOP-

2000 is a machine that can record the velocity of a fluid as a function of position. To

accomplish this, ultrasonic probes are hooked up to the machine, and their tops

directly interface with the surface to the container. As many as six probes can be

hooked up simultaneously. An application of ultrasound gel or a similar substance

between the probe-container interfaces is necessary to ensure a quality sound

connection. A cross-section of an ultrasonic probe is diagrammed in Figure 2.20.



Figure 2.19: The DOP-2000 Velocimeter, with an ultrasonic transducer attached.
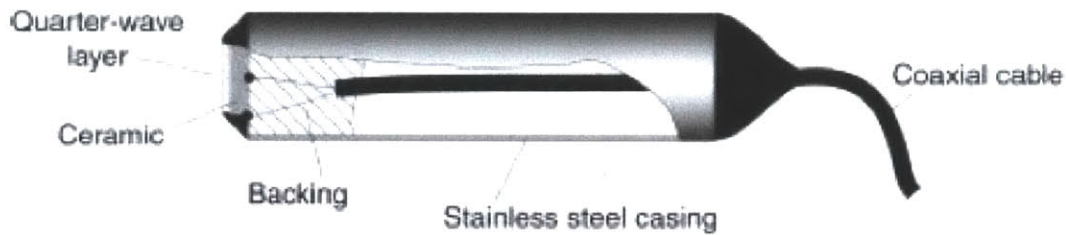
Figure 2.20: Cross section of a single ultrasonic transducer.

To actually establish velocity profiles, the probes emit small pulses of sound that are reflected off small latex particles inside the fluid [5]. Therefore, before taking any measurements, the ferrofluid must first be mixed with a solution of small latex particles; GrilTex-P1 was the brand used in these experiments. A concentration of .008 g/mL is sufficient for reliable velocity profiles.

## 2.4 Fluxball

To generate the uniform rotating magnetic field required by these experiments, a particular piece of apparatus termed a "fluxball" was used. MIT student Clinton Lawler built the fluxball in the process of completing his thesis [6]. The fluxball consists of two concentric spheres of copper wire, one "inner" and one "outer," wrapped around a polycarbonate shell (figure 2.21). Both the outer and inner sphere can be separated into halves for assembly and disassembly. The inner sphere can be placed in one of two positions, "horizontal" (upright) or "vertical" (sideways). In the horizontal position, the plane of magnetic field rotation is perpendicular to the floor; in the vertical position, the plane of magnetic field

rotation is parallel with the floor. Figure 2.23 diagrams both configurations and the direction of field rotation.
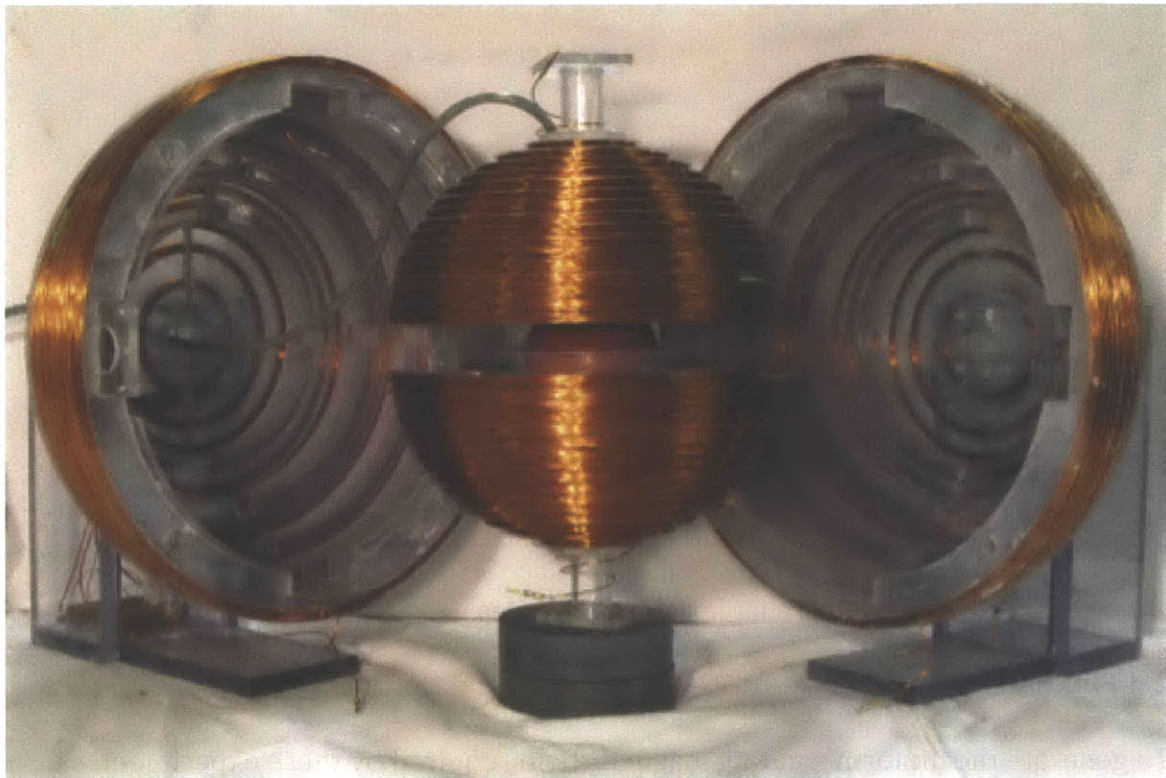


Figure 2.21: The partially disassembled fluxball. Here, the inner sphere is in the "horizontal" position.

The outer and inner coils can be independently excited with current, which produces a magnetic field. A uniform rotating magnetic field can be produced by exciting the coils with equal-amplitude sinusoidally varying current, with a 90-degree phase difference between the inner and outer coils. The plane of field rotation can be determined by using the right-hand rule, as demonstrated in Figure 2.22. The coils are driven with a power amplifier, which is controlled via LabVIEW

software. Khushrushahi wrote the LabVIEW control program used in these experiments as part of his own thesis [2].
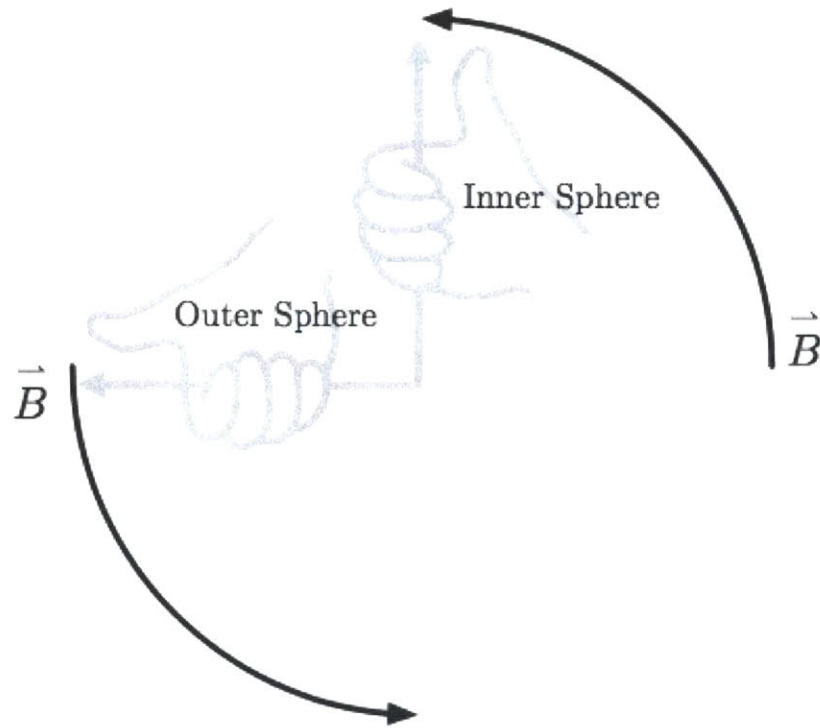


Figure 2.22: An example of using the right-hand rule to determine the plane of rotation of the magnetic field. In this example, the inner sphere is upright in the "horizontal" position, and the plane of rotation is the plane of the page. If the inner sphere were in the "vertical" position, the plane of rotation would be perpendicular to the page.

If the outer coil is excited at a +90-degree phase difference with respect to the inner coil, the direction of field rotation will be one way, and if the outer coil is at -90-degrees with respect to the inner coil, the field will rotate the opposite way. For

these experiments, the +90-degree phase difference was said to correspond to "counterclockwise" rotation, and -90-degrees "clockwise." These conventions are summarized below in Figures 2.23 and 2.24.
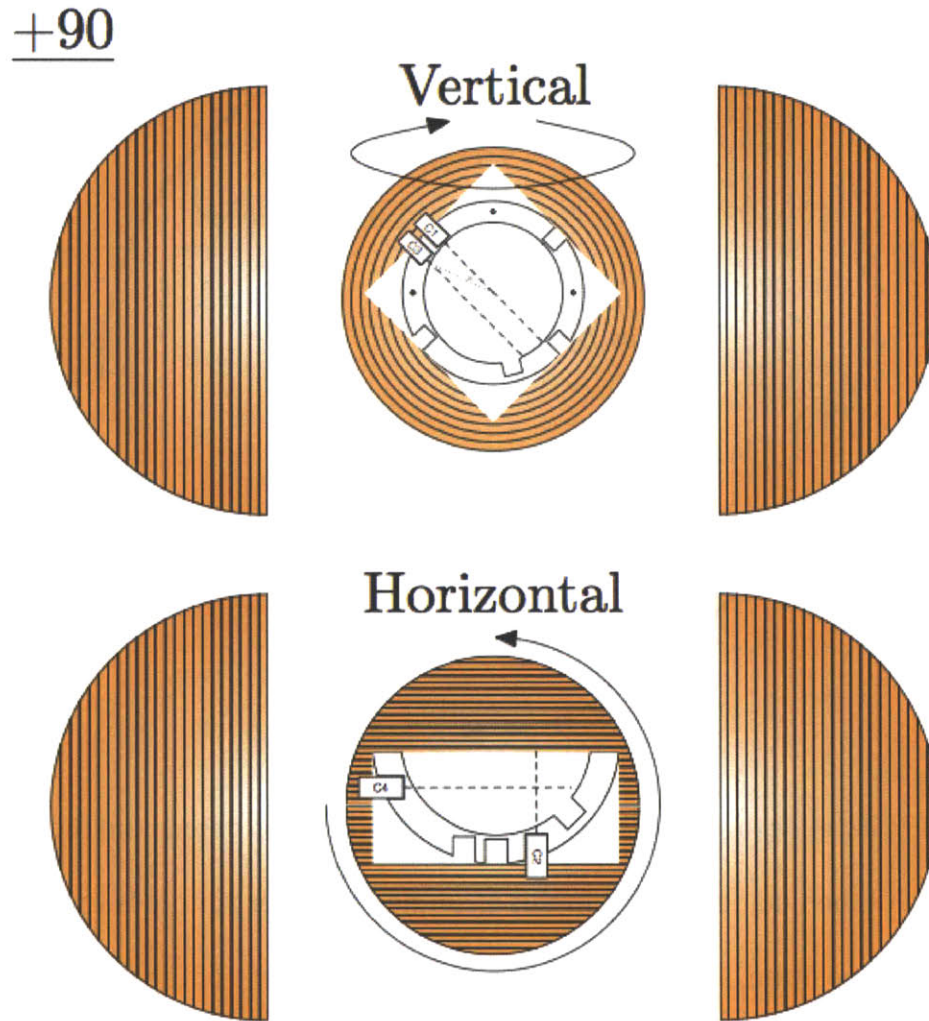


Figure 2.23: Counterclockwise field rotation that results from a +90-degree phase difference of the outer coil with respect to the inner. Arrows show the direction of magnetic field rotation. In the vertical configuration, the plane of field rotation is parallel to the floor; in the horizontal configuration, the plane of field rotation is perpendicular to the floor.
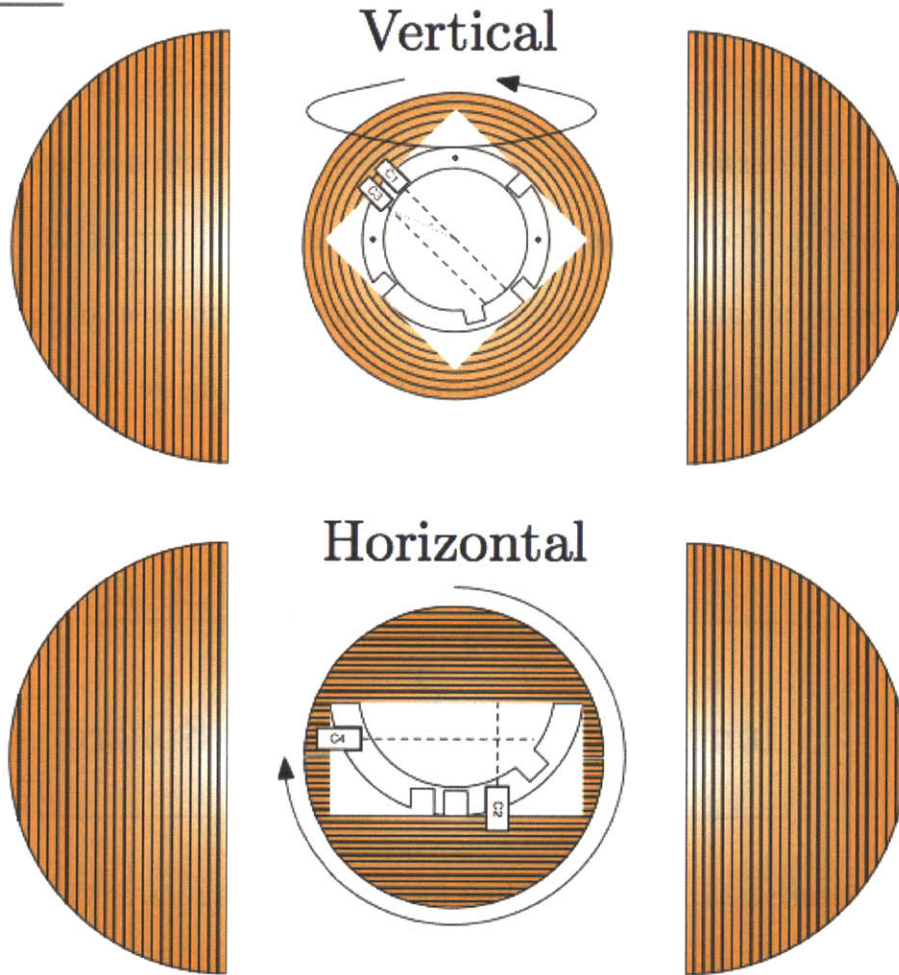
Figure 2.24: Clockwise field rotation that results from a -90-degree phase difference of the outer sphere with respect to the inner. Arrows show the direction of magnetic field rotation. In the vertical configuration, the plane of field rotation is parallel to the floor; in the horizontal configuration, the plane of field rotation is perpendicular to the floor.

### 2.4.1 Capacitor Selection for Resonant Operation

To actually generate magnetic fields strong enough to induce bulk flow in the ferrofluid, it is necessary to add capacitance in series with both the inner and outer coils, to cancel out the inductance of the coils themselves. Khushrushahi, in his thesis, derived the values of capacitors needed for two frequencies of operation: 47 Hz and 95 Hz [5]. These values are summarized below in figures 2.25 and 2.26.
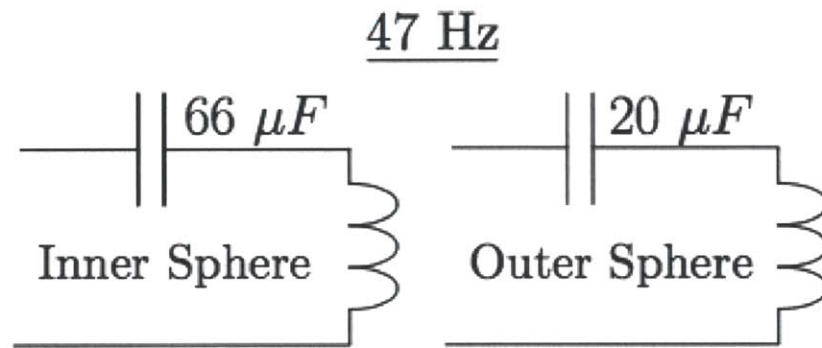


Figure 2.25: Capacitor values for resonant operation at 47 Hz.
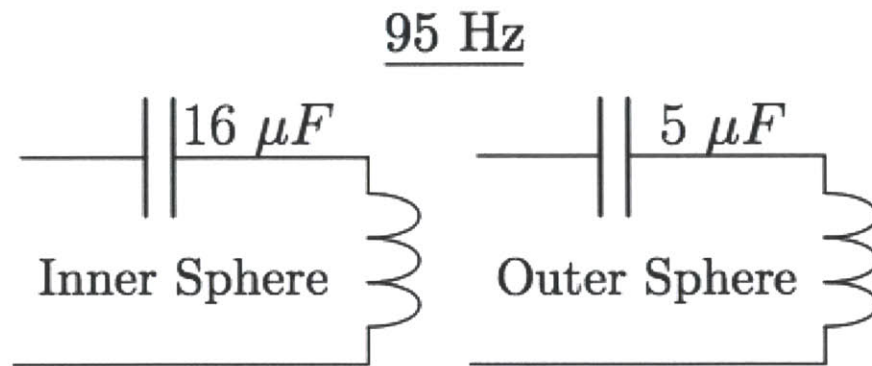


Figure 2.26: Capacitor values for resonant operation at 95 Hz.

# CHAPTER 3

## EXPERIMENTAL PROCEDURE

This chapter provides a detailed, step-by-step method to reproduce the experiments of this thesis and obtain the results produced in chapters 4 and 5, in both the spherical and cylindrical geometries.

### 3.1 Spherical Geometry

### 3.1.1 Establishing the Validity of Measurements with Probe Holder

Before experiments could be carried out with ferrofluid in the spherical containers, it was necessary to test whether the probe holder for the spheres could accurately measure fluid flow. A preliminary experiment was conducted which compared the measured results to data obtained by simulation with COMSOL multiphysics software. Khushrushahi wrote the model files necessary to produce the simulation results in the process of his own thesis.

A diagram of the experimental setup is shown in figure 3.1 below. A sphere with the top quarter cut off was placed inside the probe holder, and filled to the surface with Shell DIALA A transformer oil. Some of the physical properties of Shell DIALA A are summarized in table 3.1. The speed of sound was measured using a special feature of the DOP-2000 Velocimeter.

Table 3.1: Relevant physical properties of Shell DIALA A Transformer oil

| Viscosity (Pa s) | Density (kg/m^3) | Speed of Sound (m/s) |
|---|---|---|
| 0.0155 | 900 | 1421 |
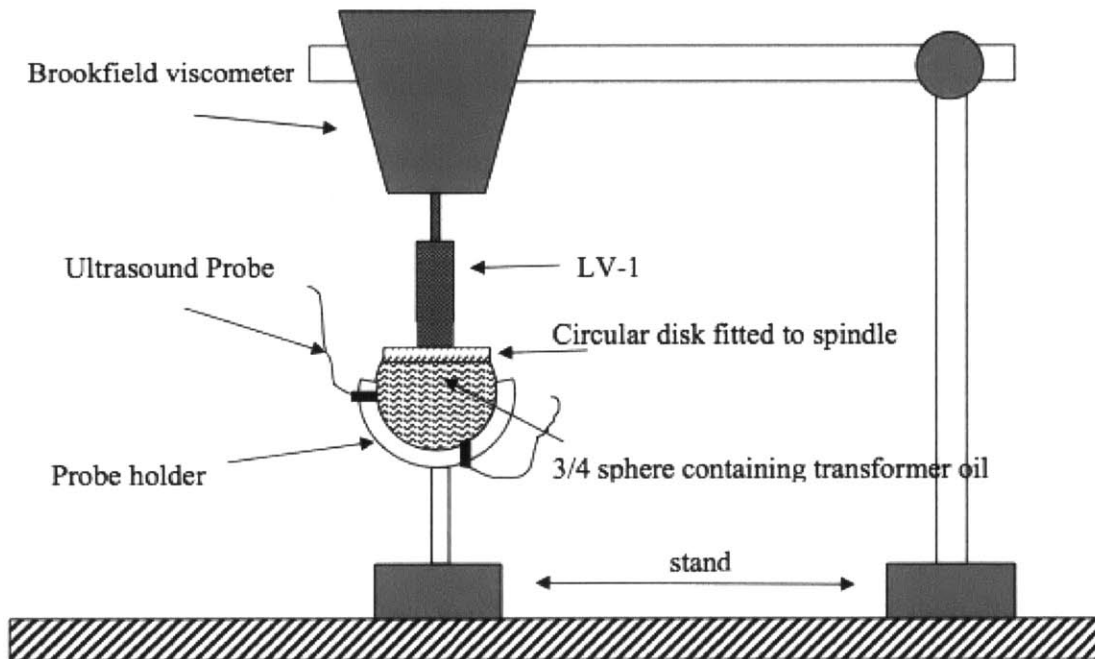


Figure 3.1: Diagram of experimental setup

After the sphere was filled with oil, a circular disk of diameter 81 mm was attached to the Brookfield Viscometer, positioned on top of the free surface of the sphere, and rotated at a constant RPM entraining the fluid layers below. One ultrasound probe was placed along the radius of the sphere, and a second offset at a 20-degree angle, which allowed for a calculation of the rotational ("phi") velocity as a function of radius. The results of this calculation are graphed in Figures 3.2-3.4. Khushrushahi set up identical flows in the COMSOL software, and the results of his simulation, as well as his own trials with an identical experimental setup, are compared against the experimental results in figures 3.2-3.4. It can be clearly seen that all results agree closely, which indicates the probe holder can successfully and accurately measure bulk fluid flow.
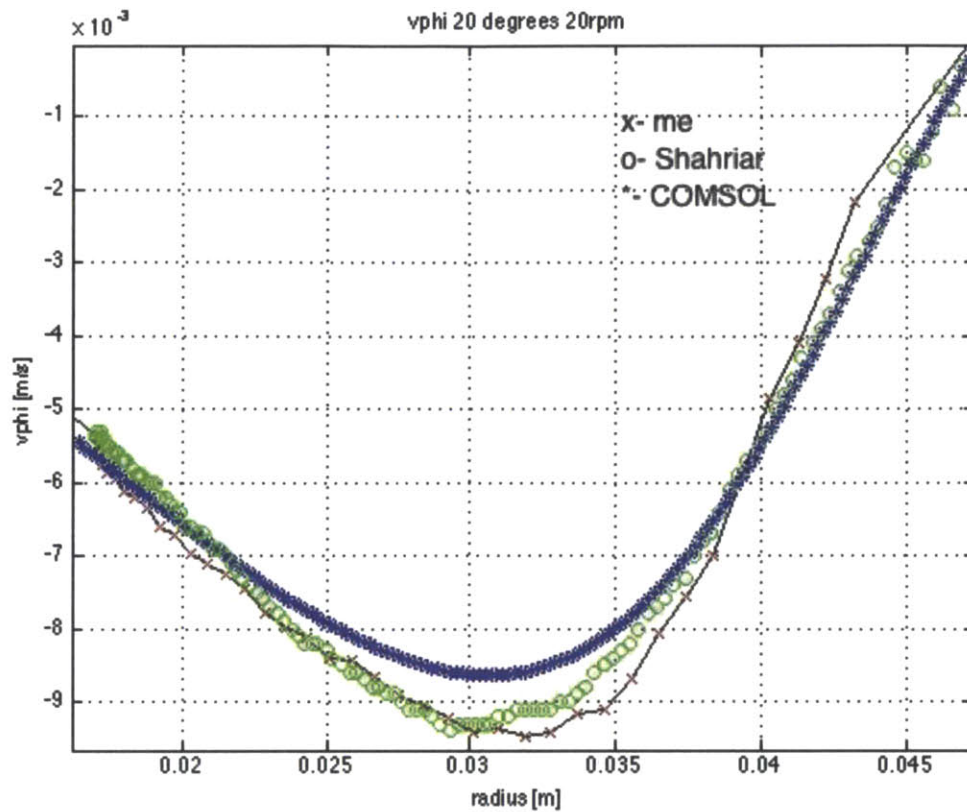
Figure 3.2: Rotational velocity Vφ as a function of radius measured at the equator of the 3/4 sphere of radius 5cm, with the Viscometer LV-1 spindle rotating the circular disk at 20 RPM. Experimental results match those previously obtained by Khushrushahi and COMSOL simulations [2].
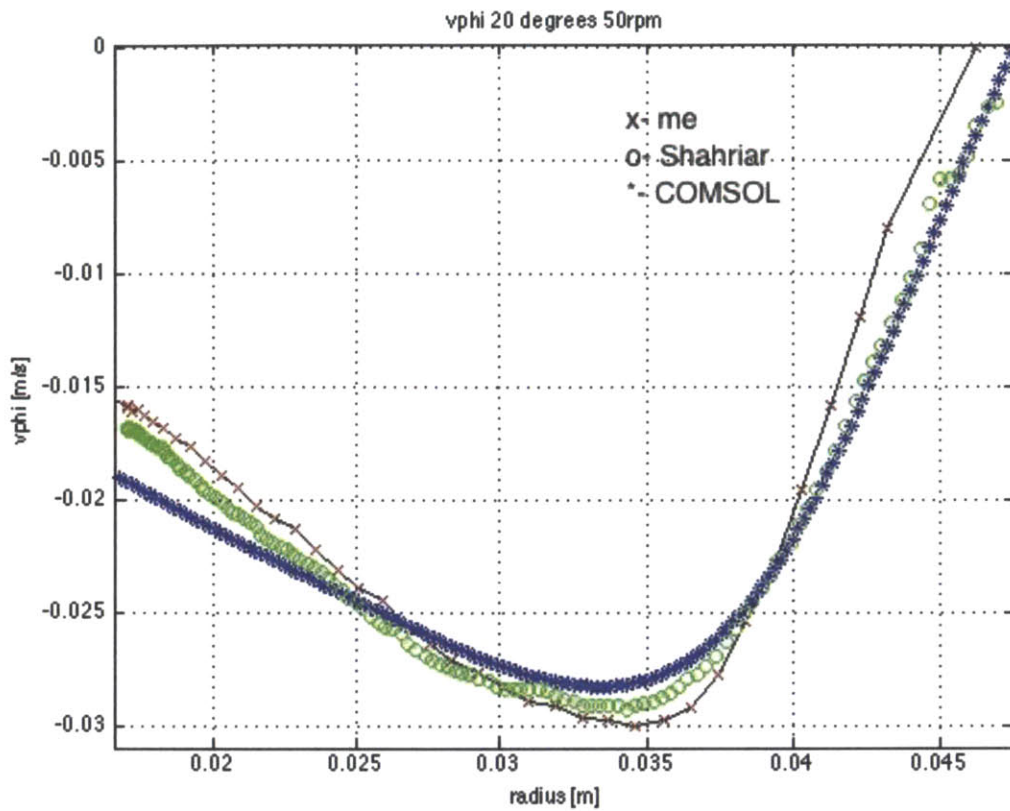
Figure 3.3: Rotational velocity Vφ as a function of radius measured at the equator of the 3/4 sphere of radius 5cm, with the Viscometer LV-1 spindle rotating the circular disk at 50 RPM. Experimental results match those previously obtained by Khushrushahi and COMSOL simulations [2].
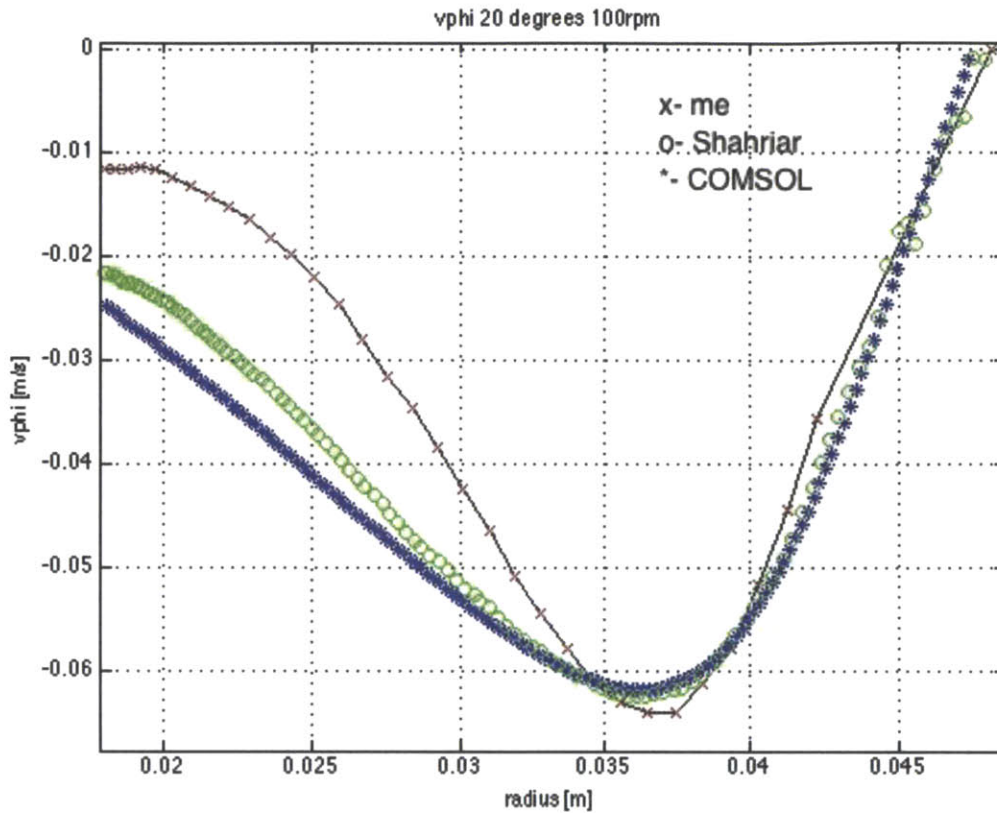
Figure 3.4: Rotational velocity Vφ as a function of radius measured at the equator of the 3/4 sphere of radius 5cm, with the Viscometer LV-1 spindle rotating the circular disk at 100 RPM. Experimental results match those previously obtained by Khushrushahi and COMSOL simulations [2].

### 3.1.2 Mix Ferrofluid in Storage Vessel

The GrillTex-P1 particles suspended in the ferrofluid will tend to settle to the bottom of its storage vessel with time. This decreases the accuracy of the velocimetry measurements, because the particles must be distributed evenly throughout the fluid for best results. Therefore, before taking any data, the storage vessel of ferrofluid should be thoroughly mixed. An orbital shaker is the best device for this purpose; anywhere from 15-20 minutes allows for sufficient mixing of the GrillTex-P1 particles. The ferrofluid storage vessel should be firmly affixed to the orbital shaker. It takes anywhere from an hour to 90 minutes for the particles to once again settle at the bottom of the container, so if data taking extends longer than this time period, re-mixing might be necessary.

### 3.1.3 Fill Spherical Container

Filling the containers is a mostly straightforward exercise; however, care must be taken to ensure that there are no air bubbles trapped within. Air bubbles can interfere with the velocimetry measurements, having an effect similar to a "wall" inside the container. To avoid this, the containers have a circular well on top, with two holes for plastic screws that can be removed, as shown in Figure 3.5.

The ferrofluid should be poured directly into the well; optionally, a squirt bottle can be used for this purpose. Once the well is filled, hold the sphere with both hands and rock it slowly back and forth in an orbital pattern. If a bubble pops out of the ferrofluid filling the well, it indicates that air has escaped from the container. If the level of the ferrofluid in the well becomes too low, simply refill the well and

continue rocking the container until no more air bubbles escape. Repeat as necessary until the container is sufficiently filled. After the container is filled and no air bubbles remain, cap the container securely with the screws. The ferrofluid-filled container is now ready to be used for data taking.
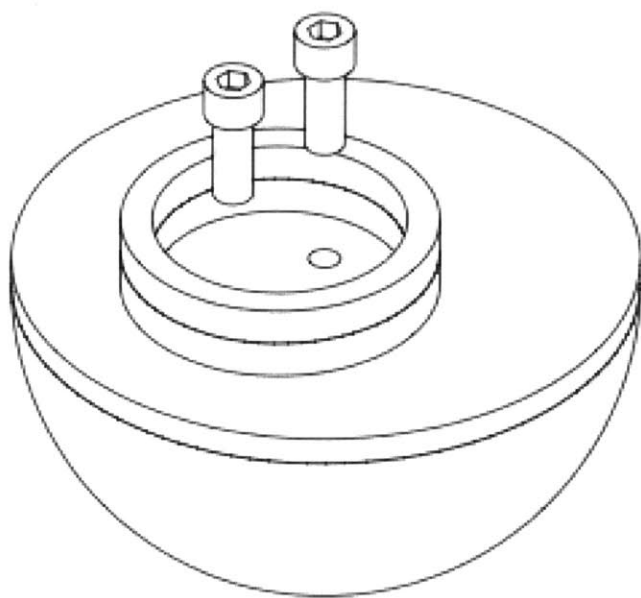


Figure 3.5: Diagram of a truncated spherical container, with the well and screw holes on top clearly visible.

### 3.1.4 Disassemble Fluxball and Insert Container

The outer halves of the fluxball have been mounted on wheels and installed on a wooden track, to assist in alignment and assembly. The wooden track is attached to a standard car jack, which can elevate it to a height of approximately 20 degrees.

If the outer halves of the fluxball are not already separated, elevate the wooden track, disconnect the winding connections between the two halves of the outer fluxball, and pull the two halves apart, sliding one half to the other end of the wooden track. Temporarily affix this half in place with a metal rod or a large screwdriver—there are holes drilled in the track for this very purpose.

Then, remove the inner fluxball sphere, making sure to disconnect the windings that attach it to the outer halves, and set it upright on the table. Disconnect the windings between the top and bottom halves of the inner sphere and remove the top. The fluxball is now fully disassembled and ready for the ferrofluid container to be placed inside.

Firmly press the ferrofluid container into the probe holder; it should be a secure and snug fit. Then, affix the bottom of the probe holder to the rod inside the bottom half of the inner sphere. The probe holder should be secure and stationary inside the sphere.

### 3.1.5 Apply Ultrasound Gel and Insert Ultrasound Probes

The ultrasound probes are now ready to be affixed to their respective positions within the probe holder. The DOP-2000 is able to have up to four probes taking measurements simultaneously. Before the probes are placed into the probe holder, ultrasound gel should be liberally applied into the probe slots and on the tips of the

ultrasound probes themselves. This ultrasound gel is critical to achieve a good sonic connection and reliable data, and if in doubt, it is better to apply more than necessary rather than less.

After the ultrasound gel has been applied, insert the probes into the appropriate probe slots, making sure they fit snugly and securely, and that they won't be jostled around when the fluxball is reassembled. If necessary, the probes can be held even more securely in place against the probe holder with some electrical tape. The fluxball is now ready for reassembly.

### 3.1.6 Reassemble Fluxball

The fluxball is now ready for reassembly. Replace the top half of the inner sphere and reconnect the windings. Place the inner sphere back inside the first outer half and reconnect those windings; finally, remove the medal rod and slide the two outer halves together, reconnect the outer windings, and release the jack to lower the elevation of the wooden track back to level.

At this point, the series capacitors should be hooked up in accordance with section 2.4.1, depending if data is to be taken at 47 Hz or 95 Hz. In between data taking sessions, these capacitors can be swapped out as necessary.

### 3.1.7 Configure LabVIEW settings

Table 3.1 below shows the configuration the LabVIEW software should be set to for all experiments. Parameters with multiple values indicate that separate trials should be performed for each one of the values. All other fields not listen in Table 3.1 can be left at their default values.

| PARAMETER | VALUE(s) |
|---|---|
| Vinner Phase wrt Vouter | +90, -90 |
| Inner fluxball | Off |
| Outer fluxball | Off |
| Same Current Inner and Outer | On |
| Inner fluxball Set Point Current (RMS) | 0, 1, 2 |
| Outer fluxball RMS Current | 0 |
| Fluxball Frequency (Hz) | 47, 95 |
| Third Coil set point current (RMS/DC) | 0 |

Table 3.1: Configuration settings for the LabVIEW software

It should be noted that the LabVIEW software should not actually be run (the "play" button should not be pressed) until the power supply has been turned on, as discussed in the next section.

### 3.1.8 Turn on Power Supply

After the LabVIEW software is configured, all fluxball and capacitor connections should be checked to make sure they're secure, and then the power supply should be turned on. It is important to turn on the power supply before the LabVIEW software is actually run; failing to do so can create an undesirable feedback loop where zero current is fed back into the software, causing the PID feedback controller to continually ramp up the current value so that a huge and potentially damaging amount of current is produced when the power supply is actually turned

on. Once the power supply is turned on and the LabVIEW program is running,

measurements can be taken.

### 3.1.9 DOP-2000 Settings for Data Taking

Table 3.2 below summarizes the "suggested" initial settings of the DOP-2000 for

measurement taking.  These settings should be viewed as a starting point rather

than as an absolute guideline; during individual trials, the settings should be tuned

as needed to get the best possible data.

| PARAMETER | VALUE(s) |
| :---: | :---: |
| PRF | 100-200 Hz |
| Emitting Frequency | 4 MHz |
| Power Level | High |
| Burst Length | 8 cycles |
| Resolution | 0.56 mm |
| Sensitivity | Very high |
| Time Gain Control (TGC) | Slope, 31 dB – 61 dB |
| Starting Depth | 10 mm |
| Number of Gates | 200 |
| Number of Profiles | 32 |
| Emissions/Profile | 128 |

Table 3.2: Suggested values for initial DOP-2000 Velocimeter settings in spherical

geometry

## 3.2 Cylindrical Geometry

Much of the procedure for the cylindrical geometry is identical to that of the spherical geometry; consequently, only those steps that differ from the above procedure significantly are expounded upon in detail.

### 3.2.1 Mix Ferrofluid in Storage Vessel

The Cylindrical containers constructed by Schoen that were used in this thesis were previously filled with ferrofluid during the course of Schoen's own experiments, so there was no separate storage vessel where the ferrofluid is held. The cylindrical containers should be directly affixed to the orbital shaker, and thoroughly mixed for 15-20 minutes.

### 3.2.2 Disassemble Fluxball and Insert Container

Disassemble the fluxball, following the procedure as outlined in section 3.1.4. The cylindrical container should be inserted into the container fixture, and then the fixture placed into the bottom half of the inner fluxball as shown in figure 3.2 below.

### 3.2.3 Apply Ultrasound Gel and Insert Ultrasound Probes

Following the procedure as outlined in section 3.1.5, apply liberal amounts of ultrasound gel to the probe slots of the container and the probes themselves, and insert the probes, making sure to create good sonic contact.

### 3.2.4 Reassemble Fluxball

Following the procedure as outlined in section 3.1.6, reassemble the fluxball with the ultrasound probes now in place.
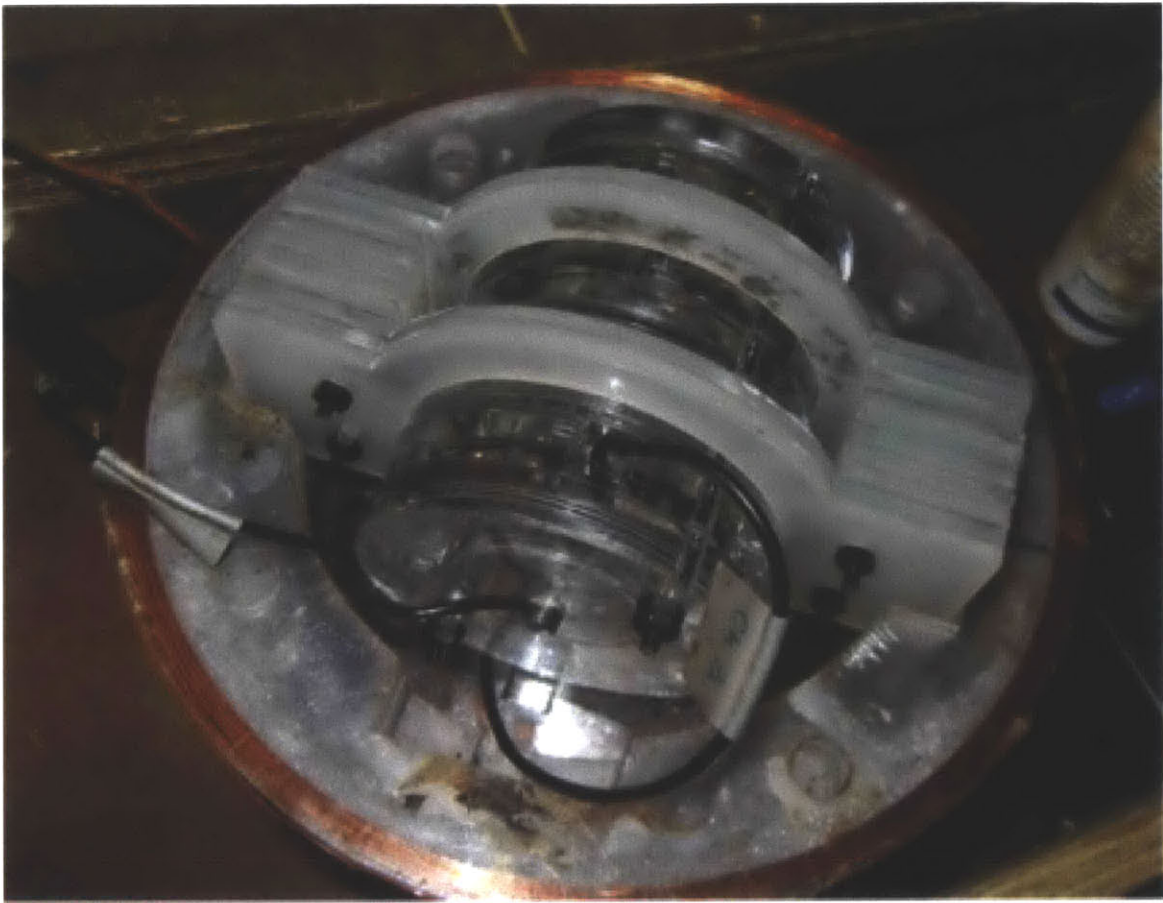
Figure 3.6: Cylinder with fixture placed inside the bottom half of the fluxball

### 3.2.5 Configure LabVIEW settings

The LabVIEW settings should be configured as outlined in Table 3.1, in section 3.1.7 above. Again, the LabVIEW software should not actually be run (the "play" button should not be pressed) until the power supply is turned on, to avoid damaging currents.

### 3.2.6 Turn on Power Supply

After the LabVIEW settings are configured, double-check all connections, and turn on the power supply. Measurements are now ready to be taken.

### 3.2.7 DOP-2000 Settings for Data Taking

Table 3.3 below summarizes the "suggested" initial settings of the DOP-2000 for measurement taking in the cylindrical geometry. Again, these settings should be seen as a starting point, rather than specific values. The parameters should be tuned as needed to obtain the best results.

| PARAMETER | VALUE(s) |
| --- | --- |
| PRF | 100-200 Hz |
| Emitting Frequency | 4 MHz |
| Power Level | High |
| Burst Length | 8 cycles |
| Resolution | 0.56 mm |
| Sensitivity | Very high |
| Time Gain Control (TGC) | Slope, 31 dB – 61 dB |
| Starting Depth | 10 mm |
| Number of Gates | 200 |
| Number of Profiles | 32 |
| Emissions/Profile | 128 |

Table 3.3: Suggested values for initial DOP-2000 Velocimeter settings in cylindrical

geometry

# CHAPTER 4

# RESULTS IN SPHERICAL GEOMETRY

## 4.1 Measurements Taken

All measurements in this chapter were taken with the fluxball in the horizontal orientation. Beyond that, there were four independent parameters that could be varied between sessions of data taking: magnetic field strength, frequency, phase offset (outer coil with respect to inner coil), and container volume (percentage of a full sphere). Measurements were taken for all possible combinations of these parameters, and any potential trends in the data were identified. Table 4.1 below summarizes the complete extent of the measurements taken for this experiment.

| PARAMETER | POSSIBLE VALUES |
|---|---|
| Magnetic Field Strength | 50.6 Gauss; 101.2 Gauss |
| Frequency of AC Field | 47 Hz; 95 Hz |
| Phase Offset (outer coil w.r.t. inner coil) | +90 degrees; -90 degrees |
| Container Volume (% of a full sphere) | 100; 90; 80; 70; 30; 10 |

Table 4.1: A summary of the measurements taken for this experiment

## 4.2 Reading Results

All of the results in this chapter are presented in graphical form, with distance from the ultrasound probe (m) along the x-axis, and flow velocity (m/s) along the y-axis.

A positive flow velocity indicates movement away from the probe, while a negative flow velocity indicates movement towards the probe. Measurements were taken at five designated "channels" which correspond to five different positions on the probe holder. The channels and their positions are shown in figures 4.1 and 4.2 below.
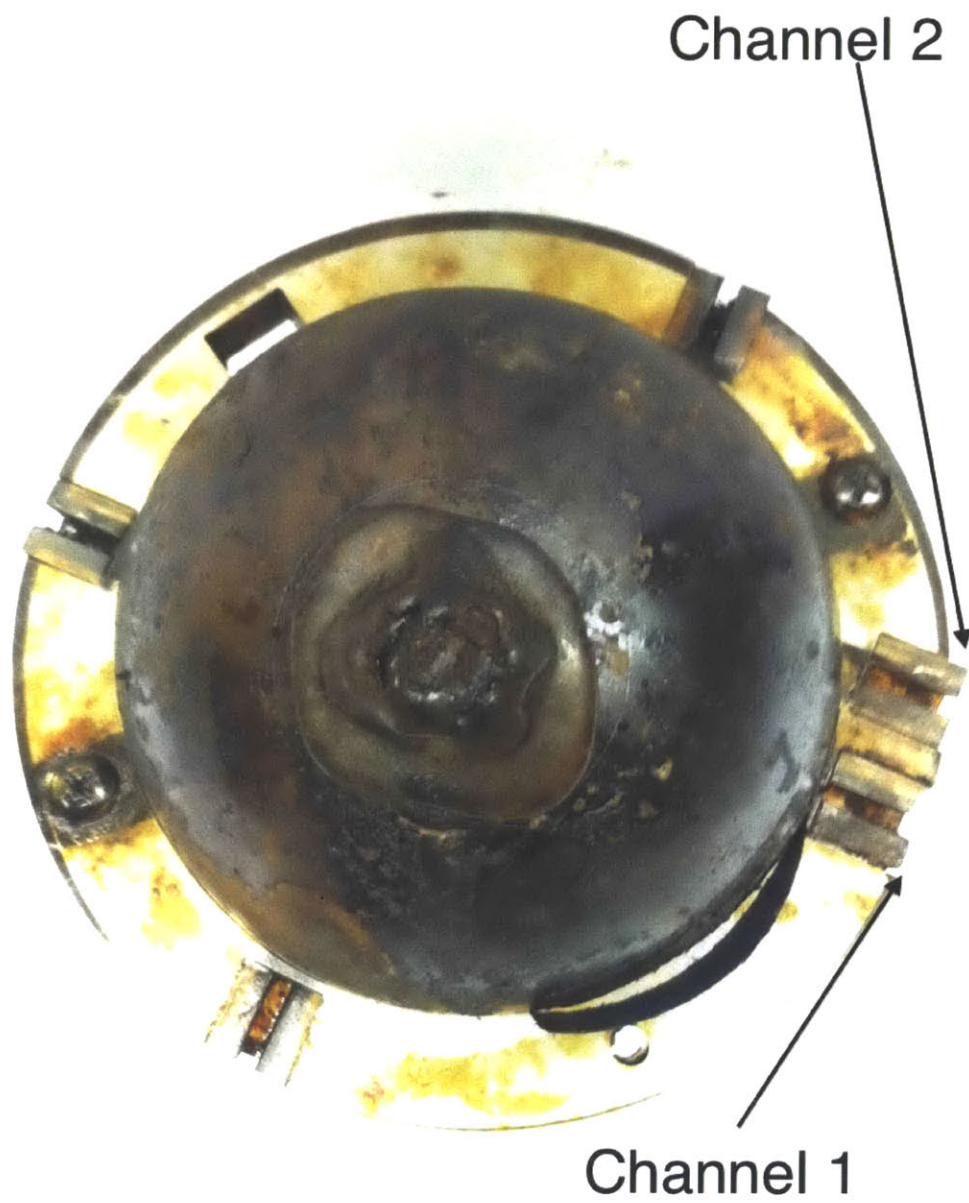
Figure 4.1: Positions of channels 1 and 2 on the probe holder. Channel 1 is centered along the diameter of the sphere.
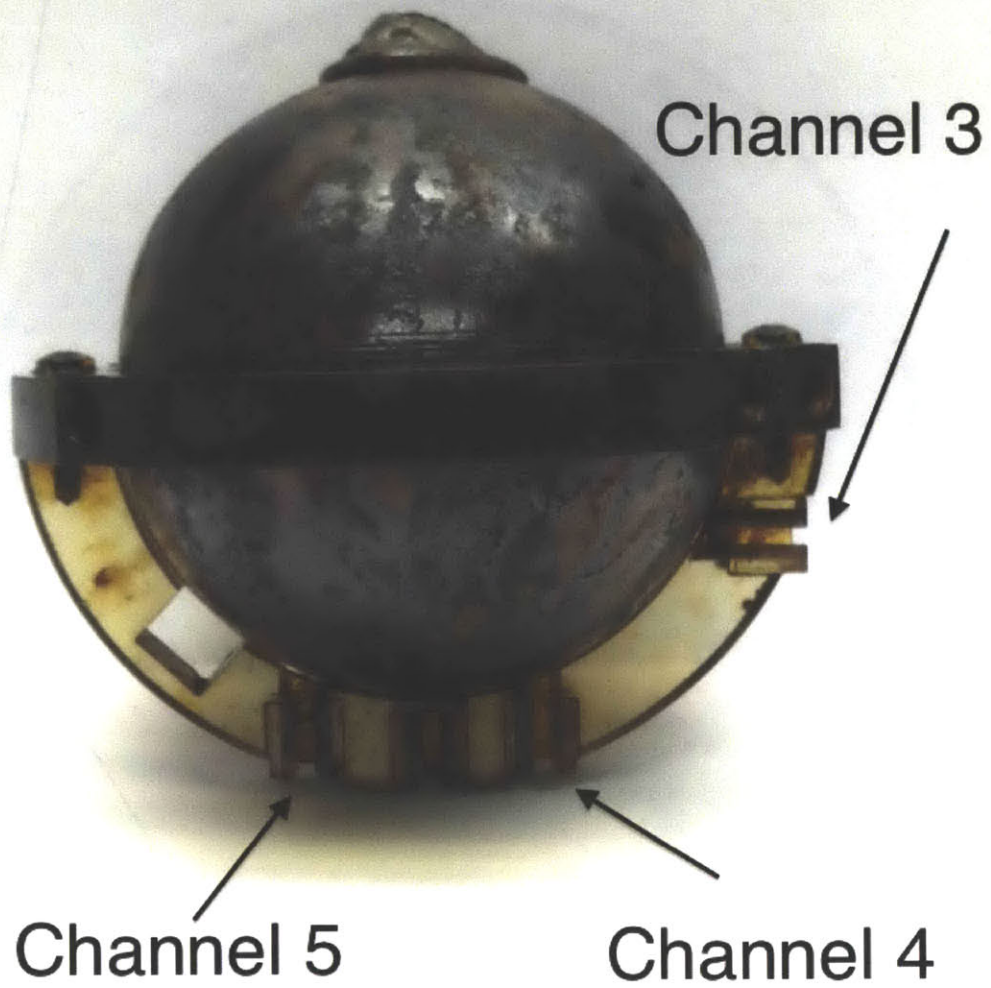
Figure 4.2: Positions of channels 3, 4 and 5 on the sphere. Probe slots for channels 1 and 2 are also visible above channel 3.

## 4.3 Results

This section discusses and presents graphs that are best illustrative of the trends found from the results of the experiment. A complete set of graphs for every channel and trial, including those in this chapter, can be found in Appendix A.

### 4.3.1 Complete Sphere (100% Volume)

As a starting point, measurements were taken on a complete ferrofluid-filled sphere. For each trial, the first measurement taken was a baseline measurement, which was a measurement with zero applied magnetic field. The baseline measurement served as a comparison point for the subsequent measurements with nonzero applied field. Generally, it was found that the flow did not deviate from the baseline significantly, and when it did, it had an extremely small flow velocity that could safely be considered negligible.

Figure 4.3 illustrates this trend. It contains two velocity profiles from channel 1 graphed on top of each other for comparison: a baseline (zero applied field) measurement and a measurement with an applied field of 50.6 Gauss. The frequency was set to 95 Hz and the phase offset at -90 degrees.

Inspecting figure 4.3, there are two preliminary things to note. First, the sharp "jumps" in the applied field measurement for x < 0.005 m. This is not representative of actual flow, but rather a signal processing error that was consistent across all trials. A likely cause of this feature was the fact that the "wall" of the container has a finite thickness, which affected the signal processing in this small region. Consequently, this feature has no real significance, and was not taken into account when interpreting the results.

61

Second, the apparent "jump" in both the baseline and applied-field profiles at around $x = .06$ m.  This also is not likely an indication of actual flow, because it is present even with zero applied field.  Rather, it is another signal processing error, which may have been caused by an "air bubble" that was present in the container, despite efforts to avoid such.  Regardless, it is still possible to make conclusions about flow in this region, as deviation from the baseline is what indicates actual flow, rather than the absolute value of the measurement.  Consequently, this feature also has no real significance.
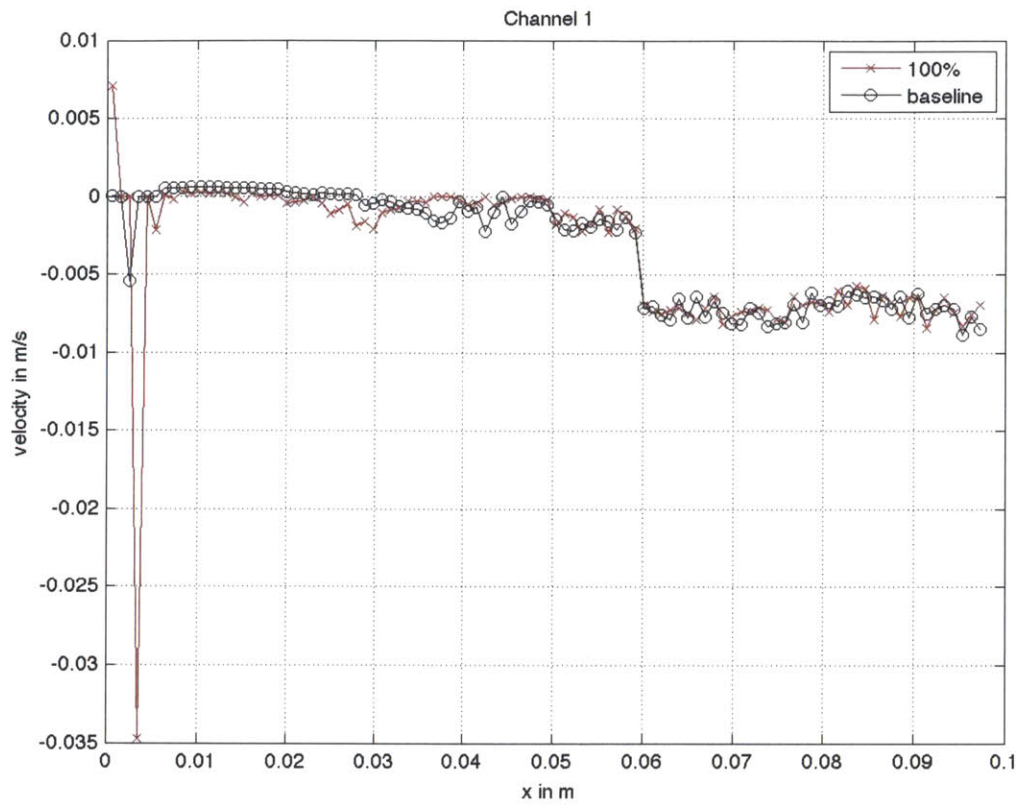
Figure 4.3: 100% Volume. A baseline velocity profile, which is a velocity profile with

zero applied magnetic field, is compared against a velocity profile with an applied

field of 50.6 Gauss, at 95 Hz, with a phase offset of -90 degrees.

It is clear from figure 4.3 that the velocity profile with the applied field does not deviate significantly from the baseline velocity profile. The largest deviances are on the order of .001 m/s, completely negligible values compared to the magnitudes of flow that were established in subsequent trials with truncated spherical containers. This is consistent with the prediction that a complete ferrofluid-filled sphere should have negligible flow established in the presence of a uniform rotating magnetic field.

**4.3.2 Truncated Spheres (90%, 80%, 70%, 30%, 10% Volumes)**

Measurements were also taken for truncated spheres varying between 90% and 10% volume of the full sphere. Generally, the trend was that the flows established in these trails were non-negligible and often had significant deviances from the baseline, in contrast to the trials for the full sphere. It should be noted that the container of 10% volume presented a specific difficulty: because the container was so small, and the "far" wall was so close to the "near" wall and the probe itself, it was difficult to obtain meaningful velocity profiles. Signal processing interference similar to that found in the first 0.005 m of the other graphs dominated the entire profile, rendering it impossible for meaningful conclusions to be drawn. The profiles for the 10% volume container are still presented in appendix A for completeness.

Figures 4.4-4.7 below show examples illustrating the trend. Again, baseline velocity profiles are plotted against velocity profiles, this time with a field strength of 101.2 Gauss. A stark contrast can be seen in these graphs compared to the graph of figure 4.3. The applied field profile has a significantly different shape and much

greater magnitude than the baseline profile. This is consistent with the prediction that demagnetizing factors drive bulk flows in ferrofluid-filled containers in the presence of a uniform rotating magnetic field.
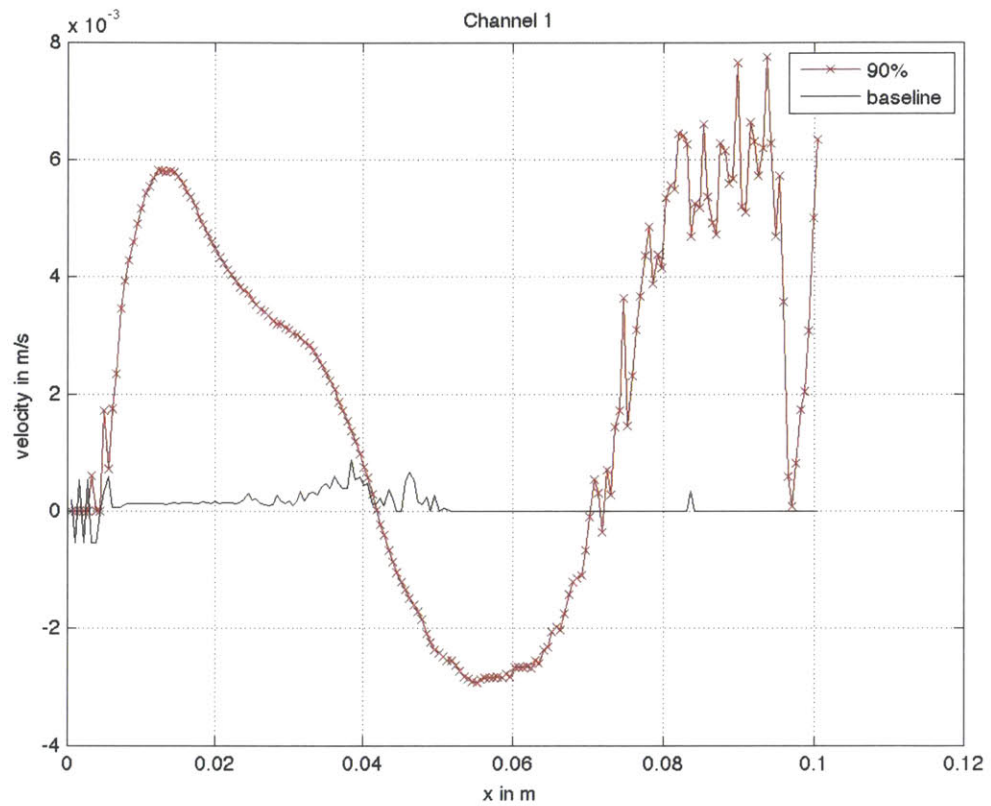


Figure 4.4: 90% Volume. Baseline velocity profile compared against a velocity profile for an applied field of 101.2 Gauss, at 95 Hz, with a phase offset of -90 degrees.
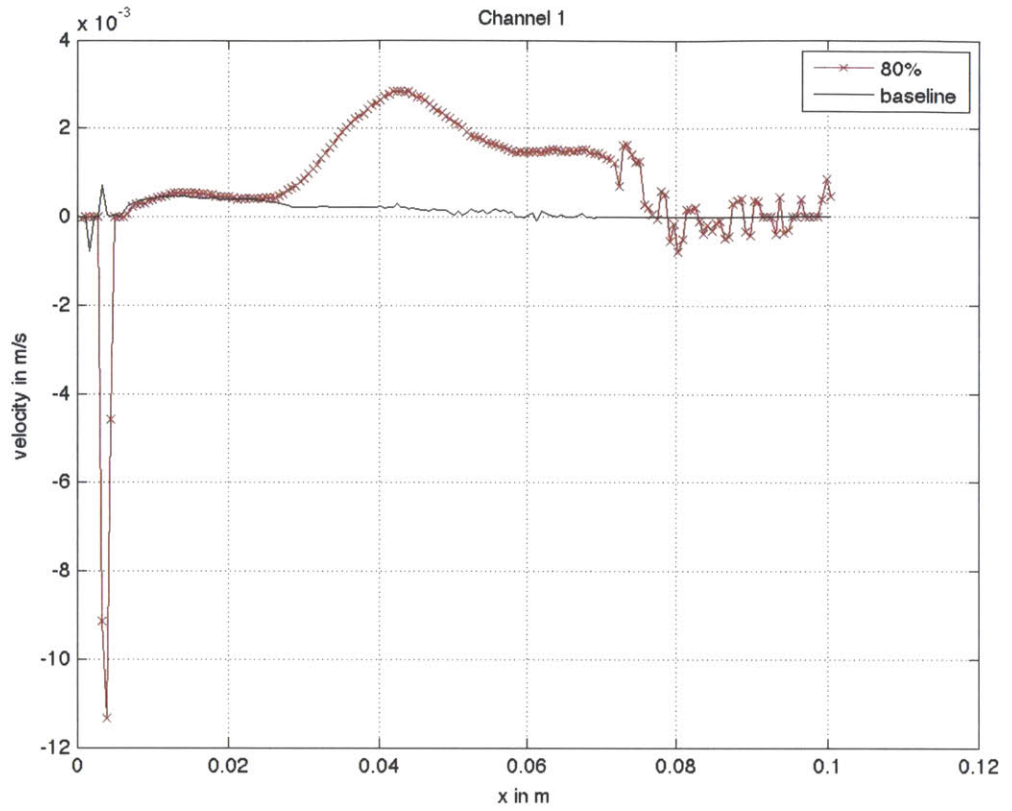
Figure 4.5: 80% Volume. Baseline velocity profile compared against a velocity profile for an applied field of 101.2 Gauss, at 95 Hz, with a phase offset of -90 degrees.
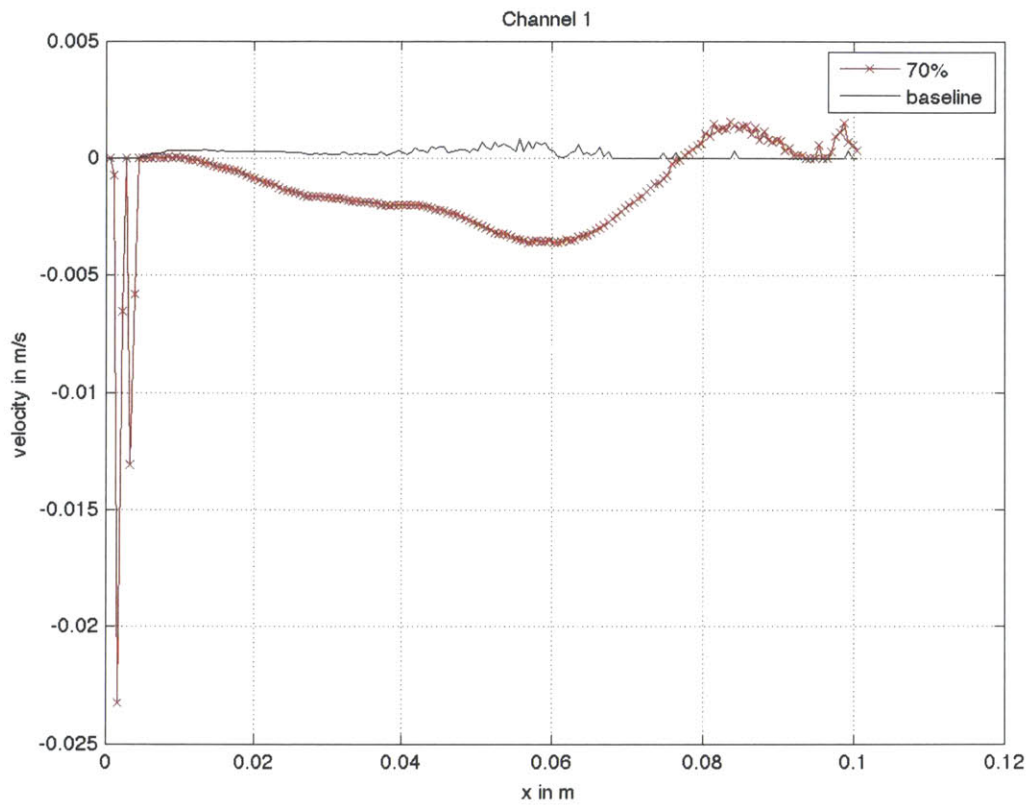
Figure 4.6: 70% Volume. Baseline velocity profile compared against a velocity profile for an applied field of 101.2 Gauss, at 95 Hz, with a phase offset of -90 degrees.
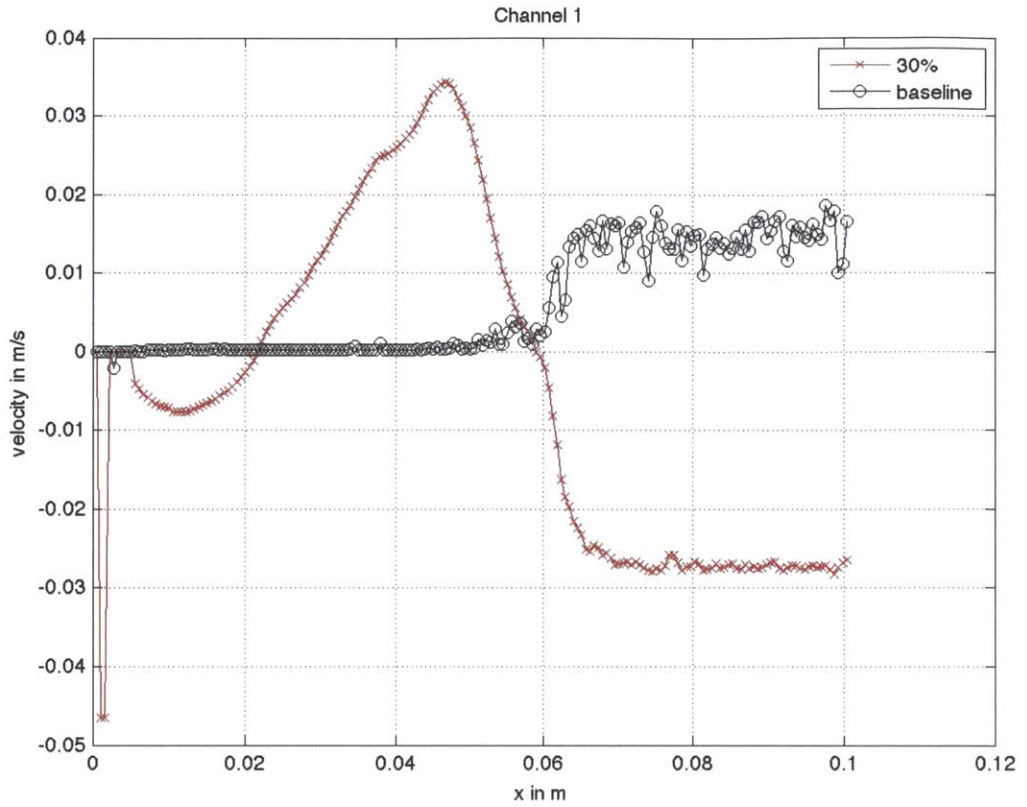
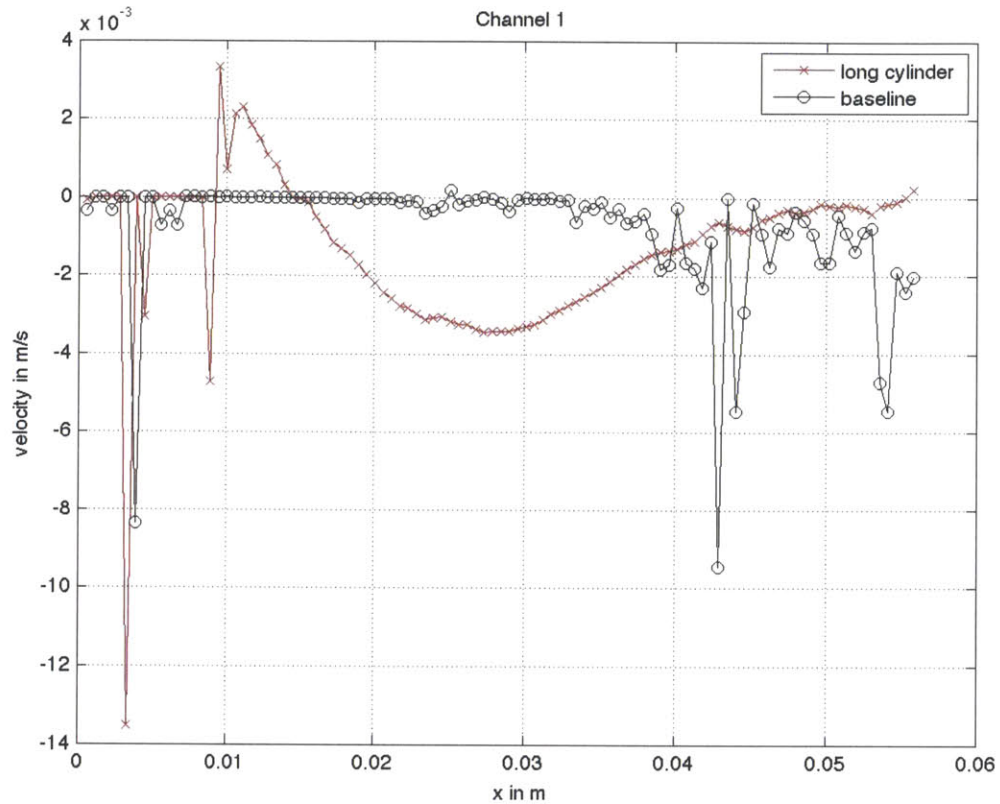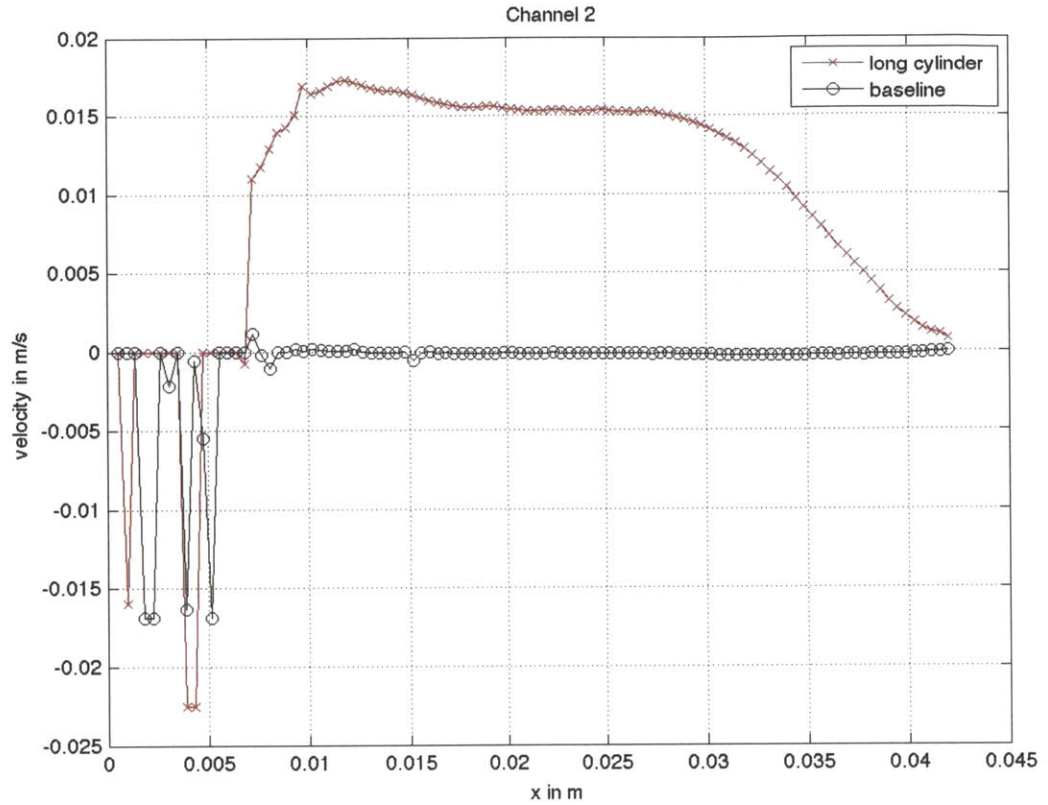Figure 4.7: 30% Volume. Baseline velocity profile compared against a velocity profile for an applied field of 101.2 Gauss, at 95 Hz, with a phase offset of +90 degrees. Note that the diameter of the 30% container is slightly less than 6 cm; consequently, velocity data for x > 6 cm is not meaningful, because it is measuring space outside of the ferrofluid container.

## 4.4 Results Interpretation

From the above graphs and discussion, it is clear that there is a significant contrast between the bulk flows driven in a full sphere and the flows driven in truncated spheres of various volumes. Negligible bulk flow is observed in the case of a full sphere, while significant bulk flow is observed in the case of the truncated spheres.

An attempt was made to find further trends in the velocity profiles as the truncated spheres decreased in volume from 90% to 10%; unfortunately, none were readily apparent. The flows that were established in these truncated containers were generally quite complex, and no discernable pattern in magnitude or profile shape was observed between containers. Therefore, the only fact that can be readily concluded is that demagnetizing factors do appear to be the main driving force behind bulk flow in spherical ferrofluid-filled containers, when placed in a uniform rotating magnetic field.

# CHAPTER 5

# RESULTS IN CYLINDRICAL GEOMETRY

## 5.1 Measurements Taken

All measurements in this chapter were taken with the fluxball in the vertical

orientation. There were four independent parameters that could be varied between

sessions of data taking: magnetic field strength, magnetic field frequency, phase

offset (outer coil with respect to inner coil), and container length (long or short).

Measurements were taken for all possible combinations of these parameters, and

any potential trends in the data were identified. Table 5.1 summarizes the complete

extent of the measurements taken for this experiment. Table 5.2 specifies exact

dimensions and other key details for both the short and long cylindrical containers.

| PARAMETER | POSSIBLE VALUES |
|---|---|
| Magnetic Field Strength | 50.6 Gauss; 101.2 Gauss |
| Frequency of AC Field | 47 Hz; 95 Hz |
| Phase Offset (outer coil w.r.t. inner coil) | +90 degrees; -90 degrees |
| Container Length | Short (1 disc); Long (7 discs) |

Table 5.1: A summary of the measurements taken for this experiment

| PARAMETER | SHORT CYLINDER | LONG CYLINDER |
| --- | --- | --- |
| Diameter | 4 cm | 4 cm |
| Height of Individual Disc | 1.27 cm | 1.27 cm |
| Total Number of Discs | 1 | 7 |
| Aspect Ratio (Height/Diameter) | 0.3175 | 2.2225 |

Table 5.2: Dimensions for both the short and long cylindrical container, each composed of Acrylic discs stacked upon one another.

## 5.2 Reading Results

All of the results in this chapter are presented in graphical form, in Figures 5.5-5.7. On these graphs, the x-axis represents distance from the ultrasound probe (m), and the y-axis measures flow velocity (m/s). A positive flow velocity indicates movement away from the probe, while a negative flow velocity indicates movement towards the probe.

The cylindrical containers themselves were constructed so that there were multiple potential slots for probes along each disc; consequently, in contrast with the spherical probe holder, there were no designated positions that corresponded to specific channels on the velocimeter. Instead, probes were placed at three general "regions:" for both the short and long cylinders, measurements were taken at the "center" region, aligned with the cylinder diameter, and along the "z-axis," or the long axis of the cylinder. The coordinate system of the container and the associated

71

regions are defined in Figures 5.1 and 5.2. For the long cylinder, additional measurements were taken at the "top" and "bottom" regions, which are defined in Figure 5.3. Note that the distinction between "top" and "bottom" is completely arbitrary, due to the symmetry of the container.
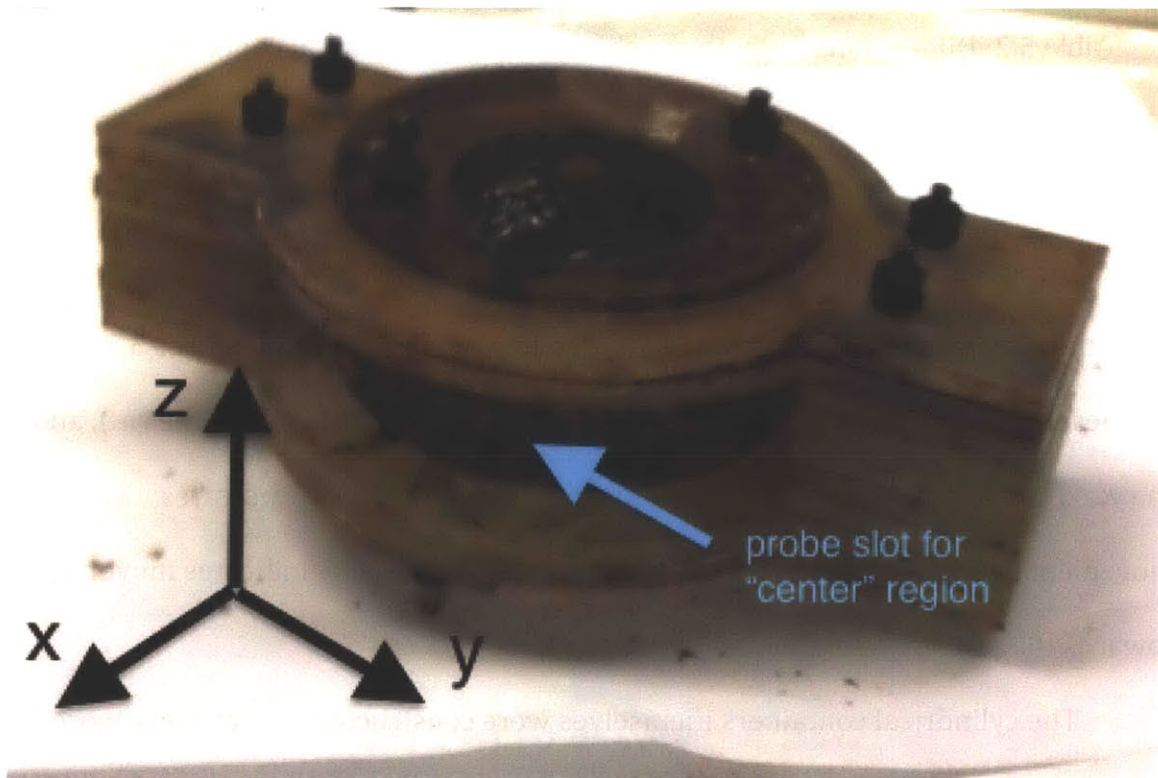


Figure 5.1: Short cylinder, three-quarters view, with conventions for the x, y, and z-axes defined. The location of the "center" region is also indicated.
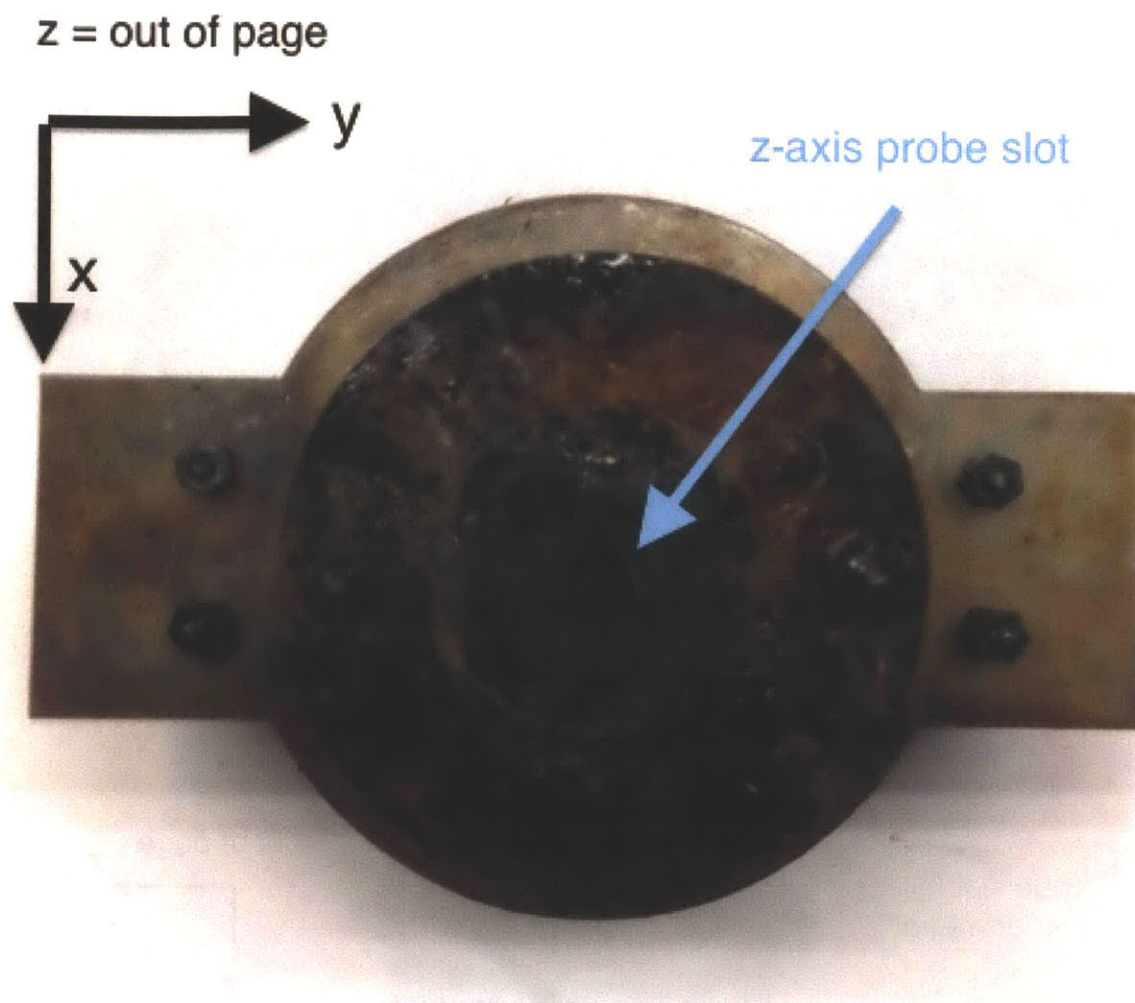
Figure 5.2: Short cylinder, top view, with the slot for the z-axis probe clearly visible.
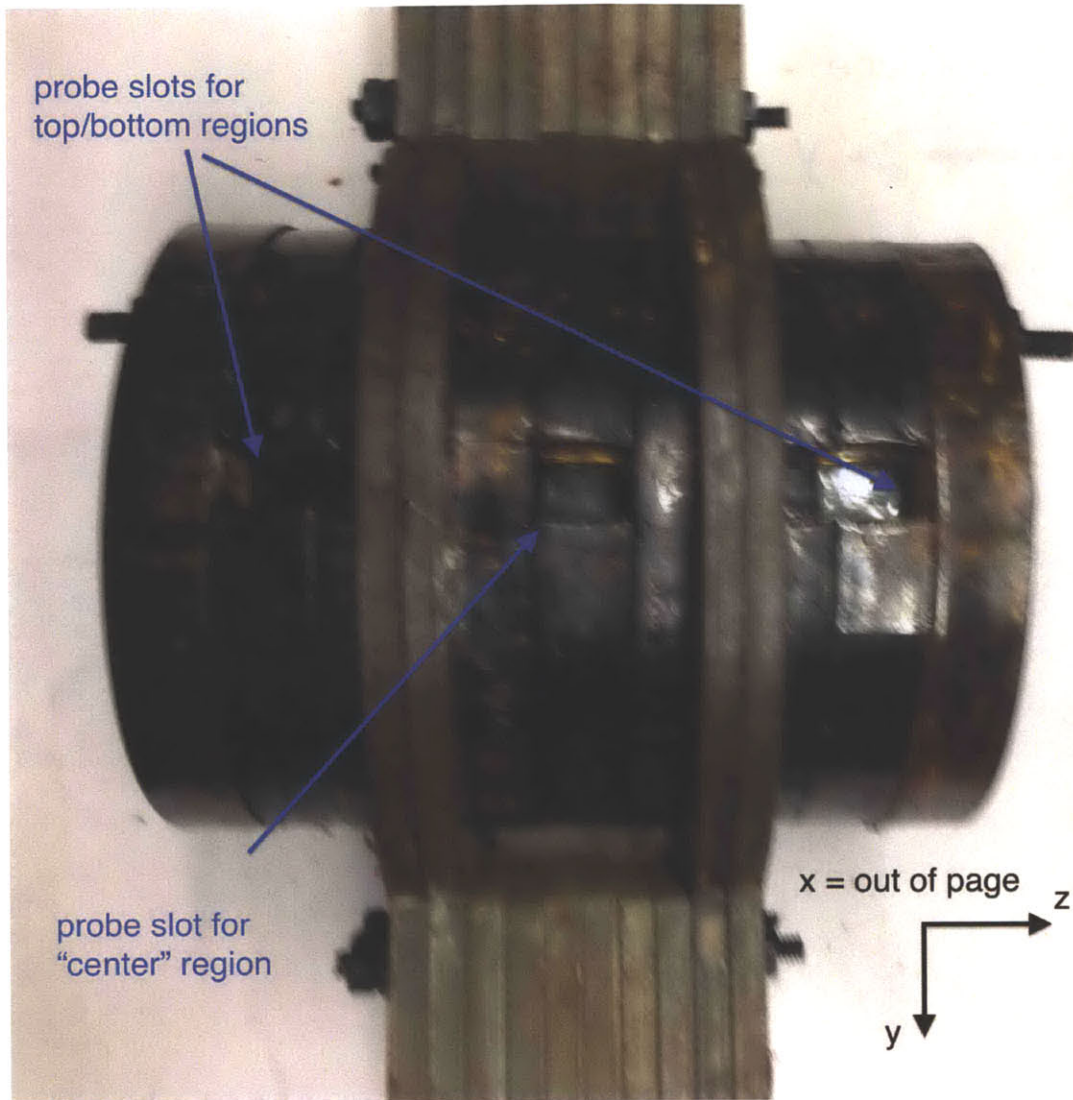
Figure 5.3: Long cylinder, side view. "Center", "Top" and "Bottom" regions are indicated.
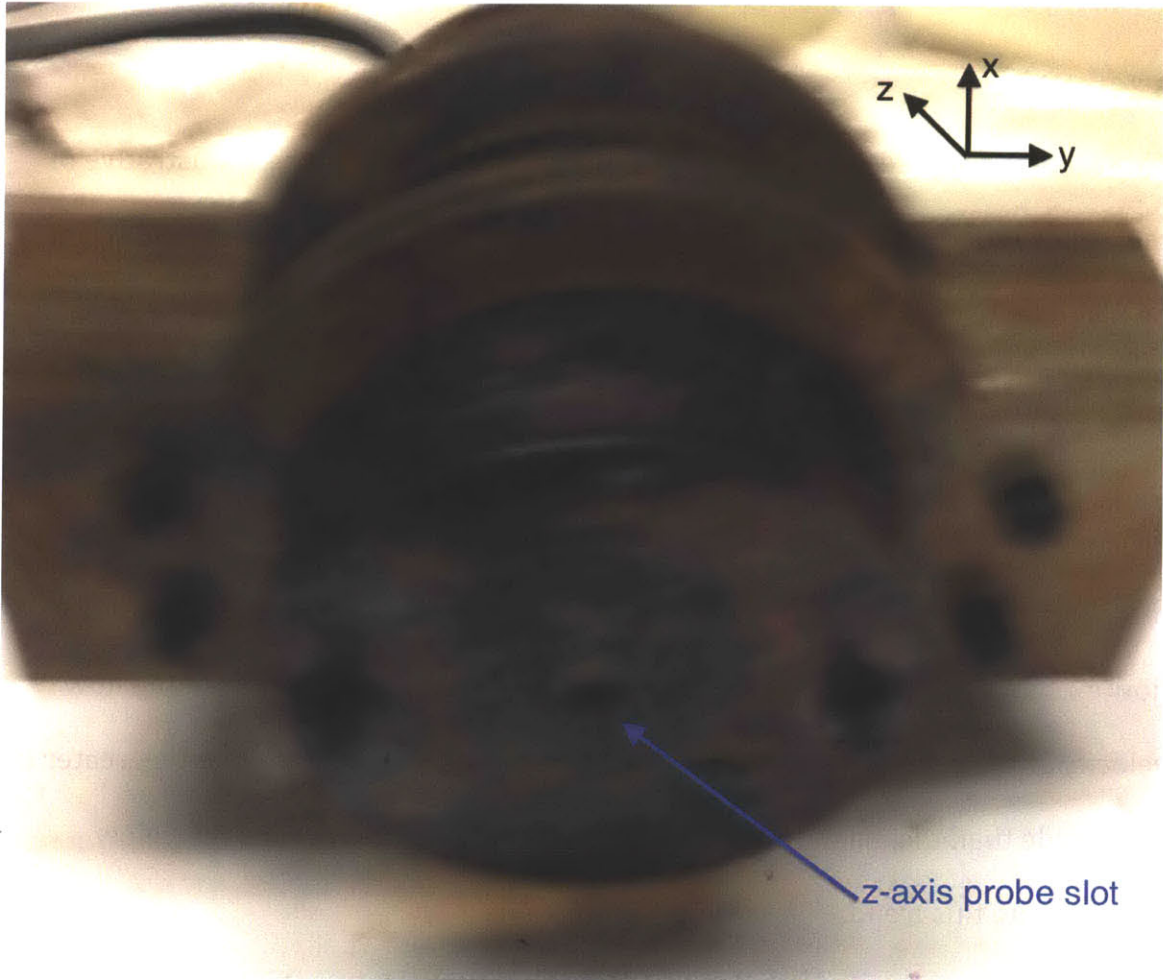
Figure 5.4: Long cylinder, three-quarters view, with the slot for the z-axis probe clearly visible.

## 5.3 Results

This section discusses and presents results and graphs that are best illustrative of the trends found from the results of the experiment. A complete set of graphs can be found in Appendix A.

### 5.3.1 Long Cylinder

Measurements were first taken on the long cylinder. For each trial, a baseline measurement with zero applied magnetic field was taken, followed by the measurements with nonzero applied field. It was found that non-negligible bulk flow existed in each region of the container. However, the magnitude of the flow velocity at the edge of the container (top/bottom region) was consistently greater in magnitude than the magnitude at the center region. Figures 5.5 and 5.6 below demonstrate this trend.

This is consistent with the idea of demagnetizing factors being the primary cause of bulk flow. According to theory, an infinitely long cylindrical container should have a negligible amount of bulk flow, because there are no demagnetizing factors to disturb the uniform external field. For a finite-length cylinder with a large aspect ratio, the region that most closely approximates the behavior of the infinite-length case is the center region. Conversely, the regions that should differ the most from the behavior of the infinite-length case are the top and bottom regions. Even though the flow velocity was non-negligible in the center region, the fact that it was consistently of a lesser magnitude than on the bottom and top regions supports the idea that demagnetizing factors were the primary cause of bulk flow.

Figure 5.5: Long cylinder, center region. Baseline velocity profile compared against a velocity profile for an applied field of 101.2 Gauss, at 95 Hz, with a phase offset of +90 degrees. Peak magnitude of flow velocity is ~3.5 mm/s. This is significantly less than the peak magnitude in the bottom region (Figure 5.6). This indicates that the demagnetizing factors of the long cylinder do not significantly disturb the uniformity of the external magnetic field in the center region. Note the "noise" present in the data for x < 0.6 cm: again, this is a signal processing error due to the finite thickness of the container wall.

Figure 5.6: Long cylinder, bottom region. Baseline velocity profile compared against a velocity profile for an applied field of 101.2 Gauss, at 95 Hz, with a phase offset of +90 degrees. Peak magnitude of flow velocity is ~ 17 mm/s, somewhat greater than that of the center region. In the top and bottom regions, the finite length of the cylinder contributes towards non-uniformities in the magnetic field, which drive the increased magnitude of bulk flow. If the cylinder were of infinite length, these non-uniformities would not exist.

### 5.3.2 Short Cylinder

Measurements were then taken on the short cylinder, and compared to the measurements of the long cylinder. It was found that the center region of the short cylinder contained bulk flow of significant magnitude, comparable to that of the bottom region of the long cylinder. The flow in the center region of the short cylinder was much greater in magnitude than the flow in the center region of the long cylinder. According to the theory, a finite-length cylinder with a small aspect ratio should indeed have significant bulk flow driven when placed in a uniform rotating magnetic field. Thus, the findings were also consistent with the idea of demagnetizing factors being the main cause of bulk flow. Figure 5.7 demonstrates this finding.
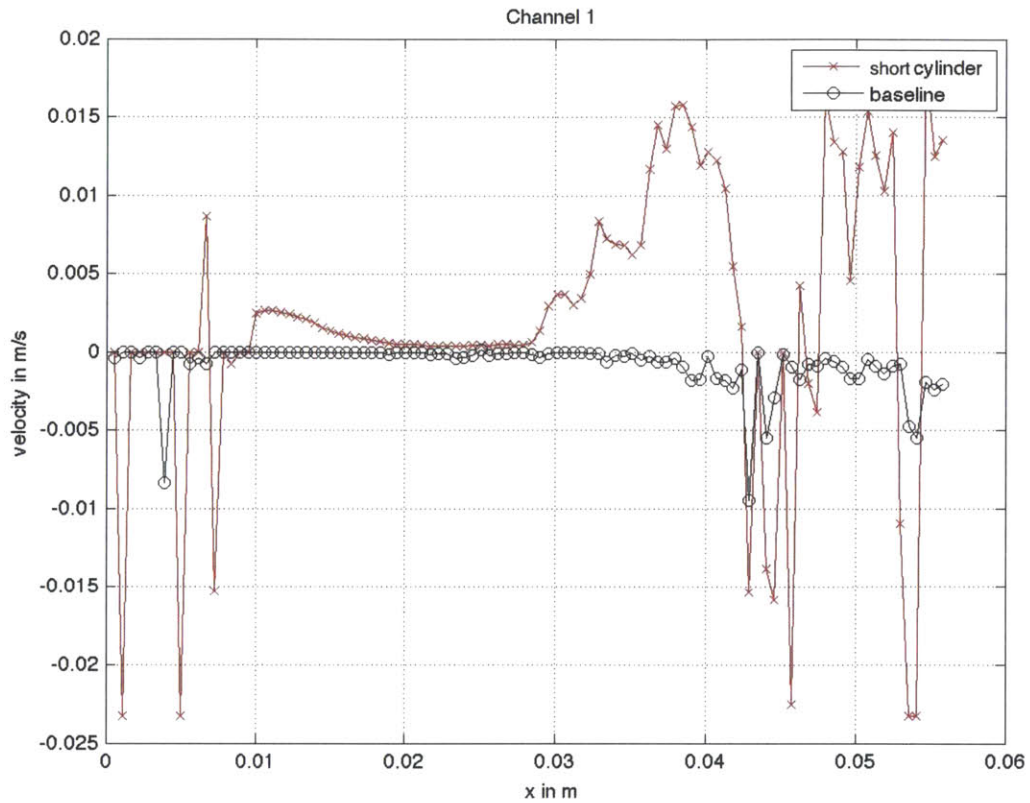
Figure 5.7: Short cylinder, center region. Baseline velocity profile compared against a velocity profile for an applied field of 101.2 Gauss, at 95 Hz, with a phase offset of +90 degrees. Peak magnitude of flow velocity is about 16 mm/s, comparable to that of the bottom region of the long cylinder. This indicates that the demagnetizing factors of the short container cause greater non-uniformities in the external magnetic field than those of the long cylinder. The result is an increased magnitude of bulk flow being driven in the center region, as compared to the long cylinder (Figure 5.5).

## 5.4 Results Interpretation

The results discussed above indicate a consistent relationship between the magnitude of bulk flow and the demagnetizing factors introduced by container geometry. For a long cylindrical container, the flow velocity was smallest when measured at the center, where demagnetizing factors had the least effect on the magnetic field, and largest when measured at the ends, where demagnetizing factors had the greatest effect. Furthermore, for a short cylindrical container, the flow velocity was significantly greater in the center region as compared to the center region in the long container. Therefore, it can be concluded that demagnetizing factors are the main driving force behind bulk flow in cylindrical ferrofluid-filled containers, when placed in a uniform rotating magnetic field.

# CHAPTER 6

# CONCLUSIONS

## 6.1 Results Summary

Truncated spherical containers and cylindrical containers of varying length were filled with ferrofluid and placed in a uniform rotating magnetic field to examine the effects of demagnetizing factors on the bulk flow of the ferrofluid. Partial sphere containers with less volume and cylindrical containers of smaller length have higher demagnetizing factors, and thus were hypothesized to drive a greater magnitude of bulk flow.

When taking measurements with the spherical containers, it was found that negligible bulk flow was driven in the case of a full sphere, because of the uniform rotating magnetic field. Conversely, when truncated spheres were placed in this uniform rotating magnetic field, significant bulk flow was observed. There was not a readily apparent pattern in flow magnitude or shape as the truncated spheres decreased in volume. This is indicative of a complicated, nonlinear relationship between demagnetizing factors and magnitude of bulk flow; a more precise relationship was unable to be established through the course of experimentation. Overall, the results were consistent with the hypothesis of demagnetizing factors being the primary cause of bulk flow, by causing non-uniformities in an otherwise uniform external magnetic field.

When taking measurements with the cylindrical containers, it was found that the magnitude of bulk flow increased as the cylinder aspect ratio (the ratio of

cylinder height to diameter) became smaller. Furthermore, in the case of a large

aspect ratio, there was significantly greater flow at the ends than at the center.

These results were also consistent with the hypothesis of demagnetizing factors

causing non-uniformities in the uniform external magnetic field being the primary

cause of bulk flow.

The results of the aforementioned experiments support the hypothesis as

posited by Khushrushahi [2], that non-uniformities in the magnetic field due to

demagnetizing factors are the primary cause of ferrofluid bulk flow in a uniform

rotating magnetic field.

## 6.2 Suggestions for Further Research

This research was mainly built upon earlier research performed by Shahriar

Khushrushahi and used equipment he designed and constructed. Equipment earlier

built by Michael Snively and Katrina Schoen [3], [4] was also integral to this

research. As a consequence, some of the constraints imposed by their equipment

prevented this research from fully exploring the effect of demagnetizing factors.

One problem in particular dealt with the probe holder and some of the

manufactured spherical containers. Spherical containers were manufactured for

50% and 60% volume; however, they could not fully fit within the probe holder, due

to a bead of excessive adhesive material interfering with the circumferential ring of

the holder. This adhesive damaged the surface of the container when removal was

attempted. Unfortunately, there does not seem to be a quick and simple solution to

this problem. If data is desired for these volumes, a complete remanufacturing of

the containers is necessary, with careful attention paid to the application of the adhesive.

Additionally, the probe slots of the cylindrical containers were slightly wider than the width of the ultrasound probes, which allowed the probes to move around inside their slots as data was being taken, negatively affecting the ultrasound signal and the integrity of the data taken. To remedy this, Teflon tape was wrapped around the body of the probes to increase their thickness, and they were also taped down to the slots with electrical tape. While this was a somewhat effective remedy, it was also sometimes unreliable, as the probe had to be placed in the perfect position or else the data would be useless due to poor ultrasound contact. A better and more permanent solution would be to make slight alterations to the cylindrical containers themselves by drilling new holes for probe slots that more closely fit the probe shape. Careful attention and a precise process would be necessary to ensure that the probe slots perfectly match the width of the ultrasound probes; however, this would make the taking of data and the repetition of the experiment considerably easier.

Due to time constraints, all testing was performed with EFH1 oil-based ferrofluid. Testing was not done with MGSW11 ferrofluid, the original ferrofluid that Khushrushahi used in his experiments. A complete repeat of the experiments in this thesis with MGSW11 would be beneficial in confirming his results. Time constraints also prevented the carrying out of experiments in spherical geometry with the fluxball in the vertical orientation. This is another set of data that could be beneficial and provide further reaffirmation of the conclusions.

# REFERENCES

[1] "What is magnetic fluid (ferrofluid)?" Web. May 2012.

http://www.rigaku.co.jp/rms_en/ technology/tech01.html

[2] Khushrushahi, Shahriar R. "Ferrofluid Spin-up Flows From Uniform and Non-uniform Rotating Magnetic Fields." PhD Thesis, Massachusetts Institute of Technology, 2010..

 [3] Snively, Michael John. "Effects of Demagnetizing Factors on Transient Motion of Ferrofluid in a Uniform Rotating Magnetic Field." Bachelors Thesis, Massachusetts Institute of Technology, 2011.

[4] Schoen, Katrina Leigh. "Design and Manufacture of a Modular Cylindrical Apparatus for Ferrofluid Experimentation." Thesis. Massachusetts Institute of Technology, 2011. Print.

[5] "DOP Velocimeters Series." *Ultrasonic Velocity Profile Doppler Measuring Instrument.* Web. May. 2012. http://www.signal- processing.com/instruments/ instruments_frame.htm

[6] Lawler, Clinton T. *A Two-phase Spherical Electric Machine for Generating Rotating Uniform Magnetic Fields.* Thesis. Massachusetts Institute of Technology, 2007. Print.

# APPENDIX A

## FULL RAW DATA SET

This section presents the graphs of data for every trial of the experiments.

### A.1 Spherical Geometry

Channel designations are as specified in Chapter 4.

### 47 Hz, 50.6 Gauss, -90°
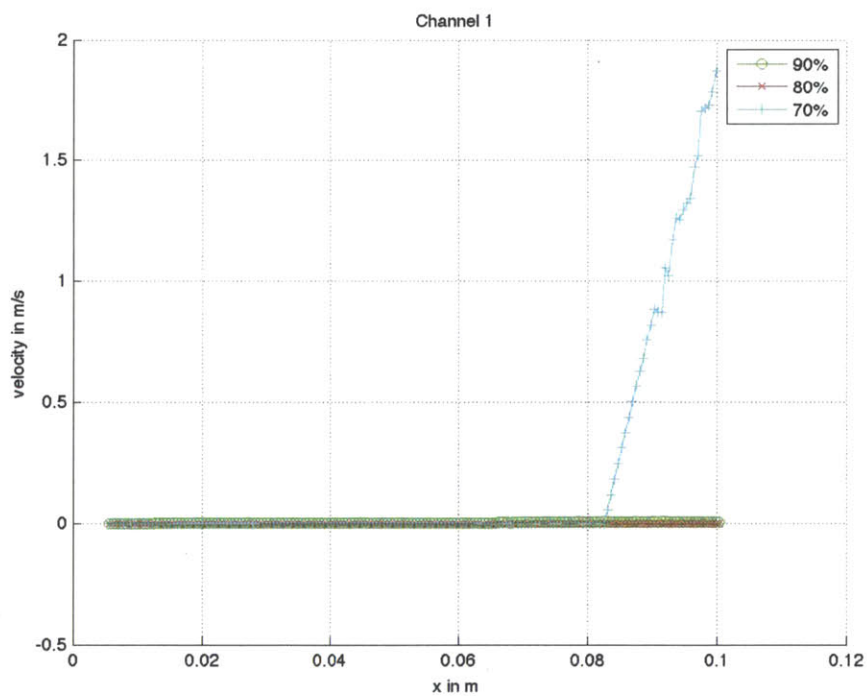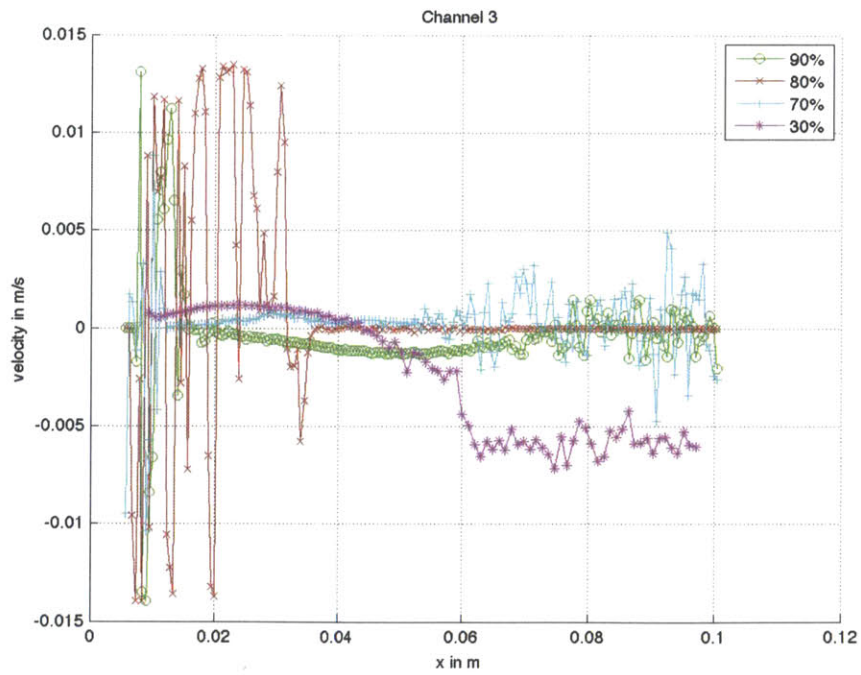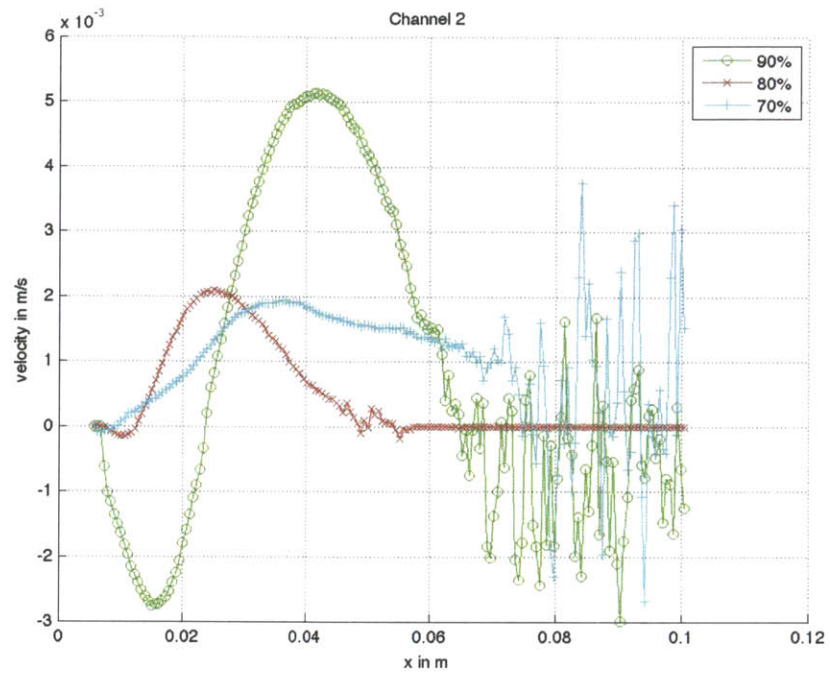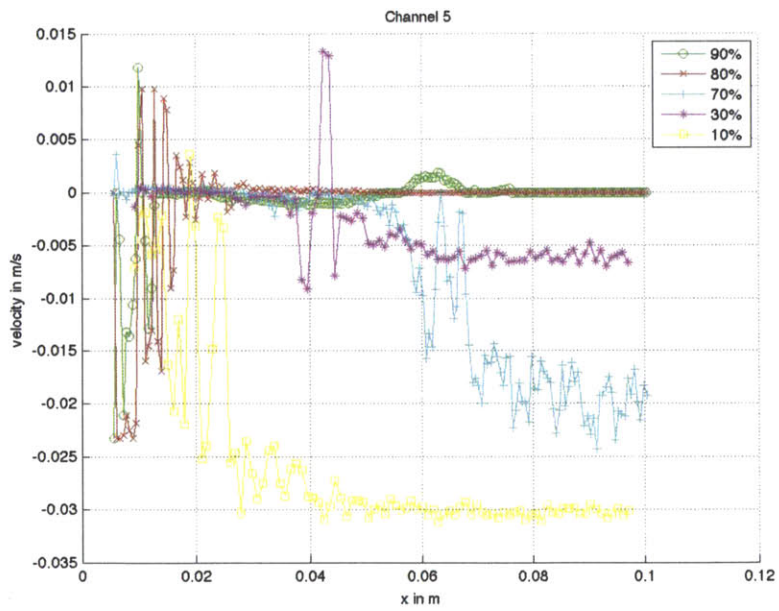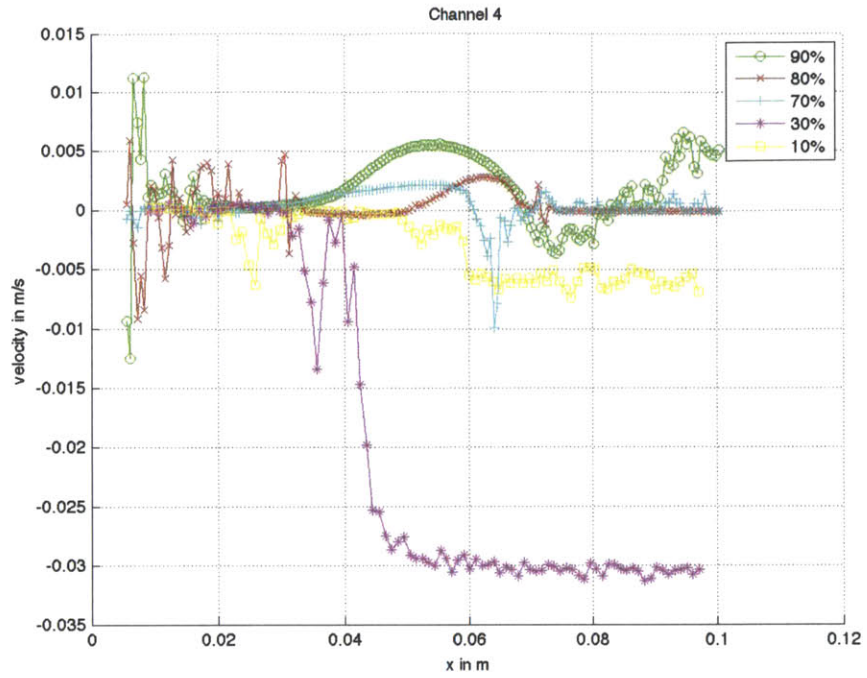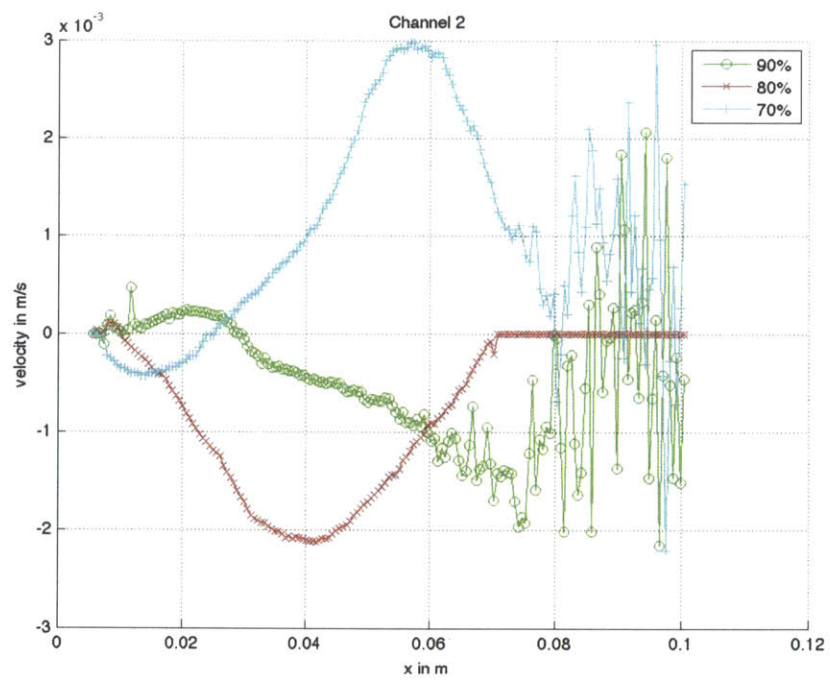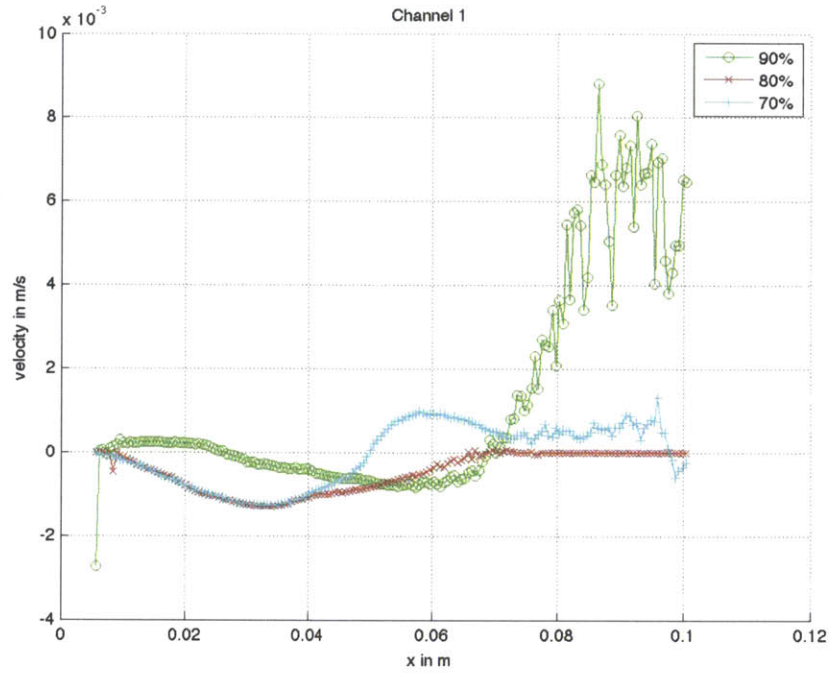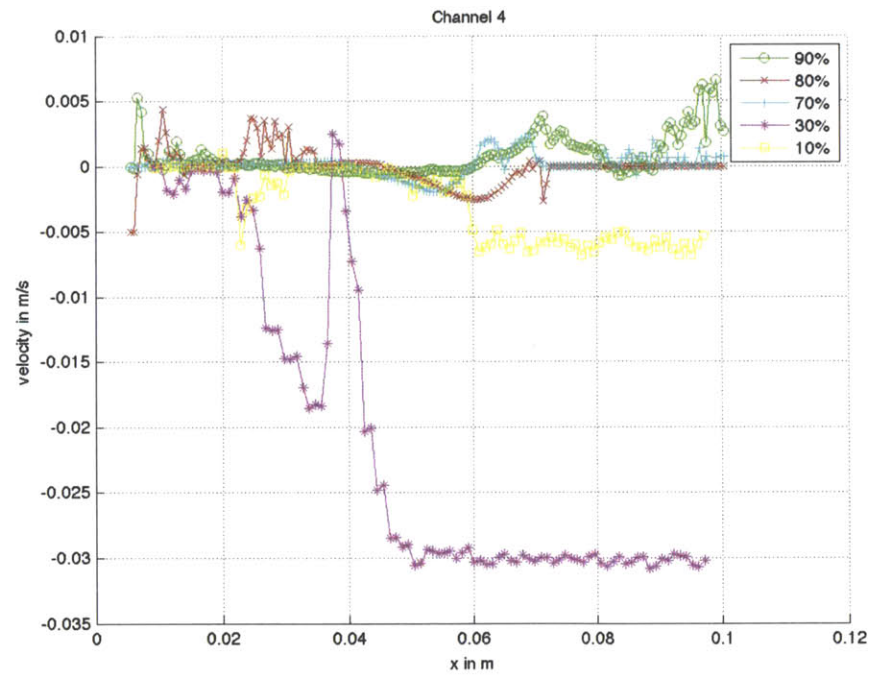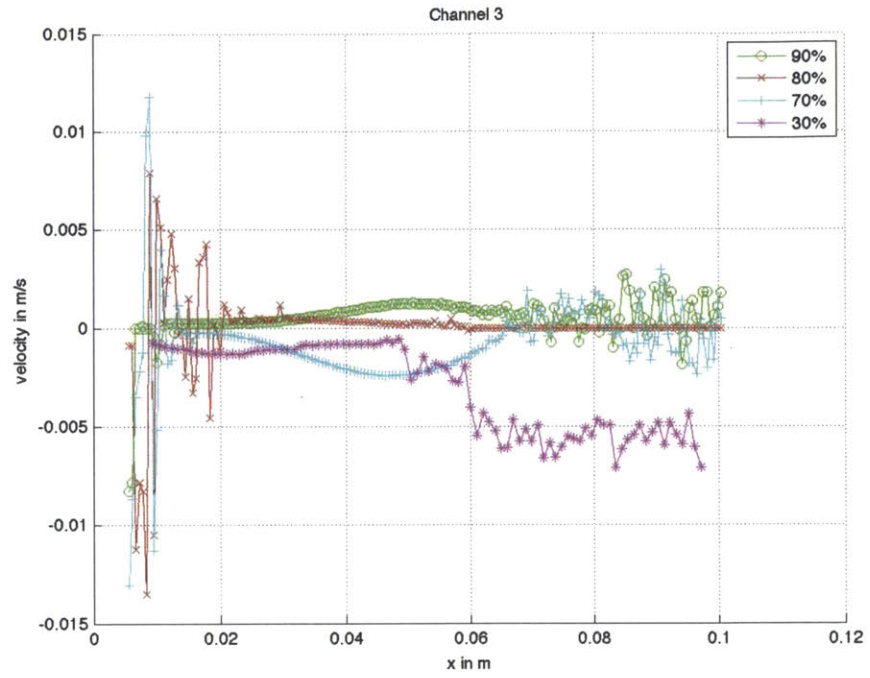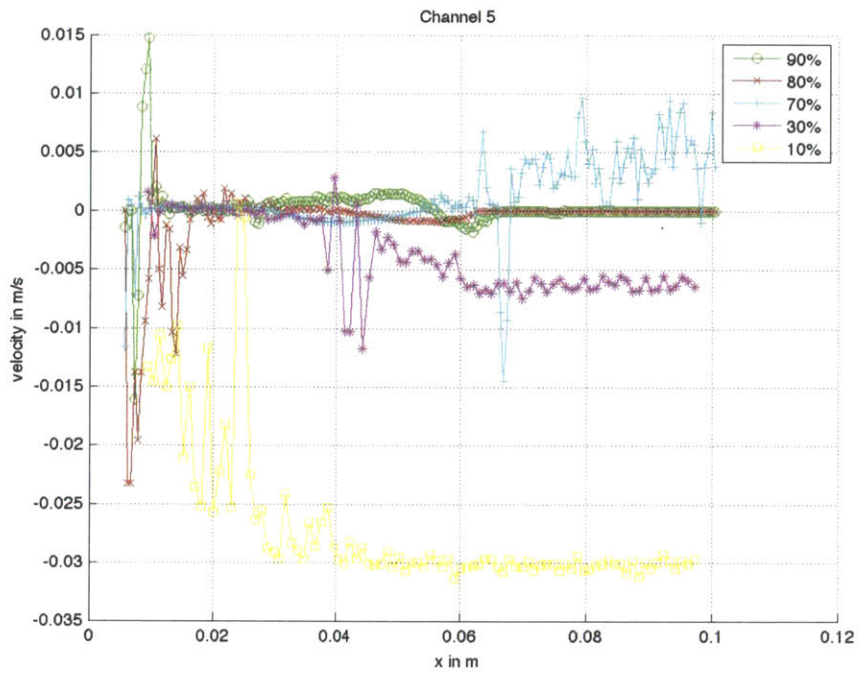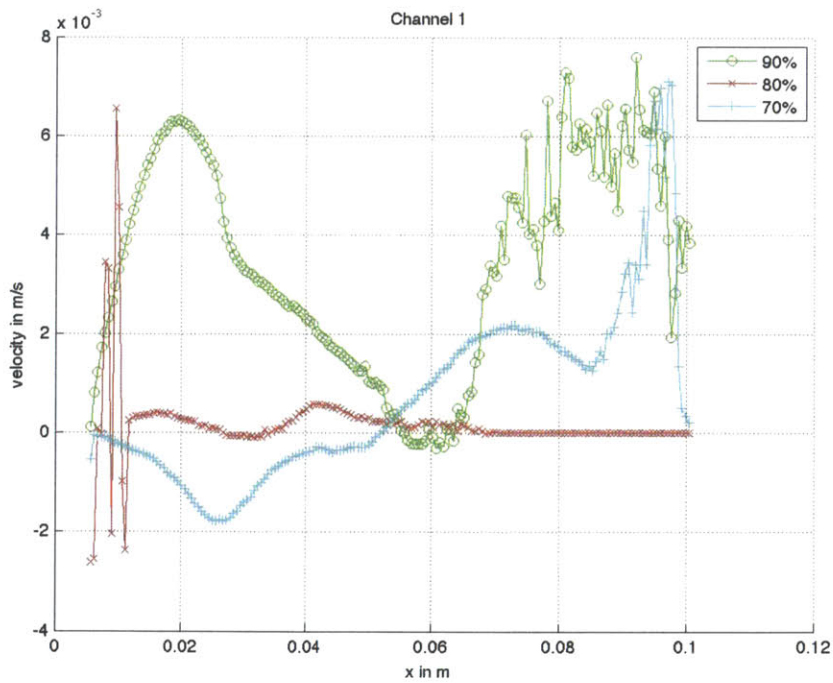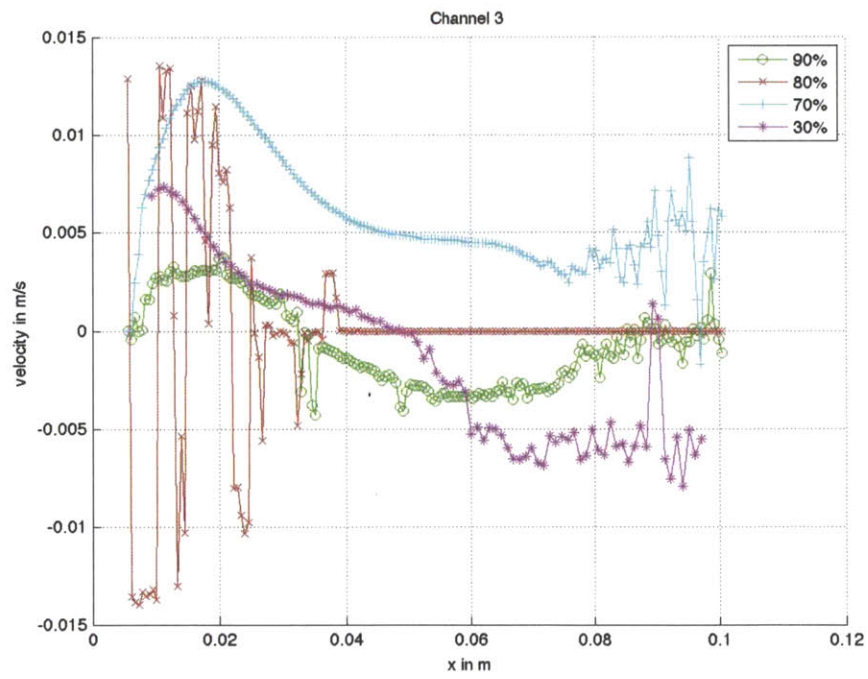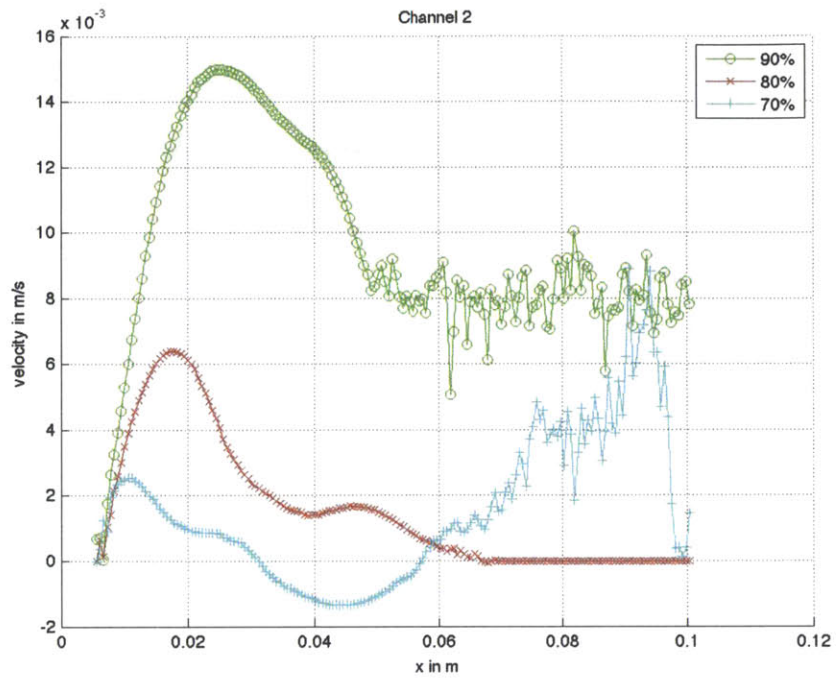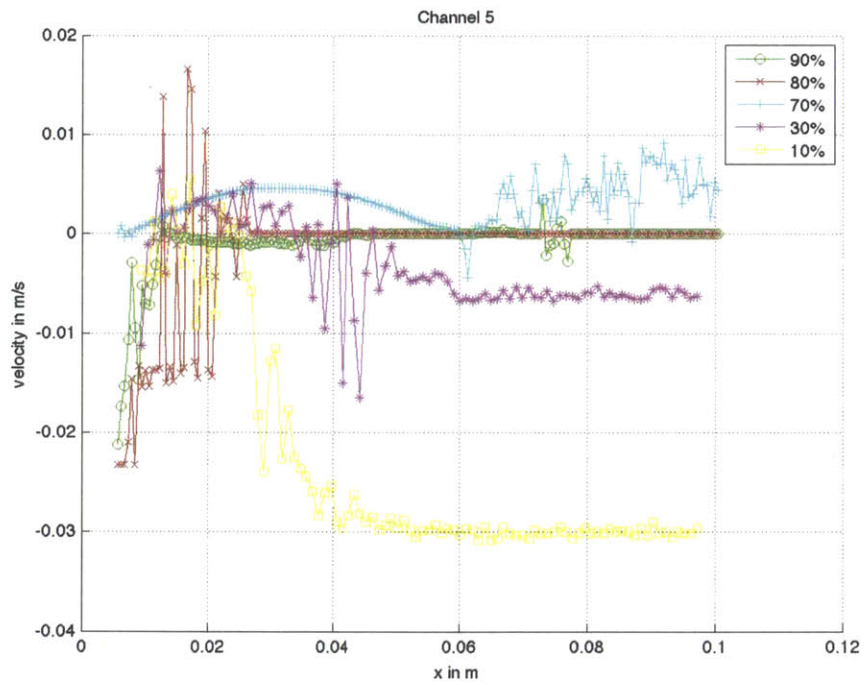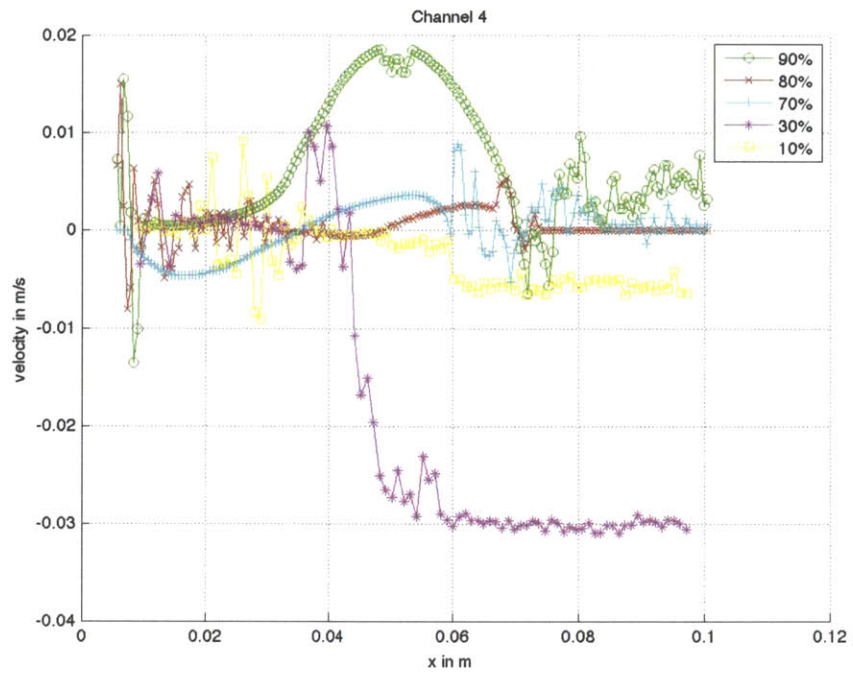
Channel 2



Channel 3

Channel 4



Channel 5

**47 Hz, 50.6 Gauss, +90°**

Channel 3



Channel 4

**47 Hz, 101.2 Gauss, -90°**

**47 Hz, 101.2 Gauss, +90°**

Channel 3



Channel 4

Channel 5

**95 Hz, 50.6 Gauss, -90°**



Channel 1

**95 Hz, 50.6 Gauss, +90°**

**95 Hz, 101.2 Gauss, -90°**

**95 Hz, 101.2 Gauss, +90°**

Channel 3



Channel 4

Channel 5
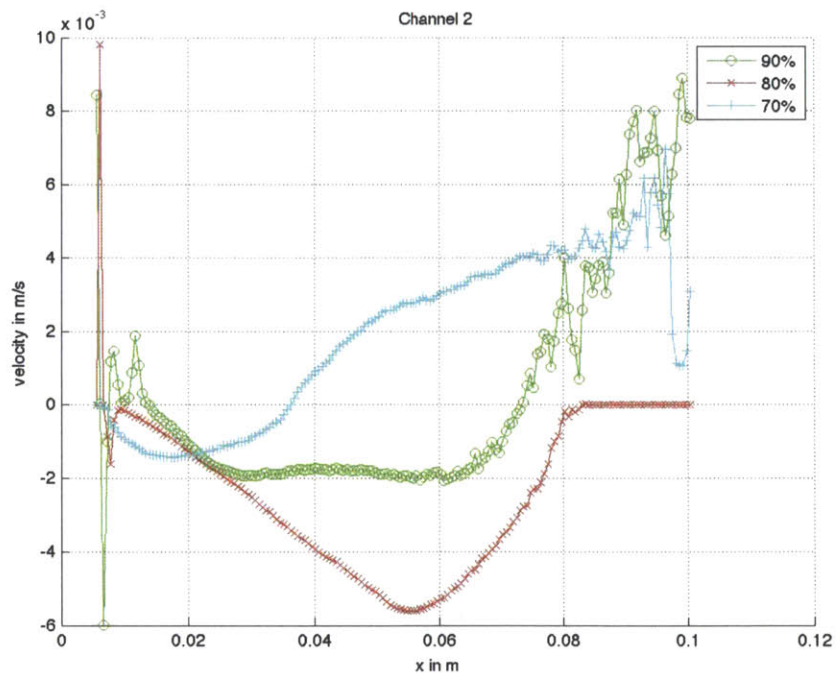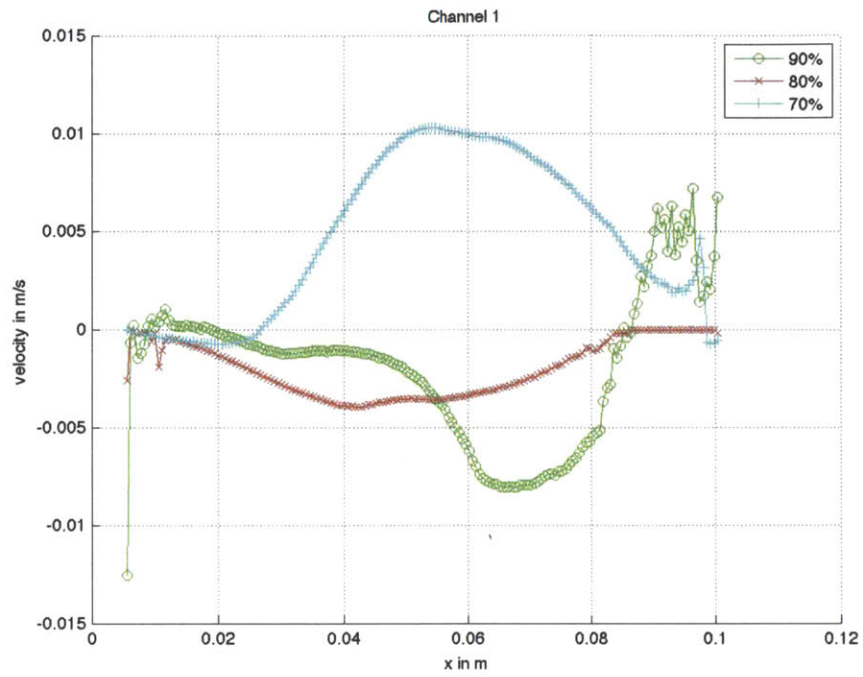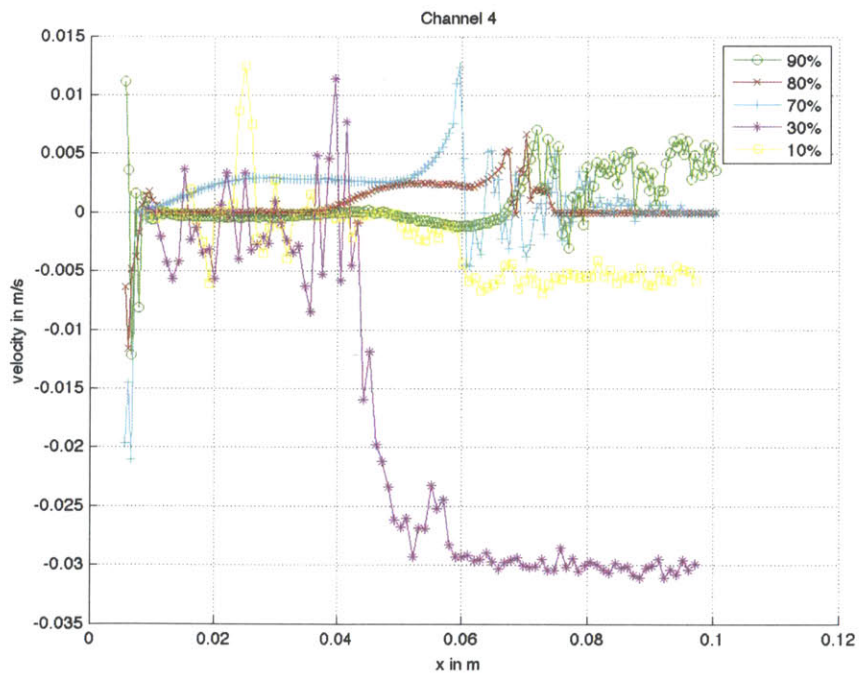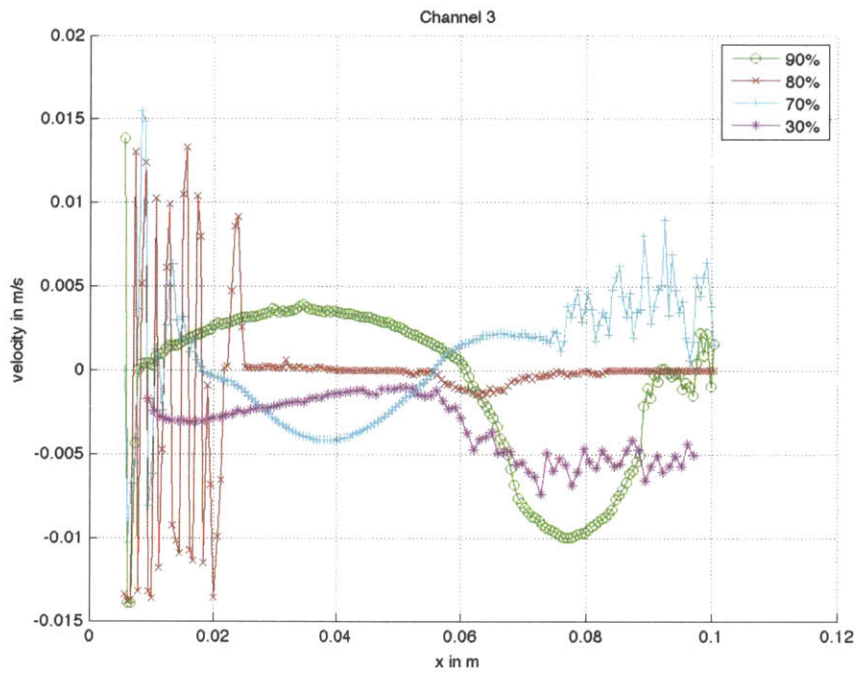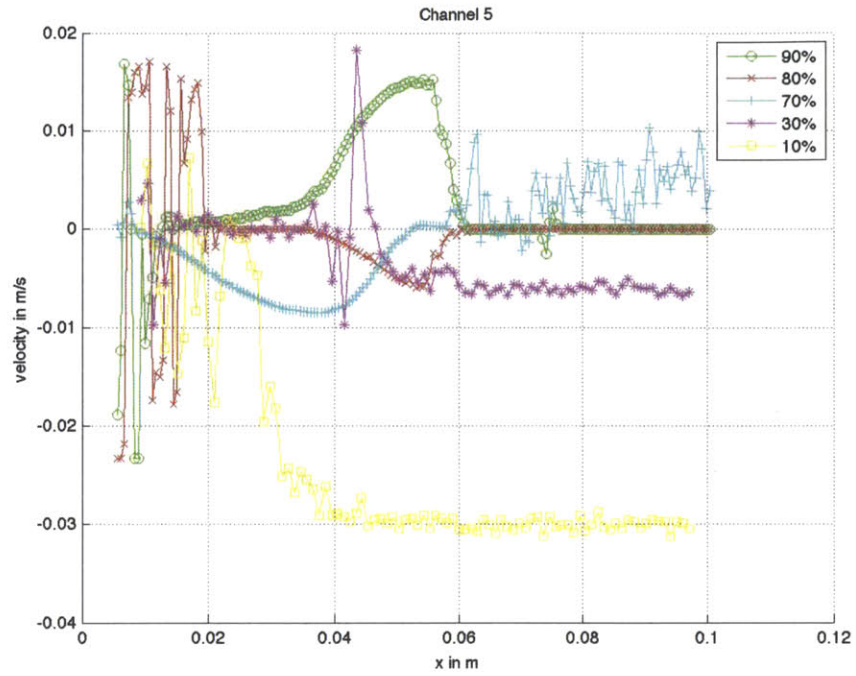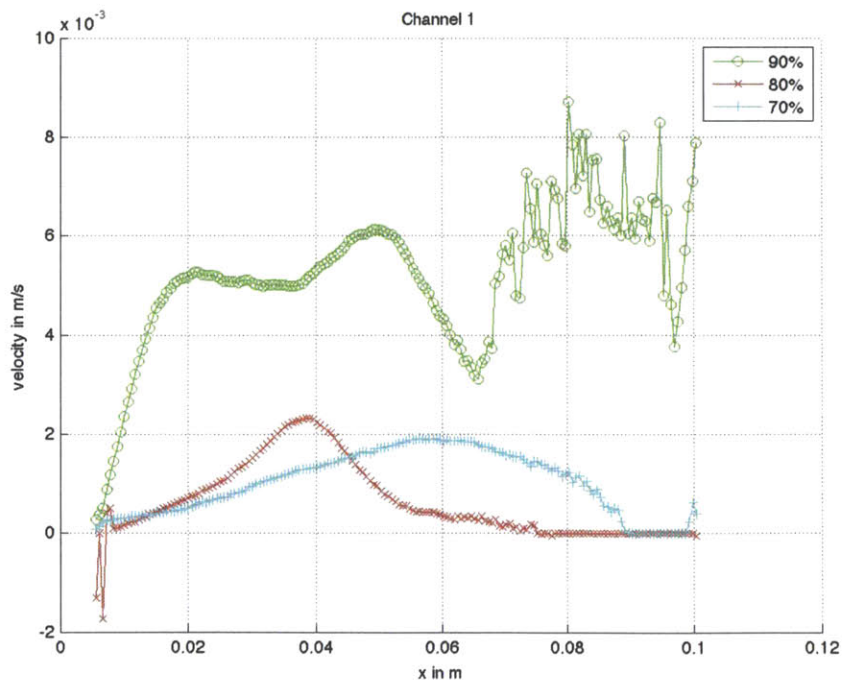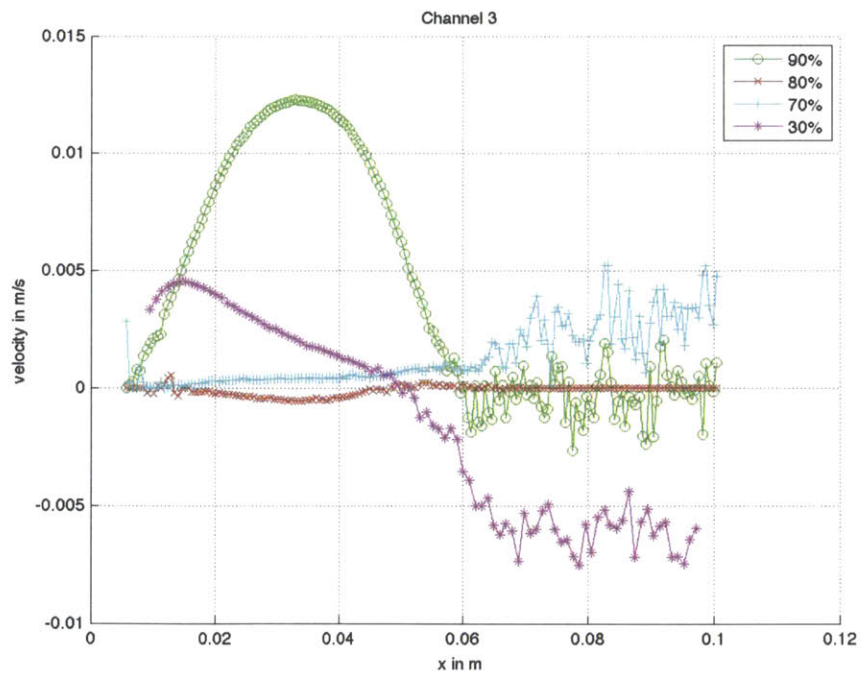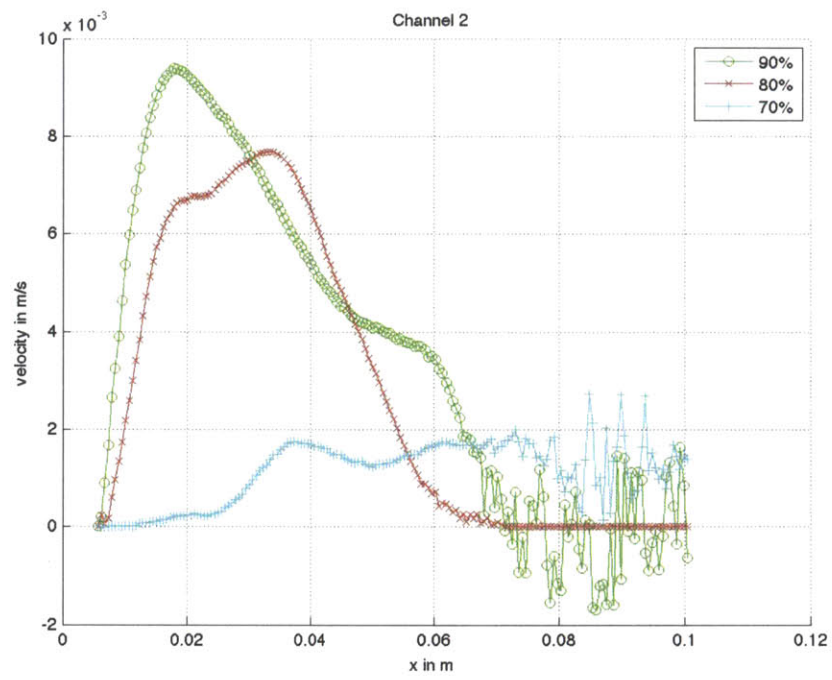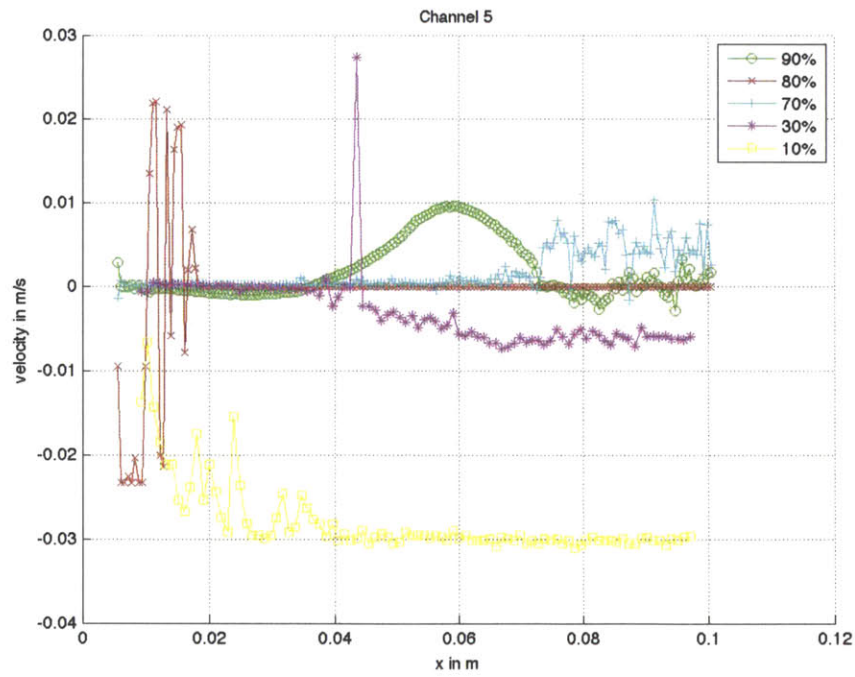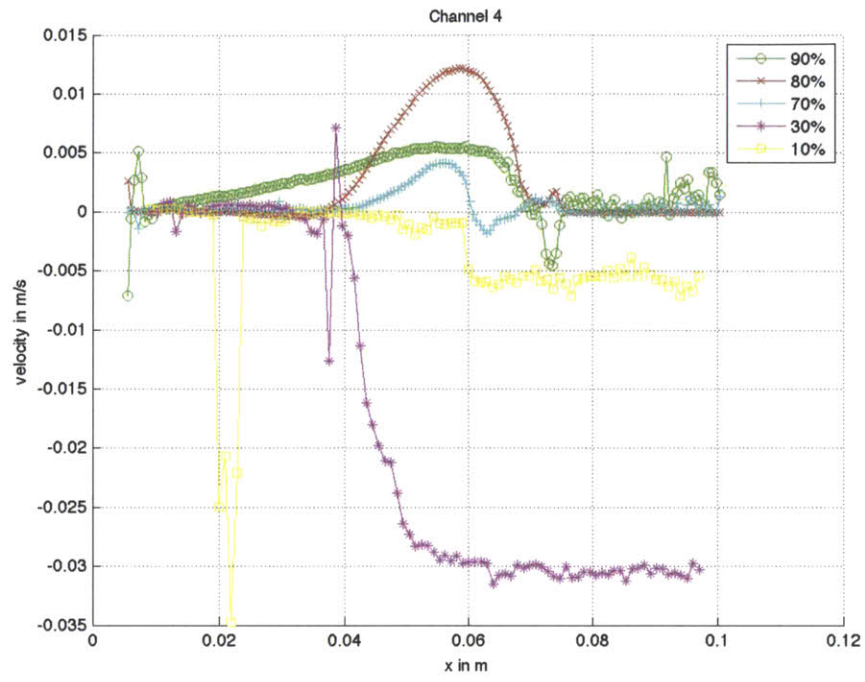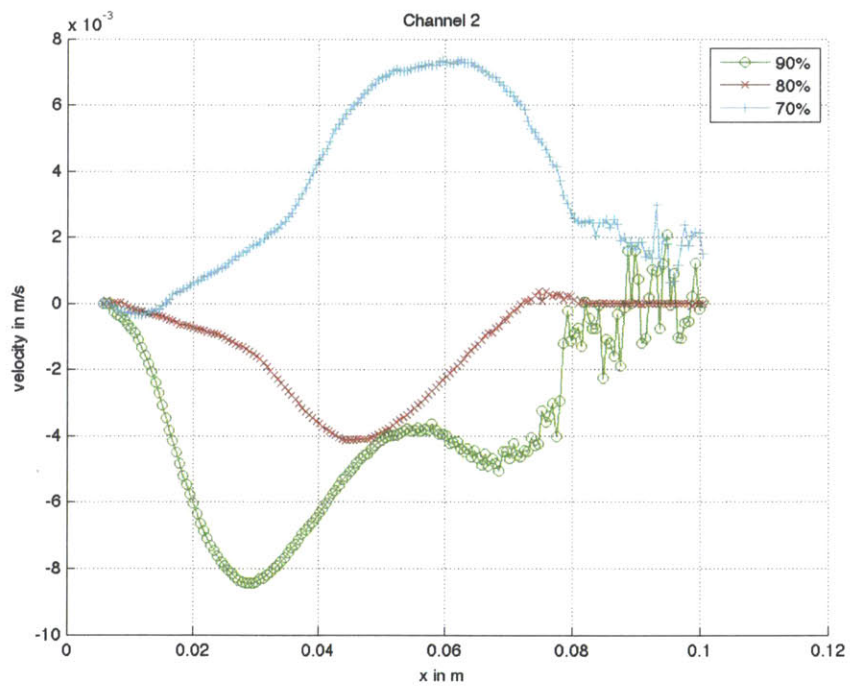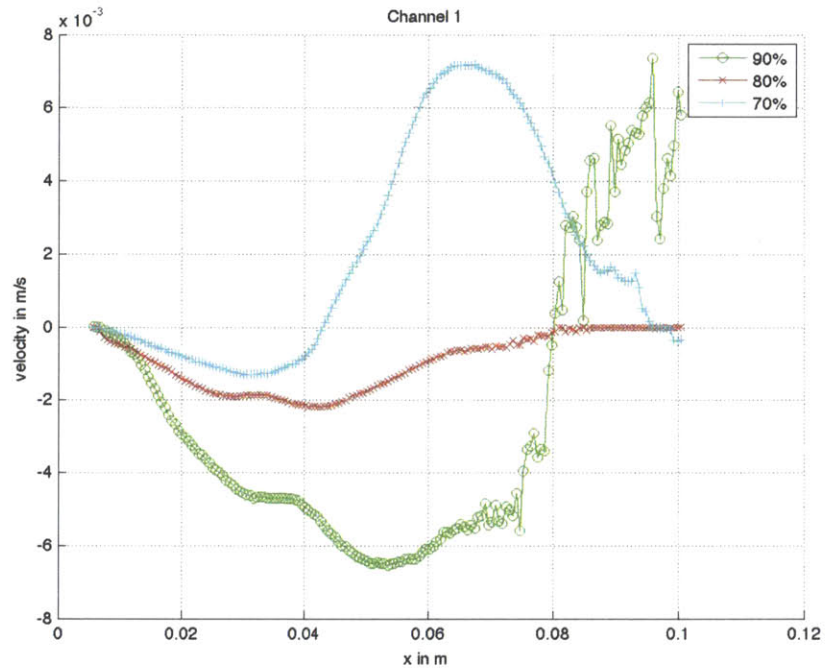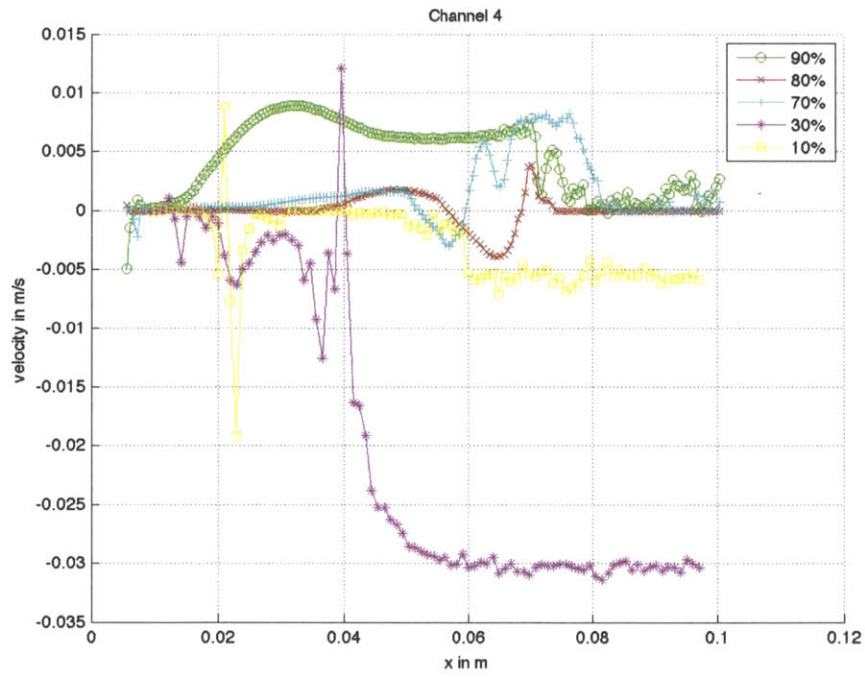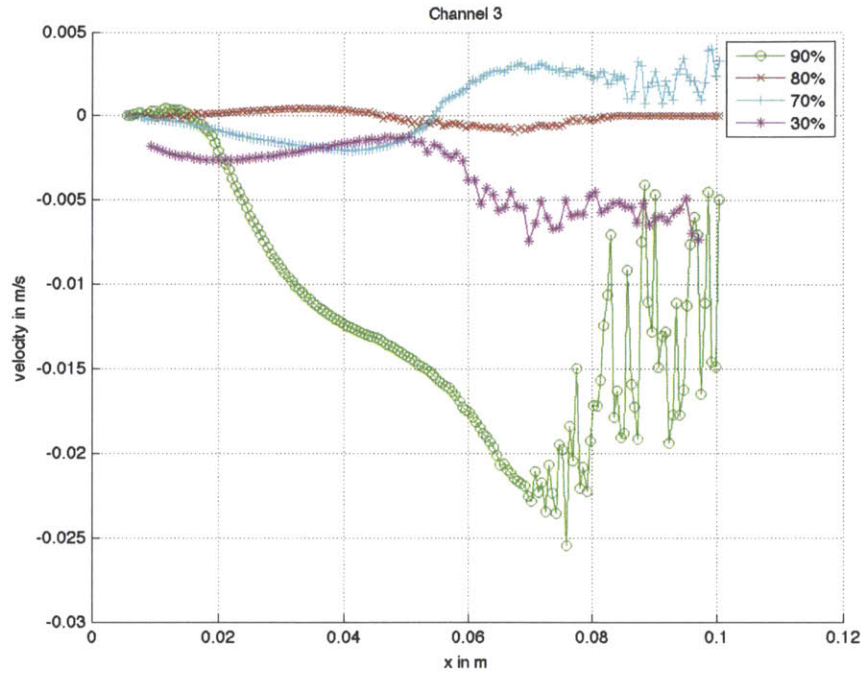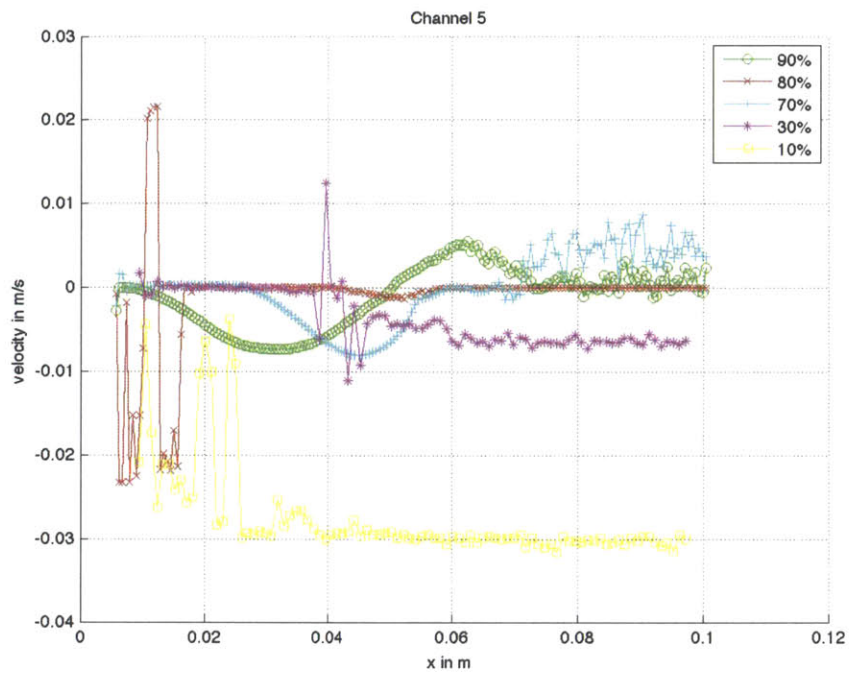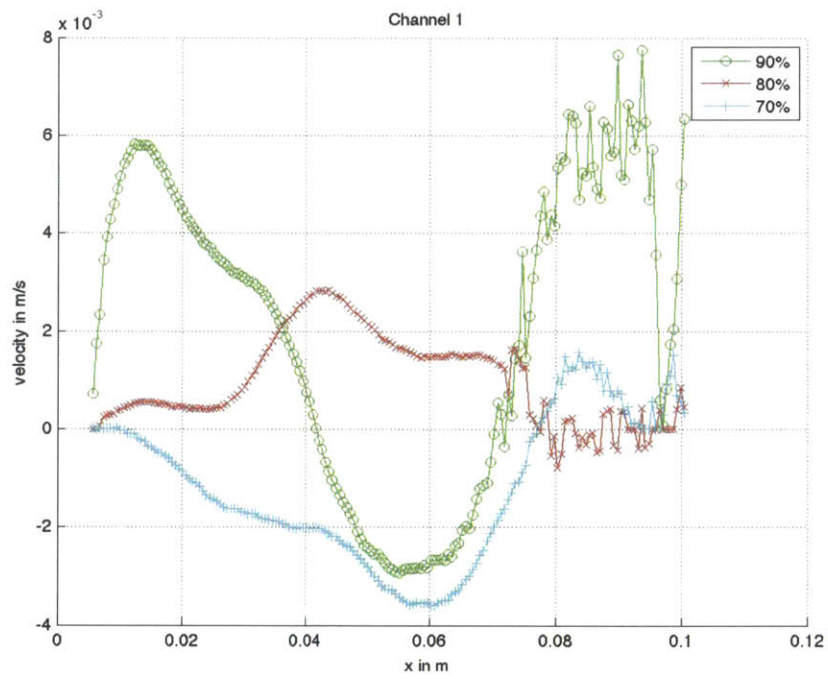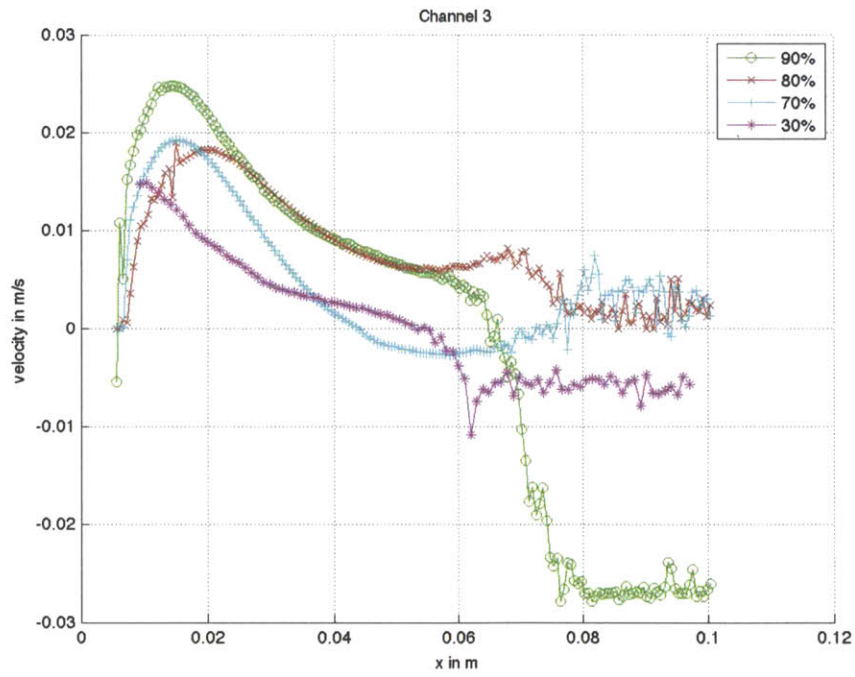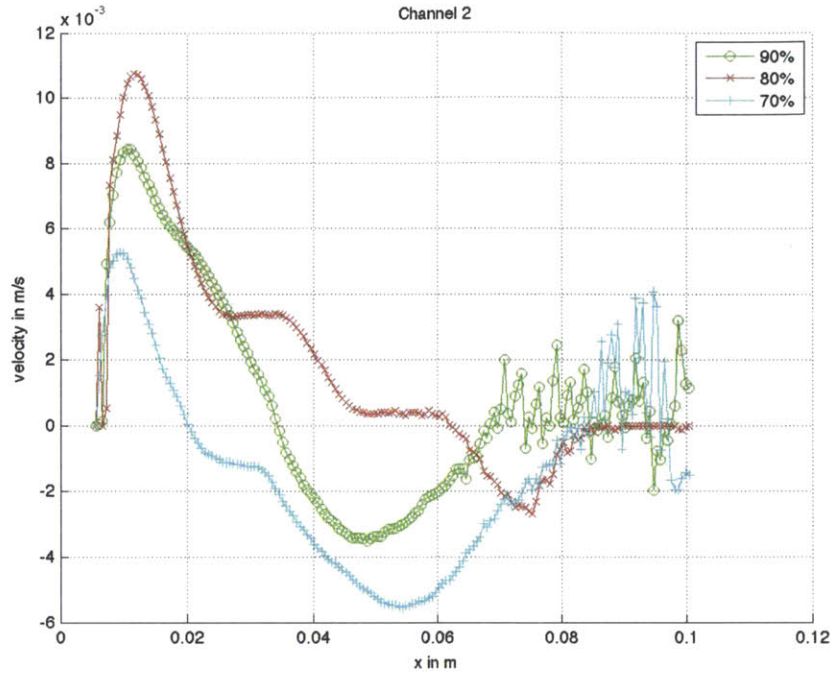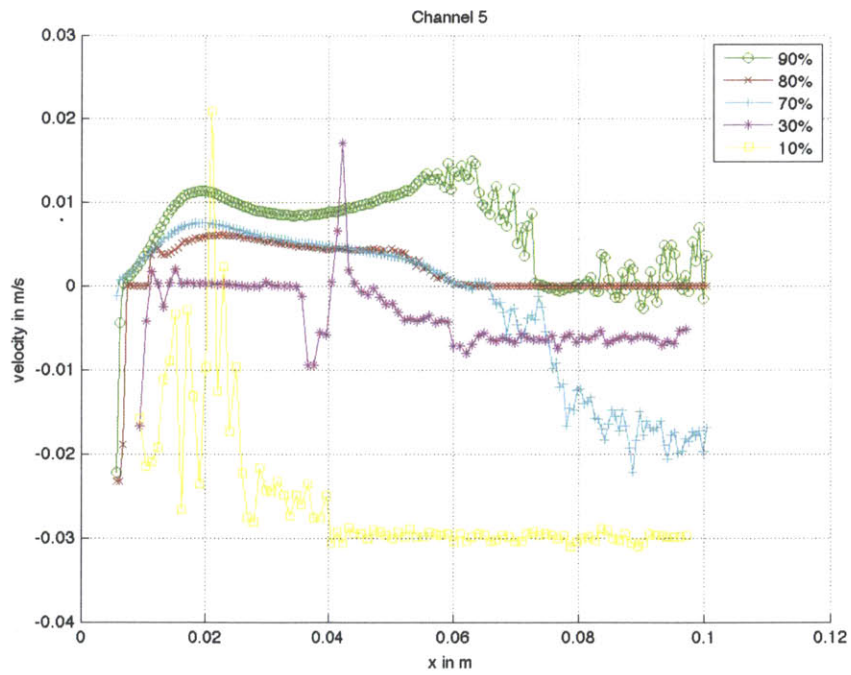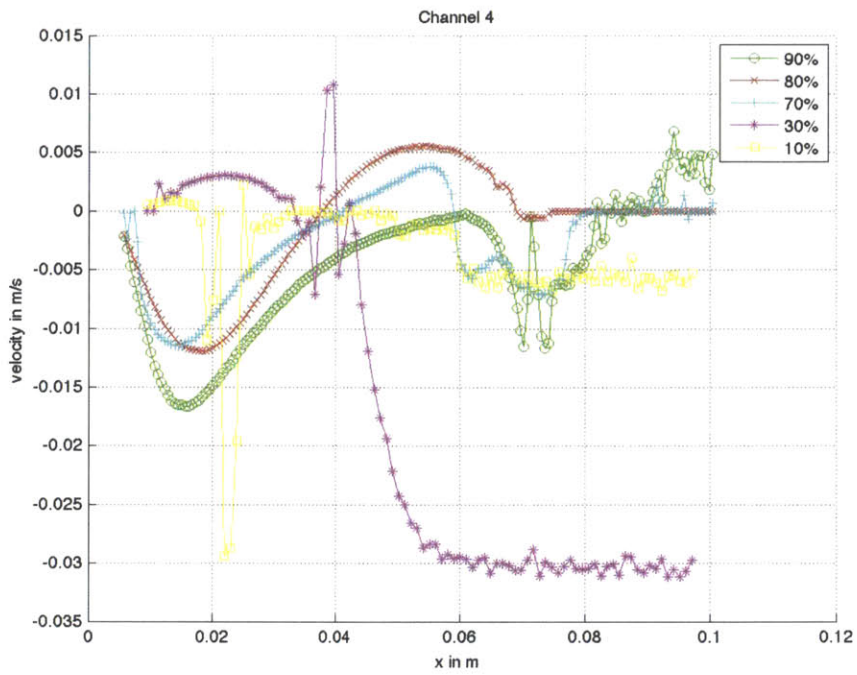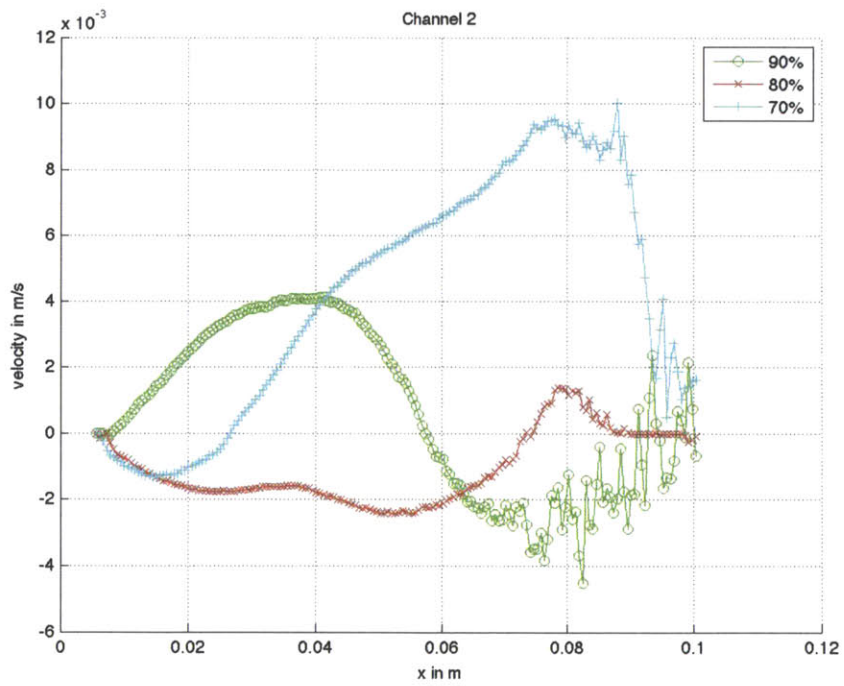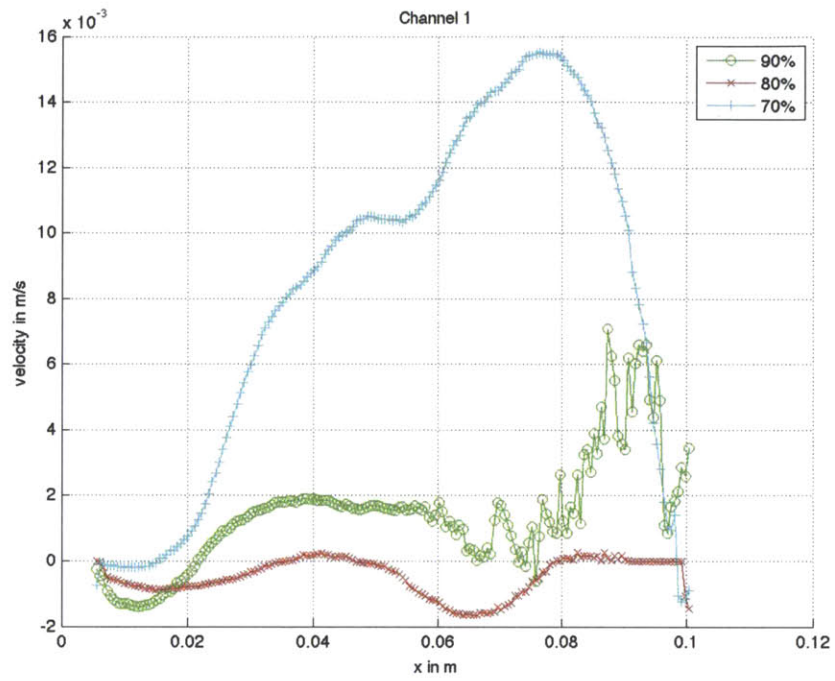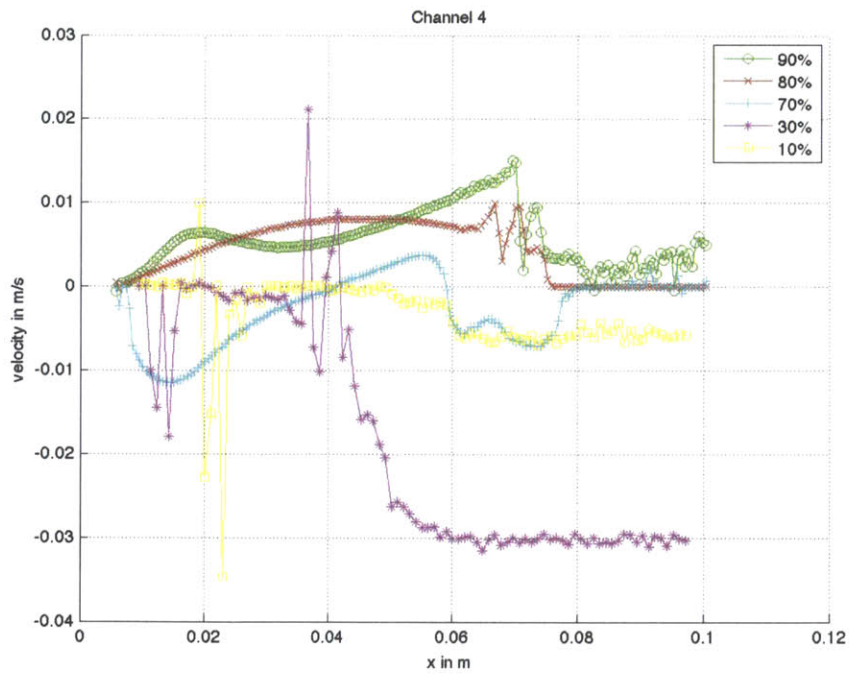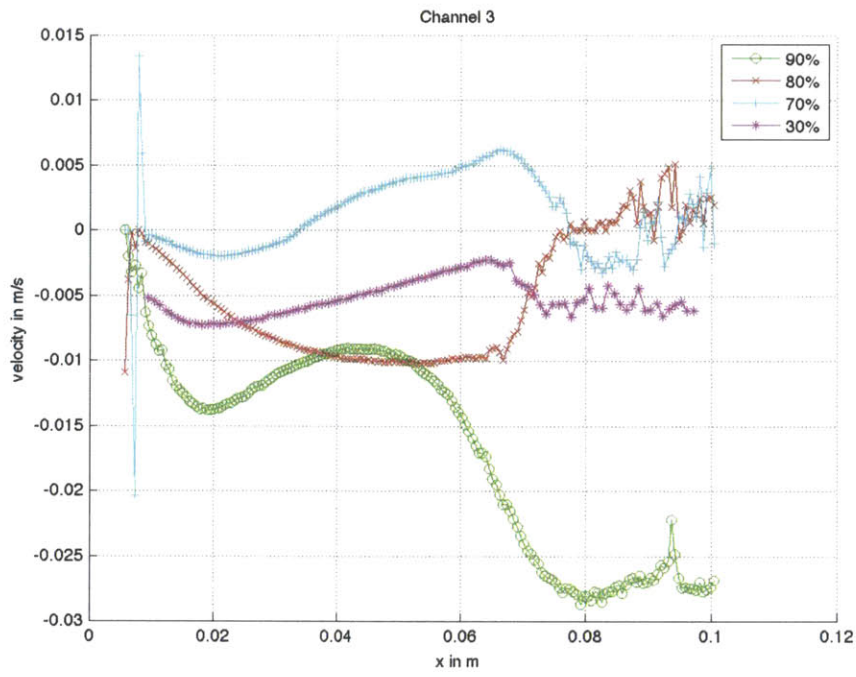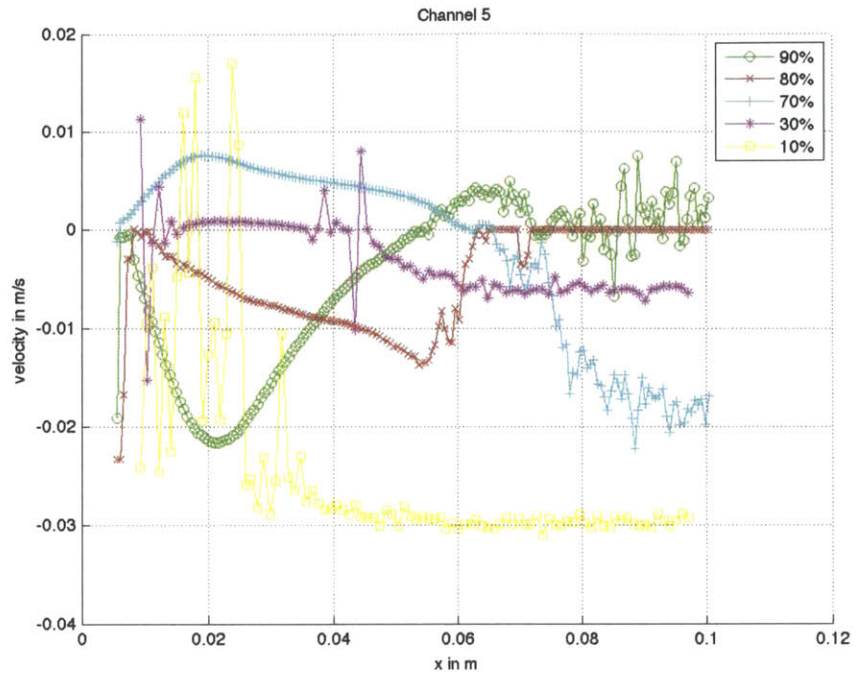
## A.2 CYLINDRICAL GEOMETRY

## A.2.1 Short Cylinder, Radial

## 47 Hz, 50.6 Gauss, -90°
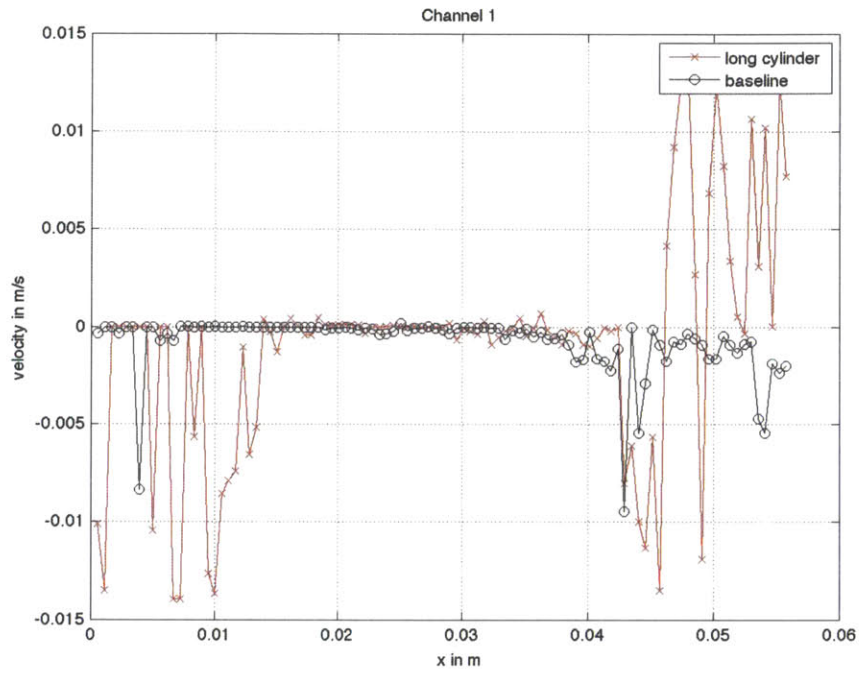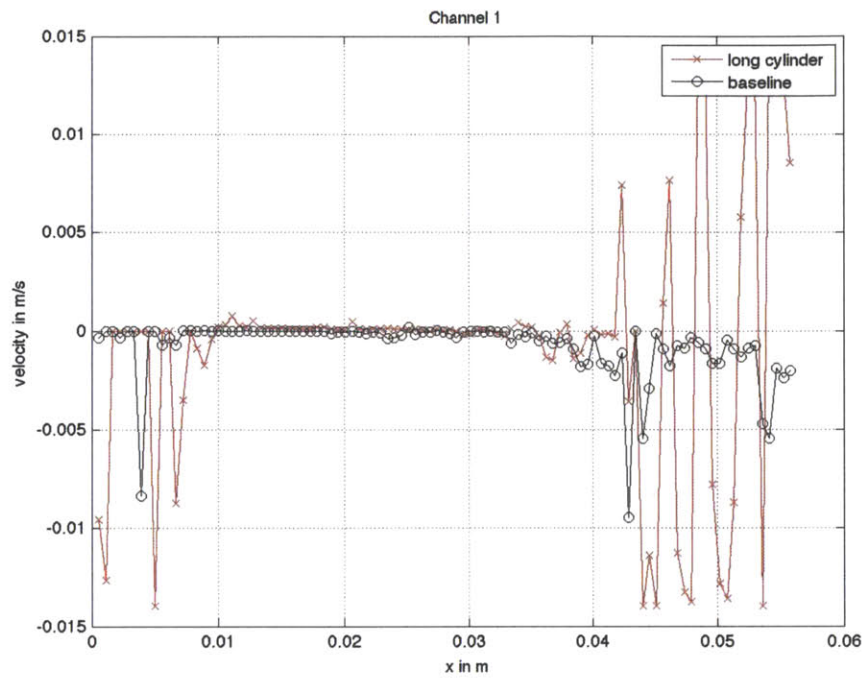
**47 Hz, 50.6 Gauss, +90°**



Channel 1

**47 Hz, 101.2 Gauss, -90°**



Channel 1
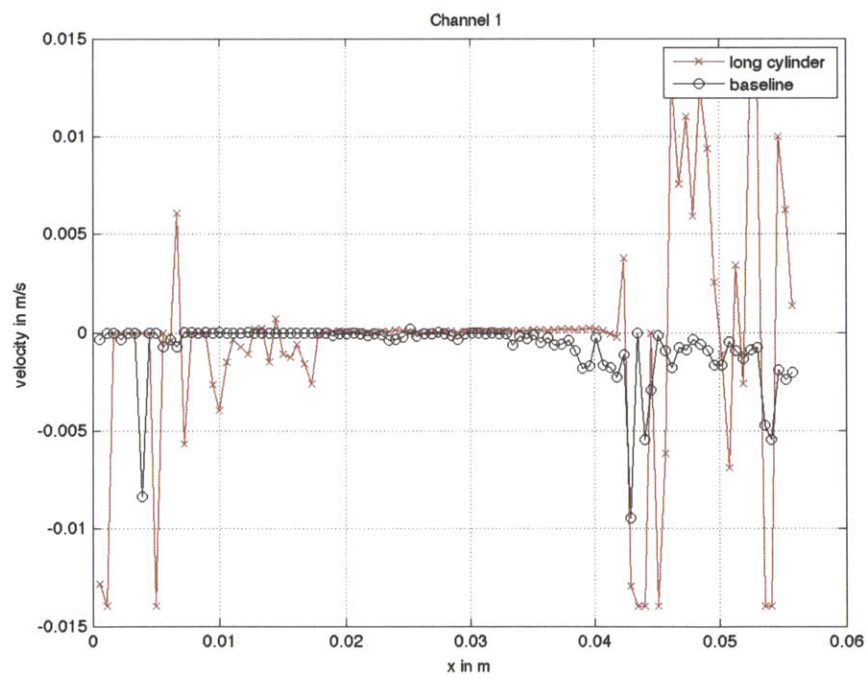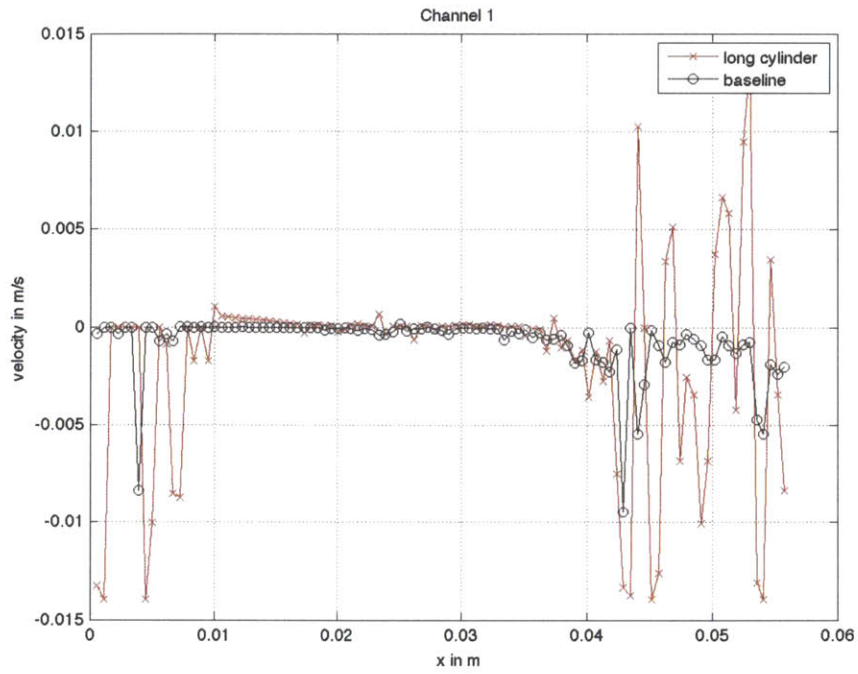
**47 Hz, 101.2 Gauss, +90°**
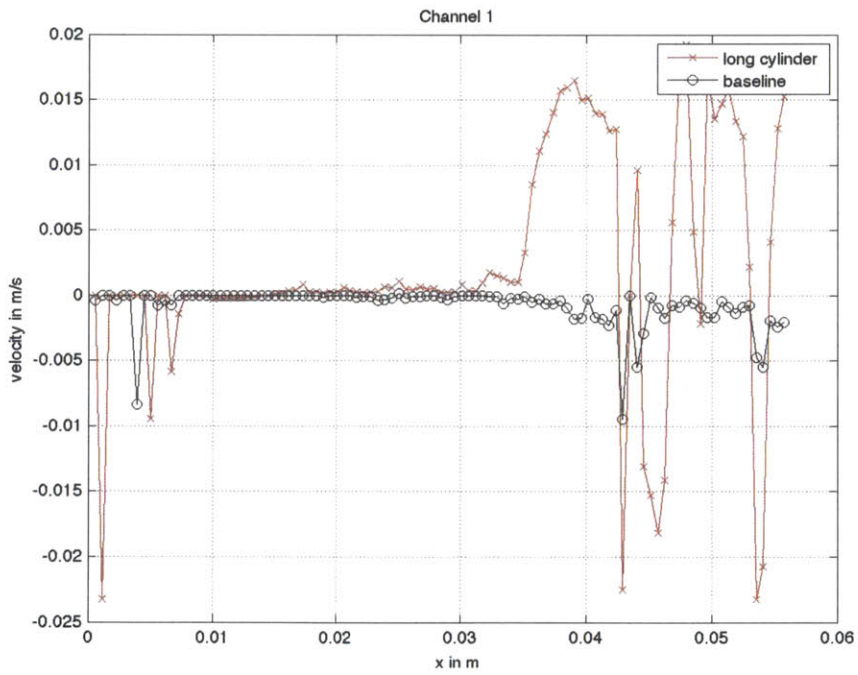


**95 Hz, 50.6 Gauss, -90°**
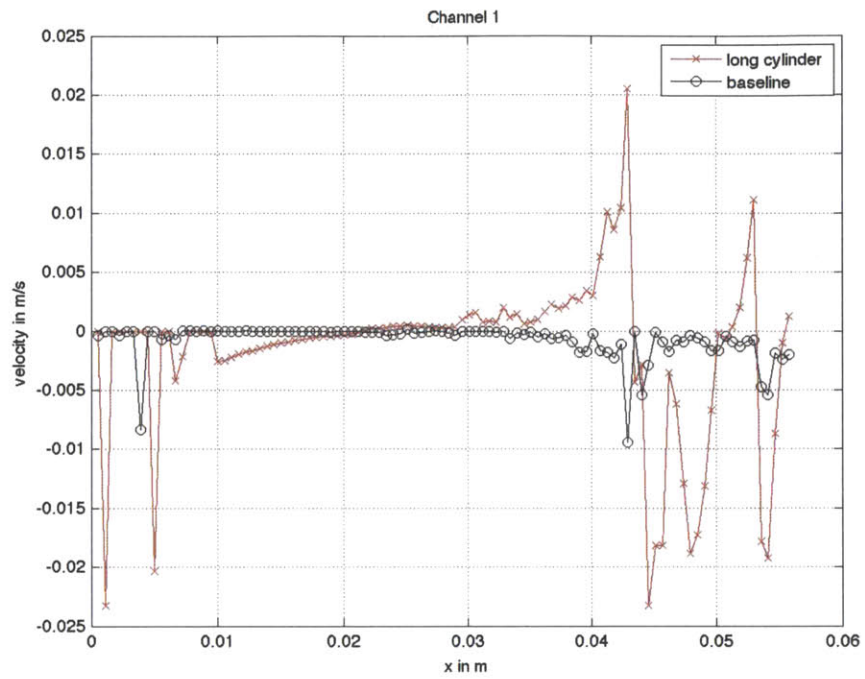
**95 Hz, 50.6 Gauss, +90°**
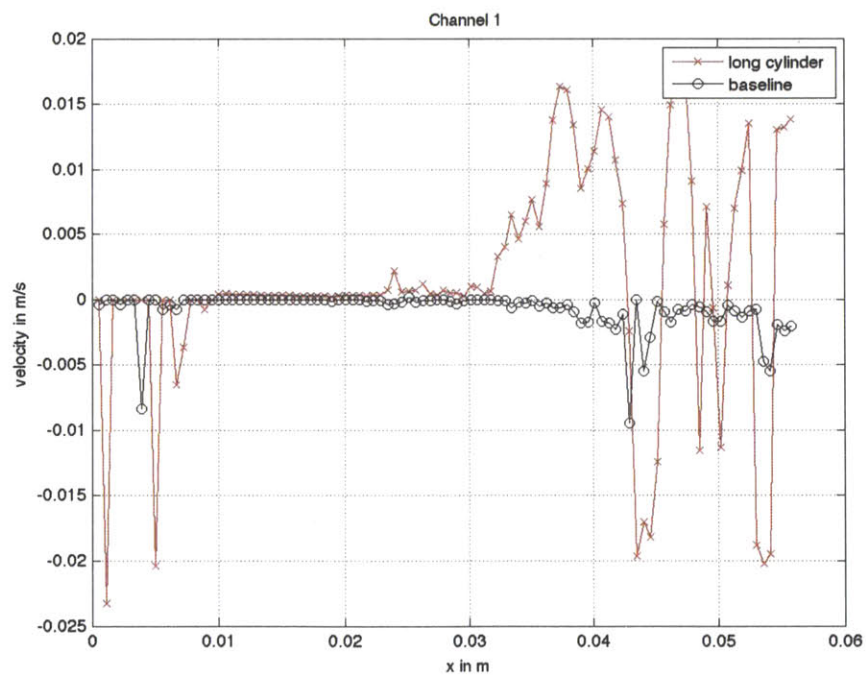


**95 Hz, 101.2 Gauss, -90°**
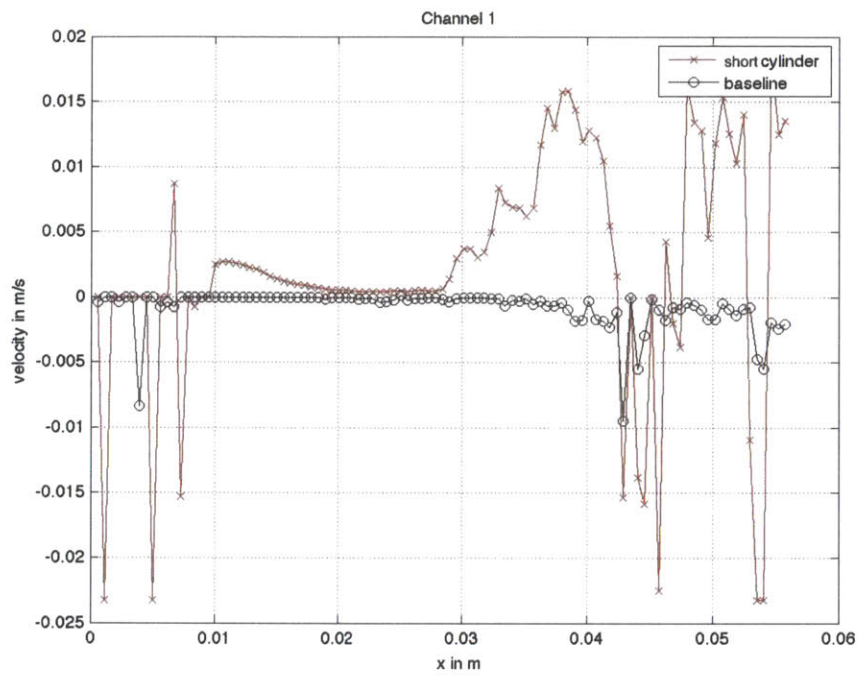
**95 Hz, 101.2 Gauss, +90°**
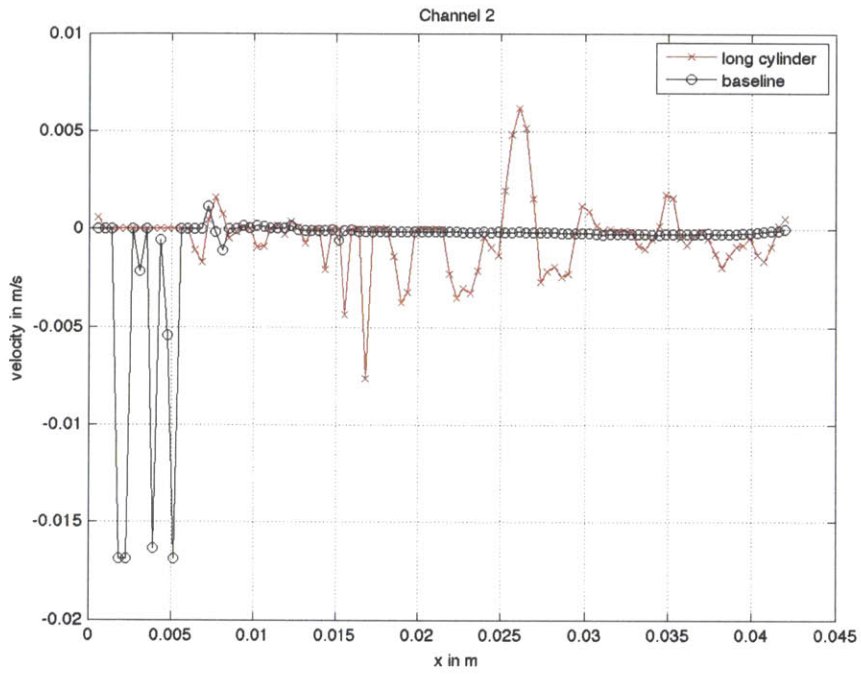
## A.2.2 Long Cylinder, Radial
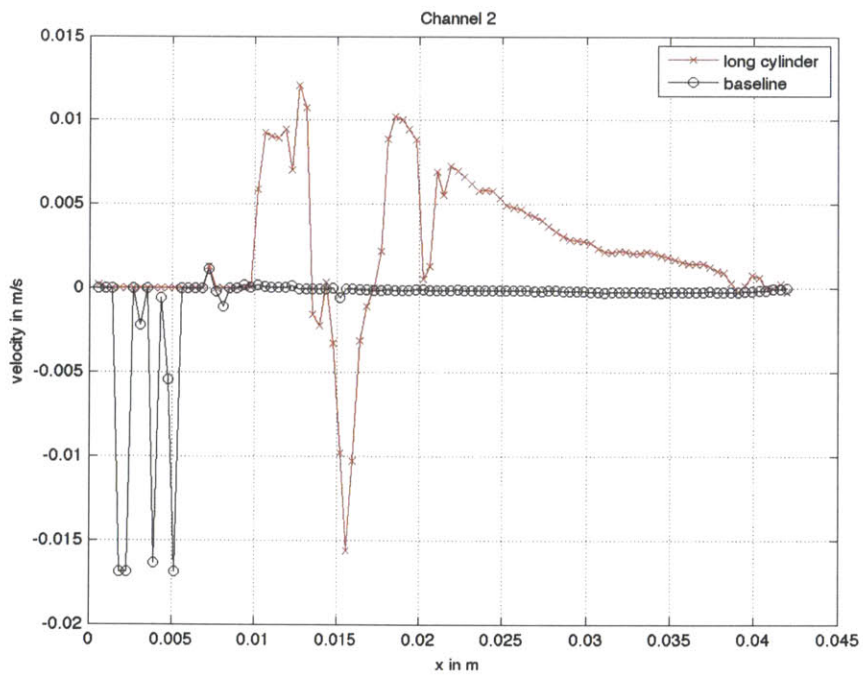
## 47 Hz, 50.6 Gauss, -90°
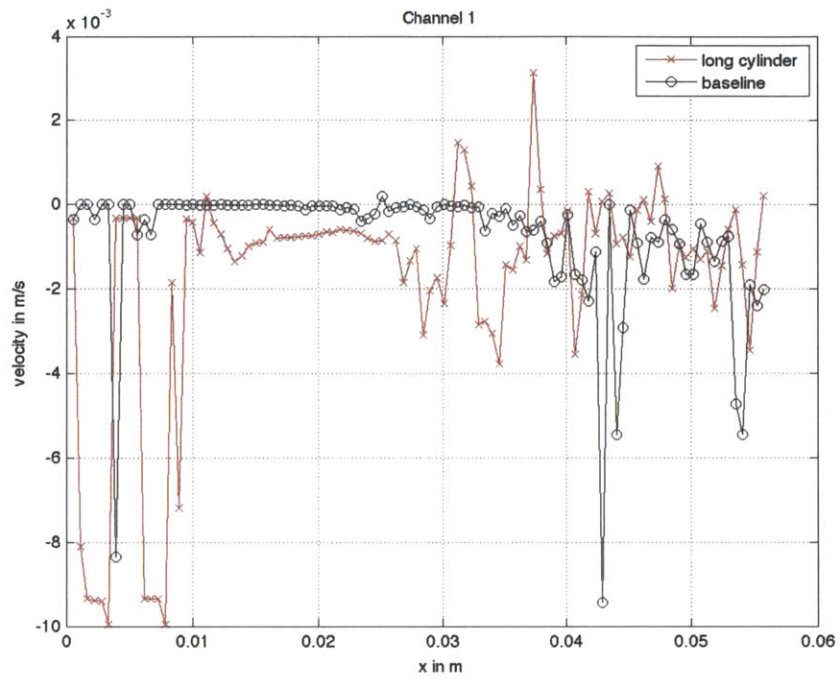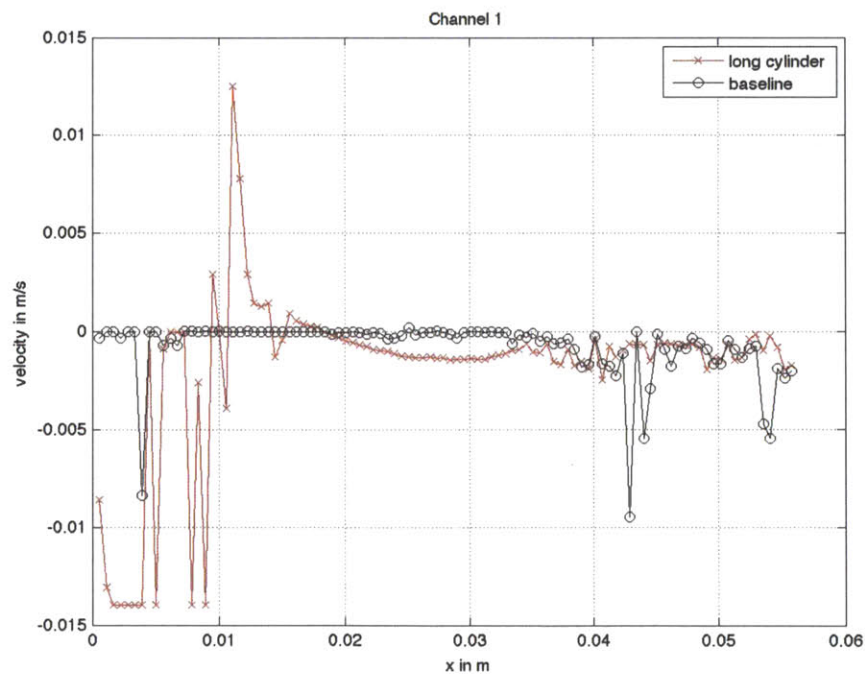


## 47 Hz, 50.6 Gauss, +90°
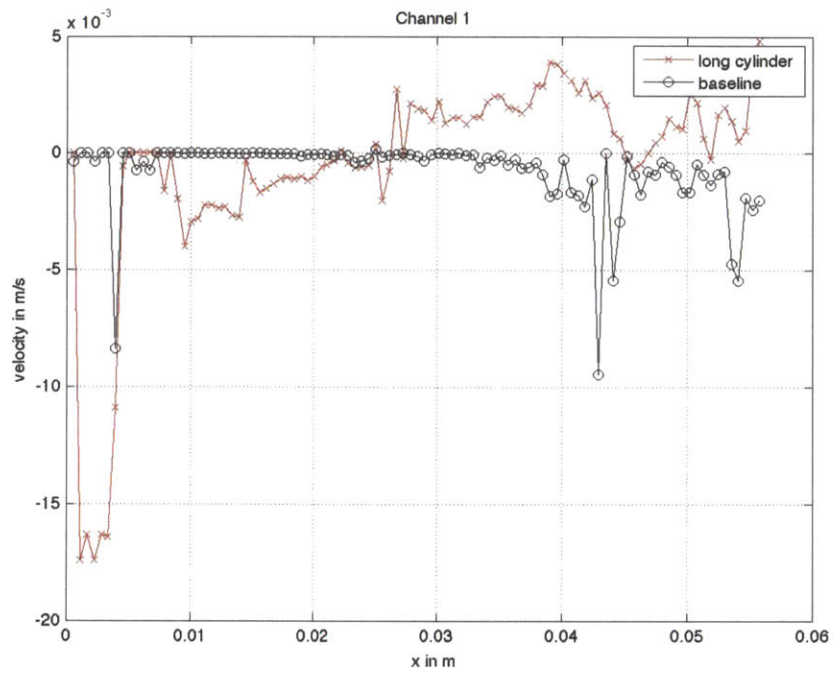
**47 Hz, 101.2 Gauss, -90°**
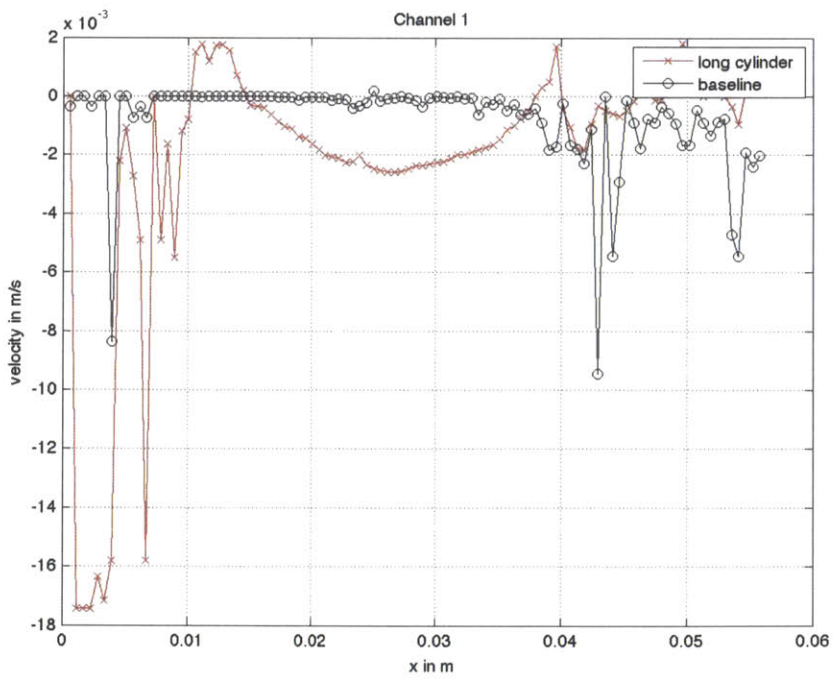


**47 Hz, 101.2 Gauss, +90°**
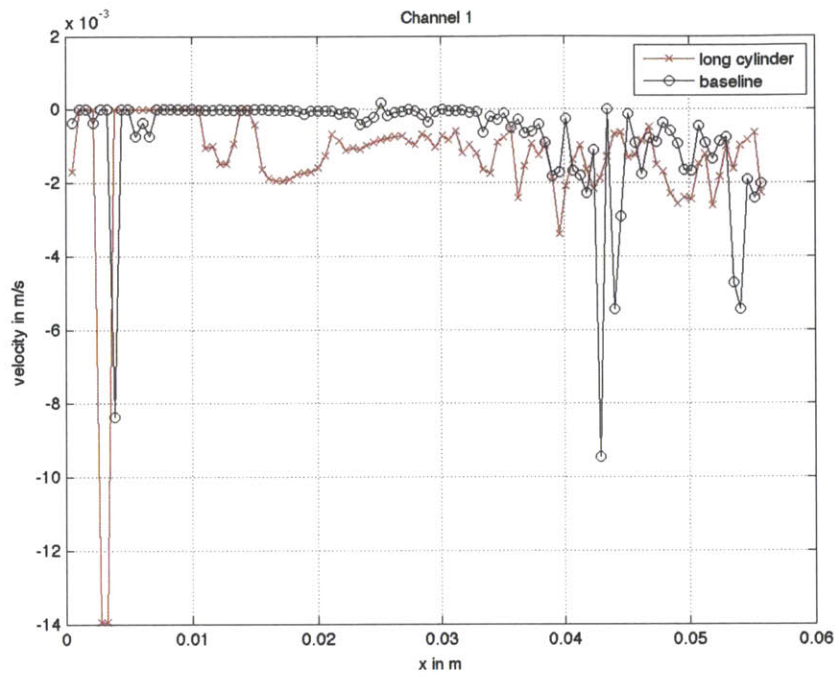
## 95 Hz, 50.6 Gauss, -90°
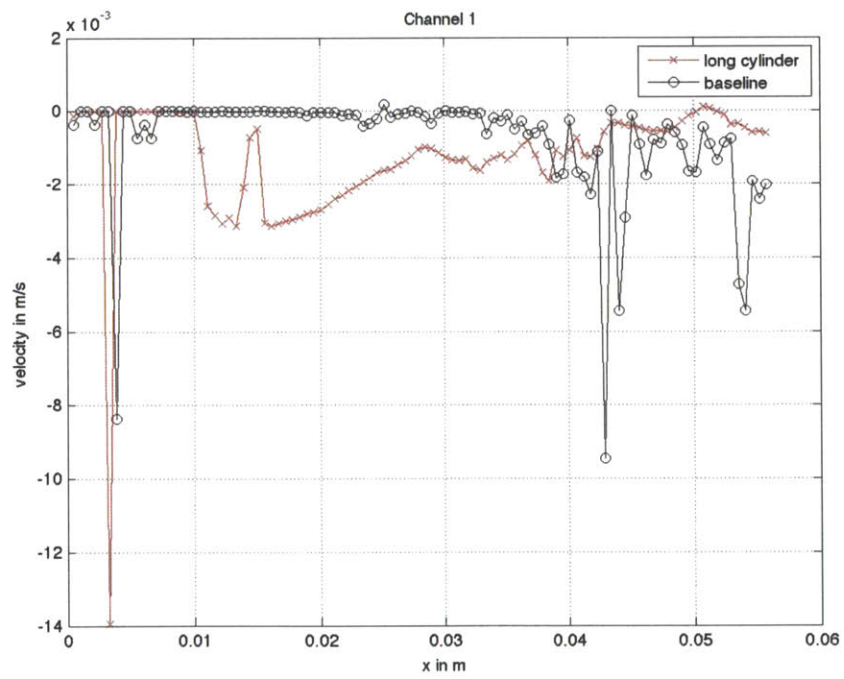


## 95 Hz, 50.6 Gauss, +90°
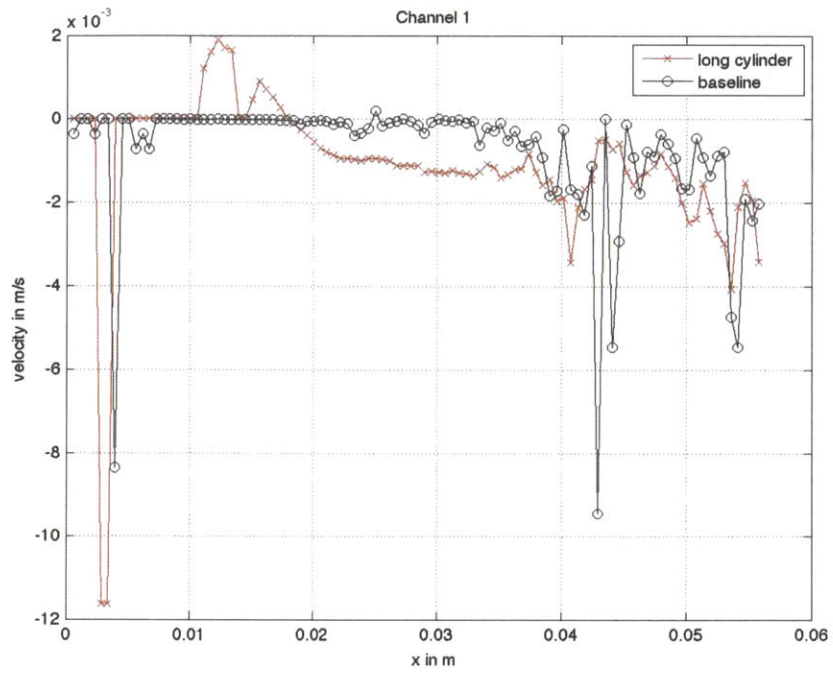
**95 Hz, 101.2 Gauss, -90°**
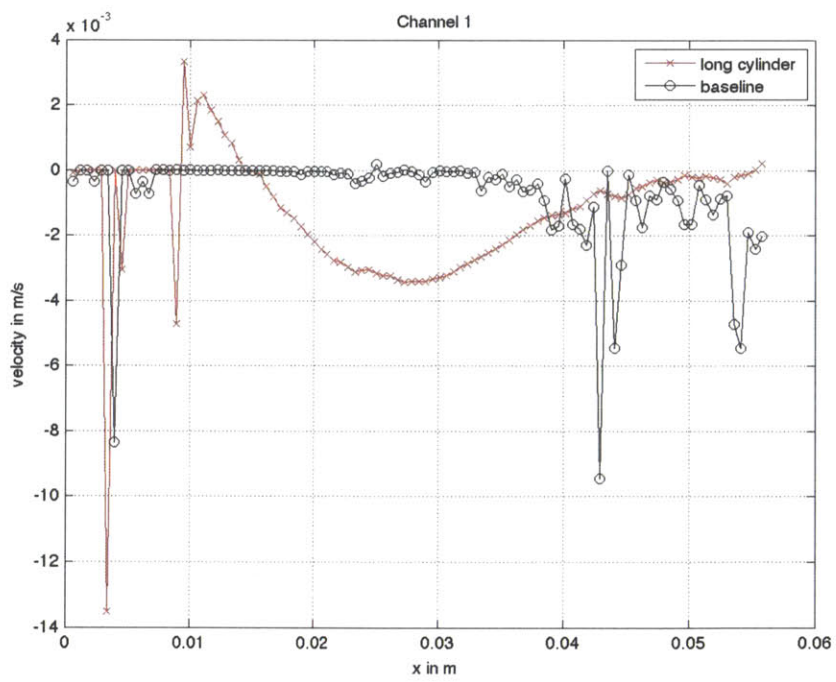


**95 Hz, 101.2 Gauss, +90°**

## A.2.3 Long Cylinder, Edge

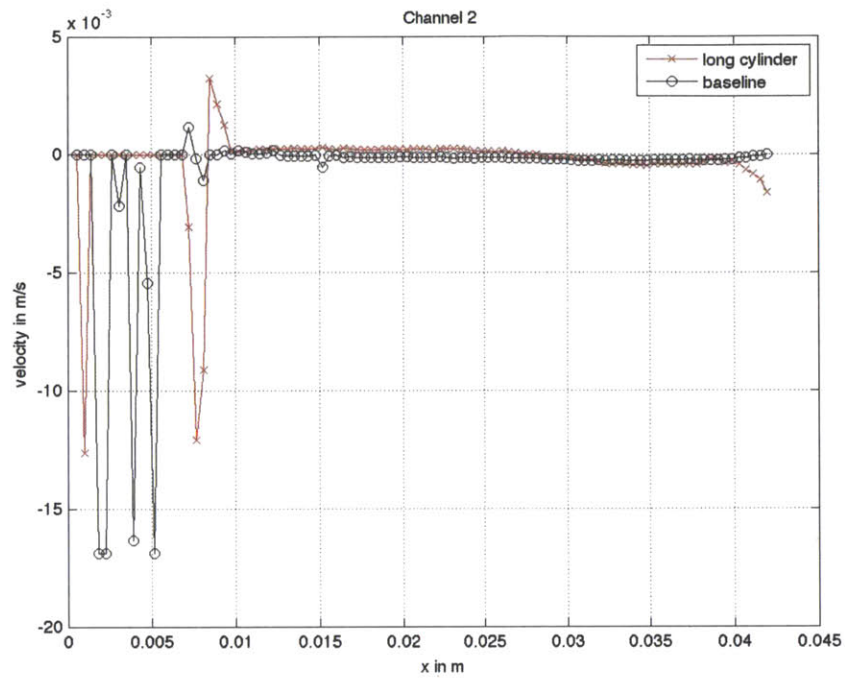## 47 Hz, 50.6 Gauss, -90°



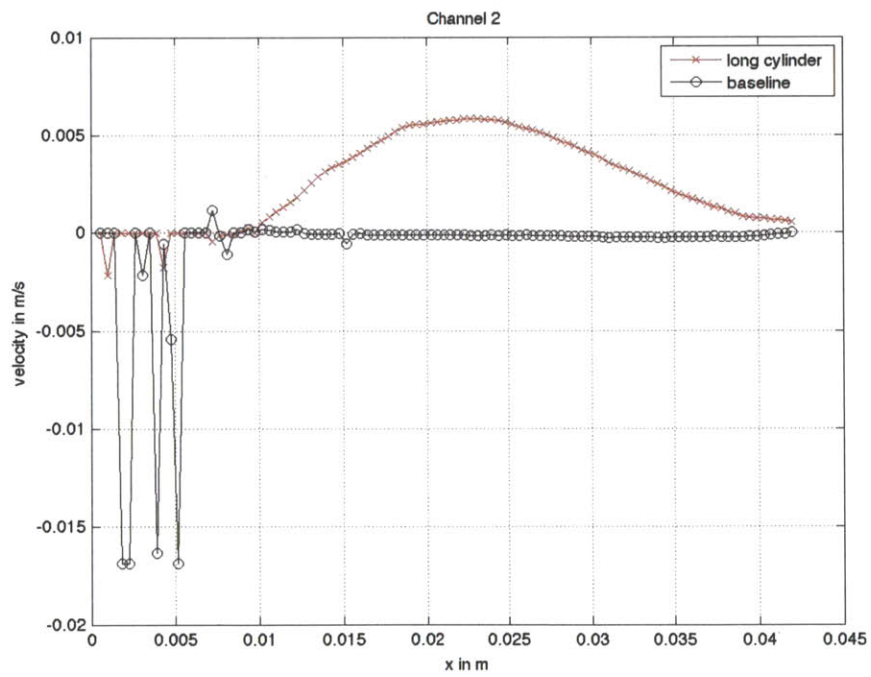## 47 Hz, 50.6 Gauss, +90°

**47 Hz, 101.2 Gauss, -90°**



**47 Hz, 101.2 Gauss, +90°**



117

**95 Hz, 50.6 Gauss, -90°**



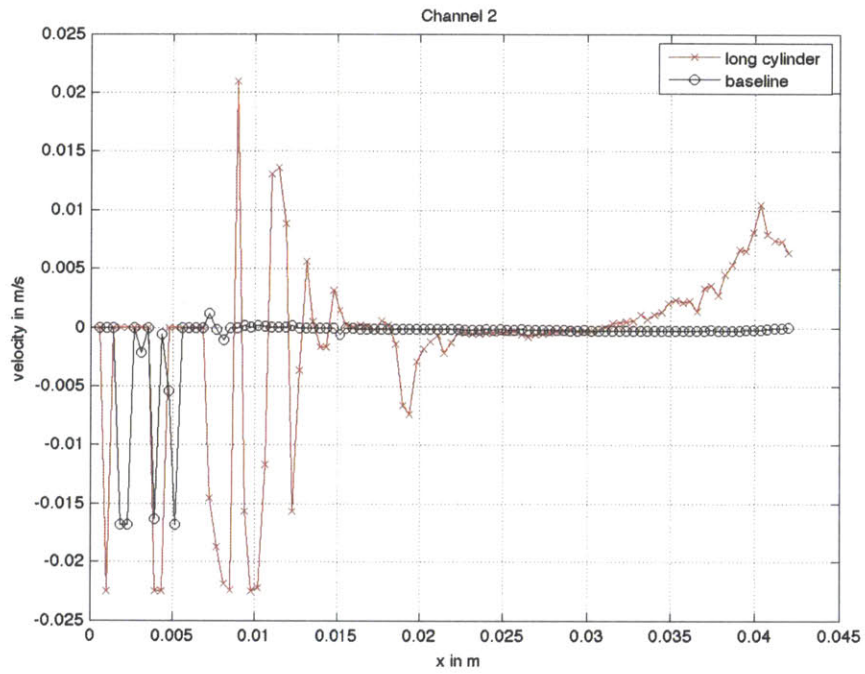**95 Hz, 50.6 Gauss, +90°**

## 95 Hz, 101.2 Gauss, -90°



## 95 Hz, 101.2 Gauss, +90°